Hairbots: The Future of Nanorobotic Coiffure

Robert A. Freitas Jr.
Senior Research Fellow
Institute for Molecular Manufacturing

Abstract. This paper describes, for the first time, the potential application of advanced nanorobotics to hair care, hairstyling, and coiffure. Nanorobots called hairbots can keep hair trimmed in a few minutes of activity every day. The nanorobots will produce no tickling or crawling sensations, can be made invisible to the naked eye of the user or bystanders, won't be easily detectable by touch if the user or someone else touches the hair when nanorobots are present, and will be secure against dislodgement from the hair by external forces such as wind or human touch. Hair extensions of any length can be manufactured in a gallon-sized hair mill – a specialized nanofactory for keratinous molecular manufacturing – then attached to native hairs in a few minutes. User defined coiffures can be assembled and maintained by nanorobots, or quickly rearranged in a timescale of minutes. Nanorobots can recolor hair, alter its curling pattern, and provide a variety of special effects such as fragrance, sound emission, and massage, or can replace the entire hairbody with new atomically-precise manufactured hair in a few minutes once it has been fabricated. Aerial hairbots positioned throughout the hairbody can lift individual hairstalks into the air against the force of gravity, enabling hairflight under user control. Bionic hair – artificial nanomechanical hair configured as tentacle manipulators – can provide the most complete solution to the challenge of coiffure flexibility, maintenance, and control, and may be able to protect the coiffured human head from physical harm due to collisional impacts if the strandbots surrounding the head can act with sufficient speed and counterforce to neutralize the threat.

Key Words and Referents: anchorbots, barber shop, beautician, beauty parlor, beauty shop, bionic hair, bleachbot, coiffure, cosmetology, databot, dyebot, flybot, guidebot, guidestalk, hairbot, hairbotics, hairdresser, hairflight, hair mill, hair salon, hairstyling, minimill, nanoflybot, nanohairbot, nanorobot, nanorobotic, nanotechnology, nodebot, strandbot

Cite as: Robert A. Freitas Jr., "Hairbots: The Future of Nanorobotic Coiffure," IMM Report No. 52, 15 April 2024; http://www.imm.org/Reports/rep052.pdf.

Table of Contents

1. Introduction

One of the most pleasant aspects of life is the beauty of the human form, and hairstyle is one of the greatest contributors to the aesthetics of that form. Of course, hair serves many practical functions. It can protect us from annoying or potentially harmful aspects of the environment such as ultraviolet radiation, dust, and debris. It helps regulate our temperature, being thick enough to shield our head from hot sunlight but thin enough to promote the evaporation of sweat which helps keep us cool. It serves as a sense organ, since our hair follicles are surrounded with nerve endings. Evolutionarily, hair provided camouflage and served as a sexual attractant. The role of hair in human psychology is essential, and an individual's hair plays a critical role in his or her identity and self-evaluation. Attitudes towards hairstyle vary widely across different cultures and historical periods.[1] Such styles are often used to reflect a person's personal beliefs, social position, group membership, age, gender, sexual preference, occupation,[2] or religion.

During one of his lectures[3] in the 1990s, Terence McKenna,[4] an American ethnobotanist and mystic, made casual humorous reference to the idea of employing nanorobots to trim people's hair: *"One of the uses suggested for nanotechnology, somewhat facetiously, was that you could have these little electronic mites that you combed into your hair. And every day they would creep out to the end of each hair, measure its length, and cut it off. So you'd have a permanent haircut, maintained by nano-mites from Clairol."*

There are many video demonstrations[5] of primitive robotic haircutting, but present-day discussions of nanotechnology in hair care[6] refer only to the simplest nanomaterials that are available today, an era in which complex atomically-precise microscopic robots cannot yet be fabricated. **The present paper is the first to combine the concepts of robotic haircutting and nanotechnology to describe, in some technical detail, the application of microscopic nanorobots to the cosmetological activities of haircutting and hairstyling**, aka. hairdressing.[7]

---

[1] Sherrow V. Encyclopedia of Hair: A Cultural History (illustrated edition). Greenwood Press, Westport CT, 2006; https://www.amazon.com/dp/0313331456.

[2] During the early years of the Roman Empire, prostitutes were required to obtain a license, pay taxes, and wear blonde hair as a mark of their profession; https://artisanhaircary.com/blog/hair-dye-history-crazy-ways-ancient-people-colored-their-hair/.

[3] "The Peculiar Humor Of Terence McKenna (Part 1)", at 6:12-6:35; https://www.youtube.com/watch?v=DKemHGIsA4k&t=371s.

[4] https://en.wikipedia.org/wiki/Terence_McKenna.

[5] e.g., "I made a hair cutting machine," Jul 2020; https://www.youtube.com/watch?v=7zBrbdU_y0s.

[6] Pereira-Silva M, Martins AM, Sousa-Oliveira I, Ribeiro HM, Veiga F, Marto J, Paiva-Santos AC. Nanomaterials in hair care and treatment. Acta Biomater. 2022 Apr 1;142:14-35; https://www.sciencedirect.com/science/article/pii/S1742706122001015.

[7] https://en.wikipedia.org/wiki/Hairdresser.

In the nanotech future likely to emerge in a few decades, wherein microscopic nanorobots[8] (image, below)[9] and the nanofactories[10] that build them (Section 4.1) are ubiquitous, hairstyling will become more convenient and simpler to perform but with vastly greater aesthetic options than are available today. In this future world, hair can be trimmed and coiffed continuously, stylistically switched frequently during the day, and arranged into coiffures that exhibit motion, reactivity to the environment, and active user control. Hair styling could be adapted to external factors like weather conditions, ensuring that the coiffure remains optimal from sunrise to sunset. The use of nanorobots could significantly reduce the time spent on hair styling by working simultaneously across the head to cut and style hair much faster than traditional methods. In addition to styling, these nanorobots could monitor scalp health, identify issues like fungal infections or dandruff at an early stage, and perhaps even administer appropriate treatments. This dual functionality could integrate health monitoring/treatment into regular grooming activities.

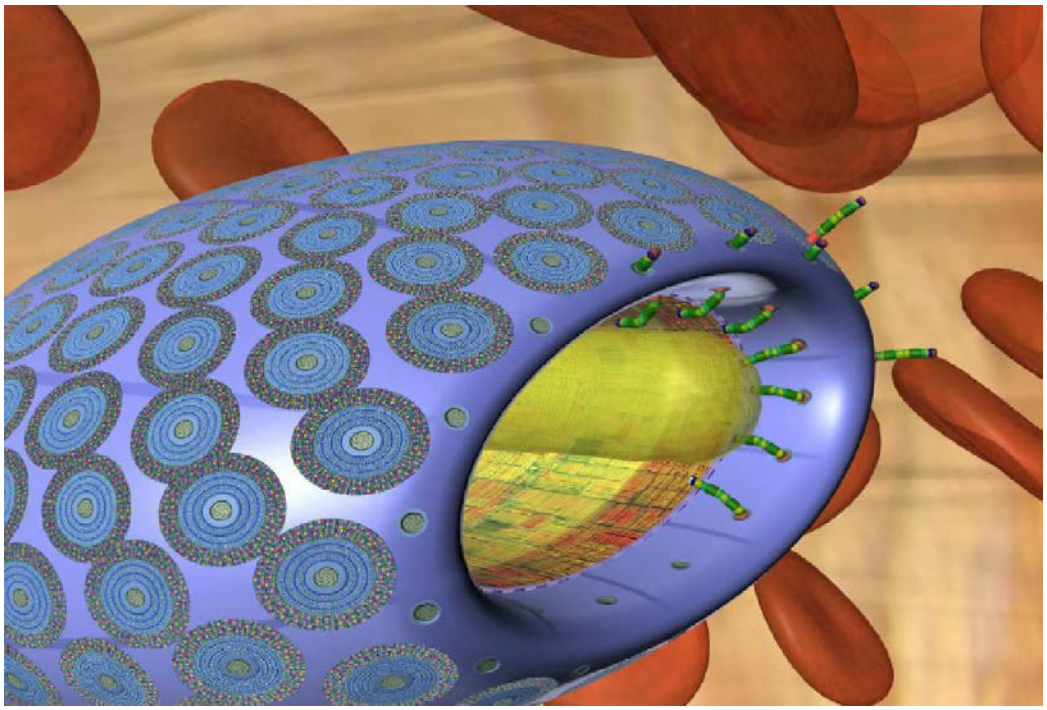

[8] http://www.nanomedicine.com/. See also: Freitas RA Jr. Nanomedicine, Volume I: Basic Capabilities. Landes Bioscience, Georgetown, TX, 1999; http://www.nanomedicine.com/NMI.htm and Freitas RA Jr. Nanomedicine Vol. IIA: Biocompatibility. Landes Bioscience, Georgetown, TX, 2003; http://www.nanomedicine.com/NMIIA.htm.

[9] "Microbivore in bloodstream" image; artwork by Forrest Bishop. Freitas RA Jr. Microbivores: Artificial Mechanical Phagocytes using Digest and Discharge Protocol. J. Evol. Technol. 2005 Apr;14:55-106; http://www.jetpress.org/volume14/freitas.pdf.

[10] http://www.molecularassembler.com/Nanofactory/. See also: Freitas RA Jr., Merkle RC. Kinematic Self-Replicating Machines. Landes Bioscience, Georgetown, TX, 2004; http://www.MolecularAssembler.com/KSRM.htm.

Nanorobots designed to manipulate individual hair strands, cutting or styling hair with precision at a microscopic level, would allow for incredibly detailed and personalized hairstyles, potentially revolutionizing the beauty industry. The role of hairstylists and hairstyling consultants will be crucial for helping people make full use of the new possibilities in nanorobotic hairstyling, aka. cosmetic hairbotics, that will undoubtedly inspire an explosion of expressive creativity.

After establishing a few general aspects of the physiology of human hair (Section 2), the present work describes the use of nanorobotic instrumentalities to trim hair to shorter lengths (Section 3), extend hair to greater lengths (Section 4), establish and maintain customized coiffures (Section 5), and alter hair color, curl, and thickness (Section 6). We then introduce the concept of mobile hairstyles that permit hairflight (Section 7), along with the concept of artificial bionic hair infused with nanosensors, nanocomputers, and nanomotors that could provide the most complete solution to the challenge of maximizing coiffure flexibility, maintenance, and control (Section 8).

2. Distribution and Properties of Human Hair

Humans have about 5 million hair follicles over the entire body.[11] Most healthy men and women who aren't partially or completely bald have 80,000-120,000 terminal hairs on the scalp of their head,[12] or typically N_{hairs} ~ 100,000. The number varies slightly by the area of the scalp and by hair color, typically ranging from a low of 90,000 for people with red hair to 100,000 for black hair, 110,000 for brown hair, and up to 150,000 for blond.[13] The typical density[14] of hair is 124-200 hairs/cm^2 on a scalp[15] of surface area 600-700 cm^2.

The diameter of all types of human hair varies from 17-180 μm,[16] but the diameter and cross-sectional geometry of terminal scalp hair varies by ancestry: 40-80 μm with oval cross-section having an ellipticity factor[17] ~1.5 (straight or wavy hair) for blond Caucasians, 50-90 μm with oval cross-section (straight or wavy hair) for red/brown/black-haired Caucasians, 60-100 μm with flat cross-section (curly hair) and ellipticity ~1.84 for African ancestry, and 80-100 μm with round cross-section (straight hair) and ellipticity ~1.28 for Asian/Native American ancestry.[18]

The hairshaft – the visible outer product of the follicle – is composed of three concentric regions:[19] (1) the medulla at the center, consisting of round cells, layered in columns and separated by air pockets; (2) the cortex, the bulk of the shaft and primary source of mechanical strength, composed of thicker spindle-shaped cells ~5 μm wide and ~90 μm long, layered vertically in parallel rows, and partaking color based on the type, number and distribution of melanin granules in the fiber; and (3) the outermost cuticle, a single 0.2-5 μm layer of transparent thin cells laid out like roof shingles, and covered with a single-molecule water-

---

[11] https://www.healthline.com/health/how-many-hairs-on-a-human-head#interesting-facts.

[12] Murphrey MB, Agarwal S, Zito PM. Anatomy, Hair. StatPearls [Internet], National Library of Medicine, NIH,14 Aug 2023; https://www.ncbi.nlm.nih.gov/books/NBK513312/.

[13] Amazing numbers in biology, Rainer Flindt, Springer 2006, pp. 212 table 4.2.2. See also: "Number of hairs on human head", Bionumbers, Harvard Univ.; https://bionumbers.hms.harvard.edu/bionumber.aspx?id=101509.

[14] Jimenez F, Ruifernández JM. Distribution of human hair in follicular units. A mathematical model for estimating the donor size in follicular unit transplantation. Dermatol Surg. 1999 Apr;25(4):294-8; https://pubmed.ncbi.nlm.nih.gov/10417585/.

[15] https://www.renefurterer.com/en-ca/tips/scalp/the-physiology-of-the-scalp.
[16] https://en.wikipedia.org/wiki/Hair#Description.

[17] Treeby BE, Pan J, Paurobally RM. An experimental study of the acoustic impedance characteristics of human hair. J Acoust Soc Am. 2007 Oct;122(4):2107-17; http://bug.medphys.ucl.ac.uk/papers/2007-Treeby-JASA-III.pdf.

[18] https://en.wikipedia.org/wiki/Hair_follicle#Variation.
[19] https://crlab.com/en_en/scientific-area/hair-and-scalp/structure-and-chemical-composition-of-hair/.

repellant lipid layer. The electron microscopy image at right shows the surface structure of a human hairstalk.[20]

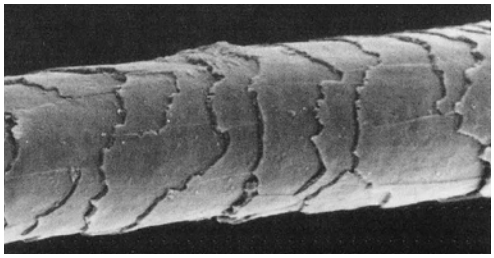

The figure below shows the average measured diameters of hairstalks, in millimeters, in relation to the location on the body of a Caucasian male.[21]

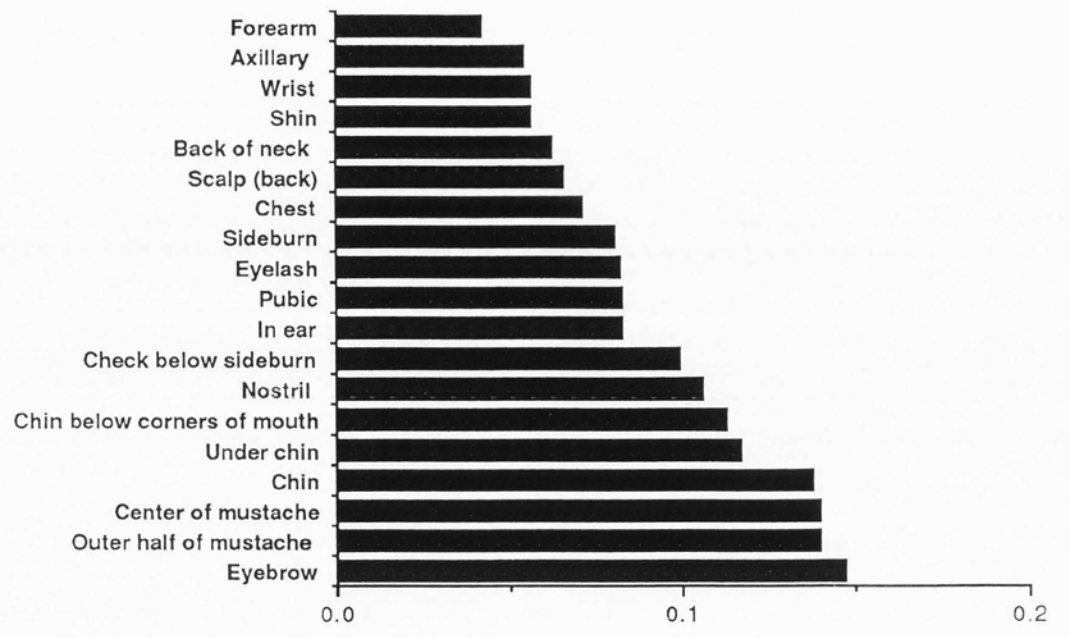

As hairs are extruded from the root of the follicle through the dermis and epidermis during growth, hairshaft cells are cut off from their supply of nourishment and die, forming a hard protein called keratin which, along with the dead cells, forms the structure of the rigid hairshaft in a process called keratinization.[22] Keratin, the main protein in the cortex, is composed of 18 amino acids including sulfur-rich cysteine (17.5%), serine (11.7%), glutamic acid (11.1%),

---

[20] Hess WM, Seegmiller RE, Gardner JS, Allen JV, Barendregt S. Human hair morphology: a scanning electron microscopy study on a male Caucasoid and a computerized classification of regional differences. Scanning Microsc. 1990 Jun;4(2):375-86, Figure 1i; https://digitalcommons.usu.edu/cgi/viewcontent.cgi?article=2022&context=microscopy.

[21] Hess WM, Seegmiller RE, Gardner JS, Allen JV, Barendregt S. Human hair morphology: a scanning electron microscopy study on a male Caucasoid and a computerized classification of regional differences. Scanning Microsc. 1990 Jun;4(2):375-86, Table 1; https://digitalcommons.usu.edu/cgi/viewcontent.cgi?article=2022&context=microscopy.

[22] Van Scott EJ. Keratinization and hair growth. Annu Rev Med. 1968;19:337-50; https://www.annualreviews.org/doi/pdf/10.1146/annurev.me.19.020168.002005. Shetty S; Gokul S. Keratinization and its disorders. Oman Med J. 2012 Sep;27(5):348-57; https://www.ncbi.nlm.nih.gov/pmc/articles/PMC3472583/.

threonine (6.9%), glycine (6.5%), and arginine (5.6%). Hair is mostly fibrous α-keratin[23] with a molecular weight of ~45,000,[24] and consists of α-helically coiled single protein strands (with regular intra-chain H-bonding) which are then further twisted into superhelical ropes that may be further coiled.[25] Mature dry hairstalks are 95% keratin plus small amounts of lipids (including triglycerides, waxes, phospholipids, cholesterol, squalene, and free fatty acids), minerals, and pigments (primarily melanin,[26] e.g., $[C_{25}H_9N_3O_{13}]_n$ for eumelanin), with a net chemical composition approximating carbon (45%), oxygen (28%), nitrogen (15%), hydrogen (6.7%), and sulfur (5.3%) for hairstalks.[27]

The density of dry human hair is $\rho_{hair} \sim 1.32$ gm/cm^3, although the hair can absorb another 0.40 gm/cm^3 of water (~60 gm for a full head of 30 cm long hair) during an exposure time of ~3 minutes.[28] Typical values for the tensile modulus, yield stress, and maximum stress for human hair are 5.1 GPa, 109 MPa, and 161 MPa, respectively.[29] A human hair "is stronger than a copper wire of the same diameter and can support a weight of 5-7 oz" (~1.6 N) under tensile stress.[30]

---

[23] https://en.wikipedia.org/wiki/Alpha-keratin.
[24] https://crlab.com/en_en/scientific-area/hair-and-scalp/structure-and-chemical-composition-of-hair/.
[25] https://en.wikipedia.org/wiki/Keratin#Disulfide_bridges.
[26] https://en.wikipedia.org/wiki/Melanin.
[27] https://crlab.com/en_en/scientific-area/hair-and-scalp/structure-and-chemical-composition-of-hair/.

[28] Zimmerley M, Lin CY, Oertel DC, Marsh JM, Ward JL, Potma EO. Quantitative detection of chemical compounds in human hair with coherent anti-Stokes Raman scattering microscopy. J Biomed Opt. 2009 Jul-Aug;14(4):044019; https://www.ncbi.nlm.nih.gov/pmc/articles/PMC2872558/.

[29] Kunchi C, Venkateshan KC, Reddy ND, Adusumalli RB. Correlation between Mechanical and Thermal Properties of Human Hair. Int J Trichology. 2018 Sep-Oct;10(5):204-210; https://www.ncbi.nlm.nih.gov/pmc/articles/PMC6290292/.

[30] Hess WM, Seegmiller RE, Gardner JS, Allen JV, Barendregt S. Human hair morphology: a scanning electron microscopy study on a male Caucasoid and a computerized classification of regional differences. Scanning Microsc. 1990 Jun;4(2):375-86; https://digitalcommons.usu.edu/cgi/viewcontent.cgi?article=2022&context=microscopy.

3. Nanorobotic Hair Trimming

While there are many aspects of maintaining living dermal, subdermal, and follicular tissue in good health, the discussion here will start with simply maintaining the desired dimensions of the mostly biologically-inactive materials in keratinized hair.

Rather than regular visits to a local barber shop, hair stylist, or beauty salon, basic hair length maintenance could be performed entirely at home. The process begins by opening a hairstyling software application package that has been downloaded to an existing personal computer, laptop, or mobile device. This package allows the user to (a) choose their desired hairstyle, (b) calculate the specific nanorobot activities needed to achieve the desired hairstyle, then (c) program the appropriate nanorobots to execute the specific activities that will maintain or create the desired hairstyle. Here we focus on continuously keeping the hair precisely trimmed to the proper length consistent with the specified hairstyle.

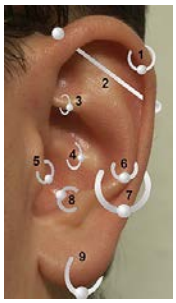

As noted below, hair length maintenance will require a set of $N_{trimbots}$ ~ 100,000 multilegged nanorobots called "hairbots" having a total packed volume of ~15 mm^3 (i.e., a tiny cube measuring $L_{storage}$ ~ 2.5 mm on a side). This entire robot fleet can easily fit inside an unobtrusive designer earring[31] (image, left),[32] or other convenient storage vessel carried on the user's body.

3.1 Prepare Scalp Map

After the software application is downloaded and the user's scalp and hair have been meticulously cleaned (Section 3.5), hairbots are activated and deployed from their storage vessel onto the user's scalp to perform the first comprehensive survey. The topography of the normal human scalp (electron microscope image, right)[33] suggests that the typical vertical surface roughness of the epidermis is ~10 μm but that ~50 μm features such as gaps and ridges in the uneven surface are widespread, especially in the vicinity of an emergent hairshaft as shown in the image. Multi-armed nanorobots with arm lengths of ~100 μm should be able to readily survey and measure the geometry of this uneven terrain, recording both the surface topography and the size and position of every hair. Note that a hair areal density of n_{hair} ~124-200 hairs/cm^2 implies a mean distance between hairs of $n_{hair}^{-1/2}$ ~ 900-700 μm.

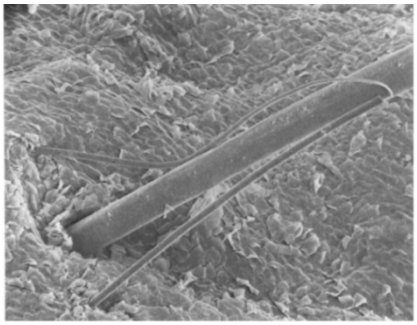

---

[31] https://en.wikipedia.org/wiki/Earring.
[32] https://commons.wikimedia.org/wiki/File:Positions_of_earrings.jpg.

[33] Montagna W, Parakkal PF. The Structure and Function of Skin. Academic Press, 1974; Third Edition, Ch. 2 The Epidermis, Fig. 6, p. 24; image courtesy of Dr. W.H. Fahrenbach; https://books.google.com/books?id=50Zgf-ZBP5gC&oi=fnd&pg=PA24.

Typical hair diameter is $d_{hairstalk}$ ~ 80 μm, and simulations of skin microstructure displacement have been done at 10 μm resolution with good results.[34] A population of $N_{trimbots}$ ~ 100,000 hairbots traveling across the scalp at v_{bot} ~ 10 cm/sec and sweeping an $x_{scanline}$ ~ 10 μm scanline with n_{scans} = 10 repeat scans for redundancy can survey an A_{scalp} ~ 650 cm^2 scalp area for the location of all hairstalks in $t_{scanscalp} \sim t_{min} + A_{scalp} / (n_{scans}\ N_{trimbots}\ v_{bot}\ x_{scanline}) = 2.6$ sec, where $t_{min} = A_{scalp}^{1/2} / v_{bot} \sim 2.5$ sec is the minimum possible time to sequentially traverse two edges of the scalp perimeter, assuming the scalp to be roughly square in shape.

With the scalp and location of every hair now mapped, the hairbots disperse to the protruding hair shafts – one robot for each hairstalk of typical diameter $d_{hairstalk}$ ~ 80 μm – and begin to climb.[35] A nanorobot with a D_{robot} = 50 μm wide body and 2-4 flexible arms on either side of the robot body (e.g., image, right),[36] with each arm having length $L_{robotarm}$ ~ 100 μm at full extension, can reach entirely around a cylindrical hairstalk of circumference $\pi d_{hairstalk} \sim 250\ \mu m \sim 2L_{robotarm} + D_{robot}$. Crawling the entire length of a single strand of hair of maximum length $L_{hairstalk}$ ~ 30 cm at v_{bot} ~ 10 cm/sec to precisely measure its length requires a maximum travel time of $t_{scanhair} \sim t_{min} + L_{hairstalk} / v_{bot} \sim 5.5$ sec for each hairbot. (An additional $t_{scanhair}$ ~ 5.5 sec will be required for the hairbots to descend their assigned hairstalks and traverse the scalp, returning to their storage vessel to download their mapping data into the hairbot control computer located there.) Achieving an arboreal climbing speed of v_{bot} ~ 10 cm/sec requires an armswing frequency of $\nu_{robotarm} \geq v_{bot} / L_{robotarm} \sim$ **1000 Hz**. This seems fairly conservative for a diamondoid nanorobot, considering it is only ~5 times faster than the $\nu_{miteleg} \geq v_{mite} / L_{miteleg} \sim$ **188 Hz** legswing frequency of the adult *Paratarsotomus macropalpis* mite, even though the mite is nearly ten times larger than a hairbot. The mite is ~700 μm in size with eight legs $L_{miteleg}$ ~ 1200 μm in length[37] and has been observed running at v_{mite} ~ 22.5 cm/sec.[38]

The power requirement for each scanning nanorobot to overcome drag from pushing through viscous air[39] is $P_{loco} = 6\ \pi\ \eta_{air}\ R_{robot}\ v_{bot}^2 = 85.4$ pW, taking air absolute viscosity η_{air} ~ 1.813 x

---

[34] e.g., Nagano K, Fyffe G, Alexander O, Barbic J, Li H, Ghosh A, Debevec P. Skin microstructure deformation with displacement map convolution. ACM Trans Graphics 2015 Jul 27;34(4):1-10; https://core.ac.uk/download/pdf/77001950.pdf.

[35] A single ~0.3 μg hairbot (Section 3.7.1) poised at the tip of a 30 cm vertically-positioned hairstalk would apply a downward force of ~0.003 μN, but ~200 μN are required to buckle the hairstalk (Section 8.2).

[36] Čížek P, Faigl J. Self-supervised learning of the biologically-inspired obstacle avoidance of hexapod walking robot. Bioinspir Biomim. 2019 May 3;14(4):046002; https://pubmed.ncbi.nlm.nih.gov/30995613/.

[37] https://www.sci.news/biology/science-mite-paratarsotomus-macropalpis-fastest-animal-01887.html. See also: Wu GC, Wright JC, Whitaker DL, Ahn AN. Kinematic evidence for superfast locomotory muscle in two species of teneriffiid mites. J Exp Biol. 2010 Aug 1;213(Pt 15):2551-6; https://core.ac.uk/download/pdf/70974452.pdf.

[38] https://en.wikipedia.org/wiki/Paratarsotomus_macropalpis.

[39] Friction by contact with neighboring hairstalks should be minimal because the typical airgap between adjacent hairstalks in coiffed dry hair is at least $x_{airgap} \geq (L_{hairstalk}\ n_{hair} / z_{pile}\ w_{patch})^{-1/2} - d_{hairstalk} \sim 64$ μm

10^{-5} kg/m-sec and R_{robot} ~ 25 μm, giving a negligible total fleet power draw of $P_{fleet} = N_{trimbots}$ P_{loco} ~ 8.5 μW. Photoelectric cells with only ε_{light} ~ 20% conversion efficiency covering the outer surface of each nanorobot can power robot locomotion if the incident intensity of visible light is $I_{light} \geq P_{loco} / \pi R_{robot}^2 \varepsilon_{light}$ ~ 0.2 W/m^2 – a requirement that should be satisfied by normal ambient light, typically 5-15 W/m^2 inside well-lighted buildings[40] but up to 200-300 W/m^2 in full daylight sun at the equator,[41] even for robots on the scalp that are heavily shaded under large volumes of opaque hair. Onboard energy storage can supplement any shortfalls in illumination-sourced power.

How big is the scalp map? Specifying the xyz scalp coordinates for each hairstalk at $x_{scanline}$ ~ 10 μm resolution requires $I_{xyz} = 3 \log(A_{scalp}^{1/2} / x_{scanline}) / \log(2)$ ~ 44 bits. Assigning each of the N_{hairs} ~ 100,000 scalp hairs a unique name requires another $I_{names} \sim \log(N_{hairs}) / \log(2)$ ~ 17 bits; specifying the length of the hairstalk to 10 μm accuracy requires $I_{length} \sim \log(L_{hairstalk} / x_{scanline}) / \log(2) = 15$ bits. Allocating another $I_{hairdata}$ ~ 24 bits of unspecified useful data per hair (e.g., a time stamp; the location and extent of "split ends" (Section 4.4) or trichoptilosis; etc.) gives $I_{scalpmap} \sim (I_{xyz} + I_{names} + I_{length} + I_{hairdata}) N_{hairs}$ = (100 bits/hairstalk) $N_{hairs} \sim 10^7$ bits per scalp map listing the names, locations, lengths, and other useful high-level data for each of 100,000 hairstalks. According to classical descriptions of high-density mechanical nanocomputing,[42] a 3D array of diamondoid register rods can achieve a storage density of $i_{nano} = 10^7$ bits/μm^3 with a $\tau_{nano} = 10^{10}$ bit/sec data access speed. So each hairbot can store all the data it has collected in an onboard ~1 μm^3 nanomechanical RAM,[43] and can upload, download, or access the entire contents in $t_{download} \sim I_{scalpmap} / \tau_{nano}$ ~ 1 msec for a power expenditure of $I_{scalpmap} E_{Landauer300K} / t_{download}$ ~ 29 pW per map-access, taking $E_{Landauer300K} \sim k_B T \ln(2)$ J/bit = 2.87 x 10^{-21} J/bit as the experimentally-confirmed[44] classical Landauer limit[45] for non-reversible computational energy dissipation, Boltzmann's constant k_B = 1.38 x 10^{-23} J/K, and temperature T ~ 300 K.

---

which is larger than the D_{robot} = 50 μm hairbot body size, for a z_{pile} ~ 1 cm thick hairpile atop the scalp, summing the height of a w_{patch} = 1 cm wide and $L_{hairstalk}$ = 30 cm long patch of overlaid hair, taking n_{hair} ~ 160 hairs/cm^2.

[40] "Lighting System Assessment Guidelines," U.S. Dept. of Energy, NREL/BR-7A20-50125, Jun 2011; https://www.nrel.gov/docs/fy11osti/50125.pdf.

[41] http://en.wikipedia.org/wiki/File:Solar_land_area.png.

[42] Drexler KE. Nanosystems: Molecular Machinery, Manufacturing, and Computation, John Wiley & Sons, New York, 1992, Chapter 12 "Nanomechanical Computational Systems"; https://www.amazon.com/dp/0471575186/. Freitas RA Jr. Nanomedicine, Volume I: Basic Capabilities, Landes Bioscience, Georgetown TX, 1999, Section 10.2.1, "Nanomechanical Computers"; http://www.nanomedicine.com/NMI/10.2.1.htm.

[43] https://en.wikipedia.org/wiki/Random-access_memory.

[44] Bérut A, Arakelyan A, Petrosyan A, Ciliberto S, Dillenschneider R, Lutz E. Experimental verification of Landauer's principle linking information and thermodynamics. Nature. 2012 Mar 7;483(7388):187-189; https://www.nature.com/articles/nature10872.

[45] Landauer R. Irreversibility and heat generation in the computing process. IBM J Res Devel. 1961;5:183-191; http://fab.cba.mit.edu/classes/MAS.862/notes/computation/Landauer-1961.pdf. Bennett C, Landauer

3.2 Process Scalp Map Data

Upon their return to the storage vessel, the hairbots download their accumulated information to the storage vessel's control computer. If the storage vessel contains $n_{datachannels} = 100$ separate input data channels, downloading the information from all $N_{trimbots} = 100{,}000$ nanorobots takes about $t_{downloadALL} \sim (N_{trimbots} / n_{datachannels})\, t_{download} \sim 1$ sec. This information is simultaneously transmitted from the hairbot storage vessel to the user's personal computer where the hairstyling application has been installed. The user's personal computer combines this data with a 360-degree headshot of the user created by stitching together several external photos or selfies taken with the camera of a mobile device to create a 3D model[46] of the user's head, face, and current coiffure.[47] The personal computer knows the exact follicle root location and precise length of every hair on the scalp, and calculates the best fit of this data to the observed configuration of the user's hair. The result is an accurate model of the current state of the user's coiffure.

3.3 Select Desired Coiffure

Starting from a visual display of the hairstalk-specific 3D model of the existing coiffure, the user can request, simulate and review the projected macroscale appearance of any desired change, ranging from a light trim to a whole new look – possibly emulating some famous person or exploring a range of alternative styles selected from an extensive menu of customized possibilities.[48] There are already numerous "AI hairstyle apps" that let people experience virtual hairstyle try-ons,[49] including one from ChatGPT4,[50] wherein the face is digitized and various hair styles are painted over the image of the face to see how it looks.

But the hairbot software application is considerably more sophisticated. The personal computer has a complete model of the exterior of the user's head at single-hair resolution, so it can simulate how a new coiffure would look under a variety of different circumstances (e.g., parted in a different place, emerging from the shower or pool, etc.) or with different hair lengths and colors. It will also simulate kinematic behavior – how the hairbody is supposed to move, e.g., when the user shakes their head or when the wind blows. In an application extension, the computer model could allow visualization of various patterns of stubble, moustaches or beards on the user's face. Of course, a user may choose to have their coiffure prepared in the traditional manner by a professional hairdresser, exactly to their liking, and then employ hairbots to create a hairstalk-specific coiffure map (Section 5.1) "snapshot" to use as the template rather than starting from a

---

R. The fundamental physical limits of computation. Sci Am. 1985 Jul;253(1):48-57; http://web.eecs.umich.edu/~taustin/EECS598-HIC/public/Physical-Limits.pdf.

[46] e.g., http://www.cs.unc.edu/~geom/HSLOD/, https://haar.is.tue.mpg.de/, https://developer.nvidia.com/blog/ai-can-render-hair-in-3d-in-real-time/, and https://magazine.viterbi.usc.edu/fall-2015/articles/big-data-for-3-d-hair-scan/.

[47] https://en.wikipedia.org/wiki/Hairstyle.
[48] https://en.wikipedia.org/wiki/List_of_hairstyles.
[49] https://www.perfectcorp.com/consumer/blog/hair/best-ai-hairstyle-testing-apps.
[50] https://chat.openai.com/g/g-jj0dzhtup-hairstyle-simulator.

computer simulation. Most people will probably wish to retain the services of a creative personal hairstylist to assist them in navigating what is likely to be a bewildering array of possibilities.

Once the desired coiffure has been selected,[51] the personal computer calculates the exact length of each individual hair and any other changes needed to achieve the selected style and creates the Desired Coiffure Map.

3.4 Trim Excessively Long Hairstalks to Specified Dimensions

The hairbots are programmed with their hair trimming instructions and are deployed from their storage vessel onto the scalp. Following a deployment pattern that permits quick matching of the observed hairstalk distribution to the recorded scalp map, each robot proceeds to its designated hairstalk and ascends the trunk, carefully measuring the exact travel distance upward from the base. Based on the desired coiffure, the personal computer calculates the ideal length of each individual hair needed to achieve the selected style and creates a cut list indicating the exact amount that must be trimmed from each individual hairstalk. For hairstalks that are too long, the hairbot trims the length by one of at least two possible methods: chemical digestion (Section 3.4.1), which leaves no detritus but is slower and more energy intensive, or mincing (Section 3.4.2), which leaves detritus but is faster and more energy efficient. Deciding which strategy is best in a given situation requires further analysis but is beyond the scope of this paper.

An extension protocol, which should be followed for hairstalks that are too short and must be made longer, is discussed in Section 4.

3.4.1 Digestion Protocol

If the hairbot is assigned to a hairstalk that is too long, the robot proceeds to the apex of the keratinous column and begins chemically digesting it, moving downward until the remaining hairstalk has the desired length. Digestion occurs as the robot employs its arms to rotate around the keratin column in a shallow spiral pattern, allowing diamondoid mandibles at the robot's ingestion port to slice a continuous ribbon of hairstalk material to be fed into a morcellation chamber. There the material is minced into small easily digested pieces and passed to a digestion chamber where the small pieces are chemically digested into small molecules, then released into the air through an exhaust port as a harmless odorless gaseous effluent (see below), analogous to the system described elsewhere for the microbivore[52] which operates in a liquid environment.

---

[51] In the 1970s, MIT computer scientist Ed Fredkin suggested using haircutting microbots to maintain existing hairlengths, reports one observer (https://groups.google.com/g/sci.nanotech/c/zhIEjAyeswQ): "You'd get a perfect haircut, just the way you'd like it to stay, and then you'd drop the microbot onto your head. It would measure the length of each hair by shinnying up and down it, and remember it. Having recorded the state of your haircut, it would continue shinnying up and down your hairs, snipping off a bit when it found a hair too long. The haircut robot would need a special 'safety' mode for shampoos."

[52] Freitas RA Jr. Microbivores: Artificial Mechanical Phagocytes using Digest and Discharge Protocol. J Evol Technol. 2005 Apr; 14:55-106; http://www.jetpress.org/volume14/freitas.pdf.

Fewer enzyme types and fewer distinct digestion cycles should be required to fully decompose predominantly keratinous hairstalk material, so the microbivore digestion cycle time can probably be reduced by tenfold, giving a modular hairbot digestion system (roughly equivalent to the microbivore's two ports and two chambers) of volume V_{module} ~ 5.5 μm^3, power draw P_{module} ~ 120 pW, and keratin digestion capacity $\delta_{keratin}$ ~ 0.7 μm^3/sec.

Since human hair grows at a typical rate of g_{hair} ~ 350 μm/day,[53] one day of untrimmed growth implies a need to remove $V_{hairtrim} \sim (\pi/4)\ g_{hair}\ d_{hairstalk}^2 = 1.76 \times 10^6$ μm^3/day from each hairstalk. Completing this removal over a brief t_{digest} = 900 sec (15 min) per day requires the equivalent of $n_{modules} = V_{hairtrim} / t_{digest}\ \delta_{keratin}$ ~ 2800 digestion modules, implying a hairbot digestion system of volume $V_{digest} \sim n_{modules}\ V_{module}$ = 15,400 μm^3 (< hairbot volume V_{robot} ~ 150,000 μm^3)[54] and continuous power draw of $P_{digest} \sim n_{modules}\ P_{module}$ ~ 0.336 μW during the 900 sec digestion process, a robot power density of P_{digest} / V_{robot} ~ 0.00224 MW/L.[55] The total energy required to complete this process is $E_{digest} = P_{digest}\ t_{digest}$ ~ 300 μJ, which can be stored in an efficient diamondoid flywheel battery[56] of energy density E_d ~ 90 MJ/L and volume $V_{battery} = E_{digest} / E_d \sim$ 3400 μm^3 (<< V_{robot} ~ 150,000 μm^3). Digestion of excess hair by an $N_{trimbots}$ ~ 100,000 nanorobot fleet costs $E_{fleet} \sim N_{trimbots}\ E_{digest}$ = 30 J and $P_{fleet} = E_{fleet} / t_{digest}$ = 33 mW. This can be replaced in $t_{recharge} = E_{fleet} / A_{dangle}\ \varepsilon_{light}\ I_{light} \sim t_{day}$ = 86,400 sec (1 day) using a tiny decorative earring photoelectric collector dangle plate[57] of area A_{dangle} ~ 3 cm^2 (~1/3 of a postage stamp) with a photoelectric conversion efficiency of ε_{light} ~ 20% exposed to the normal ambient light intensity of 5-15 W/m^2 inside well-lighted buildings,[58] especially since this power input is only required when the robots performing digestion operations are near the terminal apex of each hair and fully exposed to external illumination. Supplemental onboard energy storage can replace any shortfalls in illumination-sourced power.

Many sulfur-bearing compounds are extremely odiferous and should not be used as effluents. For example, hydrogen sulfide (H_2S) and sulfur dioxide (SO_2) are detectable to the human nose at concentrations in air (ρ_{air} = 1.29 kg/m^3) as low as c_{H2S} = 0.47 ppb[59] and c_{SO2} = 0.67 ppm,[60]

---

[53] Murphrey MB, Agarwal S, Zito PM. Anatomy, Hair. StatPearls [Internet], National Library of Medicine, NIH,14 Aug 2023; https://www.ncbi.nlm.nih.gov/books/NBK513312/.

[54] e.g., 6 roughly cylindrical robot arms of length $L_{robotarm}$ ~ 100 μm and radius $R_{robotarm}$ ~5 μm ($6V_{robotarm}$ ~ 47,400 μm^3) plus a robot body of volume V_{body} ~ 100,000 μm^3.

[55] This is comparable to the estimated peak power density of medical nanorobotic systems such as respirocytes (~0.12 MW/L), microbivores (~0.032 MW/L), and chromallocytes (~0.0029 MW/L); Freitas RA Jr. Energy Density. IMM Report No. 50, 25 June 2019; Chapter 1, "Introduction"; http://www.imm.org/Reports/rep050.pdf.

[56] Freitas RA Jr. Energy Density. IMM Report No. 50, 25 June 2019; Section 5.3.2, "Rotational Motion"; http://www.imm.org/Reports/rep050.pdf.

[57] https://en.wikipedia.org/wiki/Earring#Dangle_earrings.

[58] "Lighting System Assessment Guidelines," U.S. Dept. of Energy, NREL/BR-7A20-50125, Jun 2011; https://www.nrel.gov/docs/fy11osti/50125.pdf.

[59] https://en.wikipedia.org/wiki/Hydrogen_sulfide.

respectively, and would require an airflow velocity past a human head of circumference[61] C_{head} ~ 56 cm of $v_{H2S} \geq 4\pi\ m_S / c_{H2S}\ \rho_{air}\ C_{head}$ ~ 9.4 m/sec for H_2S or $v_{SO2} \geq 4\pi\ m_S / c_{SO2}\ \rho_{air}\ C_{head}$ ~ 0.7 cm/sec for SO_2 to odorlessly disperse the $m_S = V_{hairtrim}\ \rho_{hair}\ N_{hairs}\ f_S$ ~ 1.43 x 10^{-7} gm/sec of sulfur-containing effluent created by continuous digestion of keratin-rich hair, which is f_S ~ 5.3% sulfur by weight (Section 2). A preferable sulfur-containing effluent might be dimethyl sulfoxide, aka. DMSO (image, left). Chemically pure DMSO is odorless.[62] Plenty of atoms are available for chemical synthesis of DMSO from keratin: using DMSO (C_2H_6OS) to dispose of each sulfur atom extracted from ~75 atoms' worth of keratinous molecules requires 2 carbon atoms (from the ~23 C atoms available), 6 hydrogen atoms (from the ~40 H atoms available), and 1 oxygen atom (from the ~11 O atoms available). DMSO is a nontoxic solvent with a median oral lethal dose (LD50 ~ 14.5 gm/kg) that is higher than ethanol (~7.06 gm/kg) in rats,[63] and would require $t_{DMSO} = LD50\ M_{human} / m_S$ ~ 226 years of hair-trimming effluence to produce, hence is unlikely to build up to dangerous levels even in crowded rooms. One possible minor downside of DMSO is that this molecule is metabolized by disproportionation[64] to dimethyl sulfide and dimethyl sulfone which is subject to renal and pulmonary excretion, hence a possible side effect of DMSO is elevated blood dimethyl sulfide which might cause a bloodborne garlicky halitosis symptom in high enough concentrations.[65] Other non-odorous sulfur-containing molecules are also available for use.

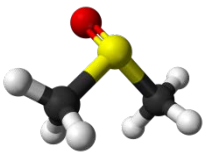

3.4.2 Mincing Protocol

An alternative to the digestion protocol described above for long hairstalks involves cutting the excess hair into tiny segments of length $L_{segment} \leq 20$ μm, creating odorless keratinous "dust" waste particles sized just below the ~20 μm visual resolution limit of the human eye (Section 3.7.2), hence invisible to the naked eye and small enough to harmlessly waft away in a gentle breeze. In this scenario, the hairbot again travels to the hairstalk apex and works backwards, progressively mincing the structure down to the desired length.

Applying the analysis of nano-morcellation systems described elsewhere,[66] cleaving a hairstalk with tensile strength[67] of 150-270 MPa (i.e., a maximum tearing strength of $T_{hairstalk}$ ~ 2.7 x 10^8 N/m^2) can be accomplished using a diamond blade with compressive strength T_{blade} ~ 5 x 10^{10}

---

[60] https://www.ncbi.nlm.nih.gov/books/NBK219999/.
[61] https://www.jasfashion.com.au/buying/buying-guides/head-n-hat-size-guide/.
[62] https://en.wikipedia.org/wiki/Dimethyl_sulfoxide#Taste.
[63] https://en.wikipedia.org/wiki/Dimethyl_sulfoxide#Toxicity.
[64] https://en.wikipedia.org/wiki/Disproportionation.
[65] https://en.wikipedia.org/wiki/Dimethyl_sulfoxide#Medicine.

[66] Freitas RA Jr. Nanomedicine, Volume I: Basic Capabilities. Landes Bioscience, Georgetown, TX, 1999, Section 9.3.5.1, "Morcellation and Mincing"; http://www.nanomedicine.com/NMI/9.3.5.1.htm.

[67] Yu Y, Yang W, Wang B, Meyers MA. Structure and mechanical behavior of human hair. Mater Sci Eng C Mater Biol Appl. 2017 Apr 1;73:152-163; http://meyersgroup.ucsd.edu/papers/journals/Meyers%20434.pdf.

N/m^2,[68] length L_{blade} = 80 μm, and cutting edge width W_{edge} = 25 nm that can apply a cutting force up to $F_{blade} \sim (L_{blade}\ W_{edge})\ T_{blade}$ = 0.1 N to a hairstalk of thickness $d_{hairstalk}$ = 80 μm, because the minimum force required to cut the stalk is $F_{min} = (L_{blade}\ W_{edge})\ T_{hairstalk}$ = 0.00054 N << F_{blade}. The chopping energy for each full blade stroke is $E_{stroke} = F_{min}\ d_{hairstalk} = 4.3 \times 10^{-8}$ J and the continuous power requirement of the blade (neglecting drag during the return stroke) is $P_{blade} = E_{stroke}\ \nu_{blade}$ = 13,000 pW where the chopping frequency ν_{blade} = 0.3 Hz and the hairstalk is completely cut through in $t_{cut} \sim 3.3$ sec after one stroke of the blade. The fleet power requirement is $P_{fleet} \sim N_{trimbots}\ P_{blade}$ = 1300 μW, again assuming a fleet of $N_{trimbots} \sim$ 100,000 nanorobots.

We require $n_{cuts} = g_{hair} / L_{segment} \sim 18$ cuts to trim away one day's growth, requiring $t_{cuts} = n_{cuts}\ t_{cut} \sim 60$ sec to complete with the expenditure of $E_{cuts} = P_{blade}\ t_{cuts} \sim 0.78$ μJ of energy which can be stored in an efficient diamondoid flywheel battery[69] of energy density $E_d \sim 90$ MJ/L and volume $V_{battery} = E_{cuts} / E_d \sim$ 9 μm^3 (<< $V_{robot} \sim$ 150,000 μm^3). Mincing one day's worth of hair growth by a 100,000 hairbot fleet costs $E_{fleet} \sim N_{trimbots}\ E_{cuts}$ = 0.078 J, which can easily be produced by onboard hairbot photoelectric collectors or by the $L_{storage}^2\ \varepsilon_{light}\ I_{light}\ t_{day} \sim 1$ J generated over the course of a day by a photocell-coated storage vessel of size $L_{storage} \sim 2.5$ mm on a side at the I_{light} ~ 5-15 W/m^2 illumination levels commonly found inside well-lighted buildings.[70]

If more than one day's growth needs to be trimmed, the mincing protocol can still be used with similar time and power requirements if we allow a single full cutline through the hairstalk, a single terminal cutting of the excess length (rather than being fully chopped), with disposal of the cutting either by nanorobot carriage to a convenient disposal site or by simple hair rinsing.

According to one expert,[71] the practice of razor-cutting hair can produce "a more textured, lived-in look while scissors will give a more blunt uniform look....Razors are used to add texture, volume, and movement to the hair. When hair is cut with a razor the ends are cut at an angle, which creates a bevel on the end of the hair strand. When hair is cut with scissors, the ends are cut perpendicular, or like a cross. The hair that has a bevel on the ends has the ability to achieve more volume because the hair can actually climb up the other strands of hair. The hair cut with scissors has a harder time balancing on the other hairs, so it tends to lay flatter."

---

[68] The calculated uniaxial ideal compressive strength of flawless diamond, using pseudopotential density functional theory, is -223.1 GPa, -469.0 GPa, and -470.4 GPa along the ⟨100⟩, ⟨110⟩, and ⟨111⟩ crystal lattice directions, respectively. Luo X, Liu Z, Xu B, Yu D, Tian Y, Wang HT, He J. Compressive Strength of Diamond from First-Principles Calculation. J Phys Chem C. 2010 Oct 21;41(114):17851-3; https://www.researchgate.net/profile/Xiaoguang_Luo/publication/225376850_Compressive_Strength_of_Diamond_From_First-Principles_Calculation/links/0fcfd5126365a800dc000000.pdf. The ~50 GPa failure strength used here was conservatively estimated as 10%-20% of the uniaxial figures and ~5% of the known 1050 GPa Young's modulus for diamond. Freitas RA Jr. Nanomedicine, Volume I: Basic Capabilities. Landes Bioscience, Georgetown, TX, 1999, Table 9.3; http://www.nanomedicine.com/NMI/Tables/9.3.jpg.

[69] Freitas RA Jr. Energy Density. IMM Report No. 50, 25 June 2019; Section 5.3.2, "Rotational Motion"; http://www.imm.org/Reports/rep050.pdf.

[70] "Lighting System Assessment Guidelines," U.S. Dept. of Energy, NREL/BR-7A20-50125, Jun 2011; https://www.nrel.gov/docs/fy11osti/50125.pdf.

[71] https://laurakcollins.com/will-a-razor-cut-be-good-for-my-hair/.

However, razor cuts can also produce split ends (Section 4.4) unless the blade is very sharp.[72] Split ends can be avoided by hairbots employing the mincing protocol applied at an angle – the beveled cut in the image at right[73] is ~100 μm in length.

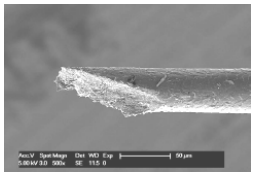

3.5 Daily Cleaning

The trim cycle (Section 3.4) can be continuous or repeated at regular intervals of the user's own choosing, though at least daily trims are recommended to maintain a consistent appearance and to keep maintenance execution time and robot fleet numbers at reasonable levels.

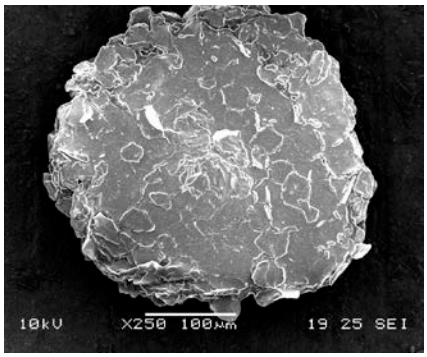

A meticulous cleaning cycle should be performed prior to preparing the initial scalp map (Section 3.1) and should also be repeated at least daily, in which the fleet of hairbots removes dirt, lint, excess oils and waxes,[74] mineral deposits from sweat or other sources, and other unwanted materials such as dandruff (electron microscope image, left),[75] from the scalp and from all hairstalks. A modest fleet of hairbots can handle normal such accumulations in reasonable execution times, but larger numbers or more time might be required in cases involving heavy deposits (e.g., large masses of mud or blood caked in the hair).

For example, the total mass of dandruff to be removed from a previously uncleaned scalp of area $A_{scalp} \sim 650\ cm^2$ that is $f_{dandruff} = 10\%$ covered with mature flakes of dandruff of diameter $d_{flake} \sim 300\ \mu m$, mean thickness $x_{flake} \sim 12\ \mu m$, and density $\rho_{flake} \sim 1.2\ gm/cm^3$ (similar to stratum corneum),[76] is $M_{dandruff} = f_{dandruff}\ A_{scalp}\ x_{flake}\ \rho_{flake} \sim 0.094$ gm, of volume $V_{dandruff} = M_{dandruff} / \rho_{flake} \sim 0.078\ cm^3$. This will require $t_{dandruff} = V_{dandruff} / N_{trimbots}\ n_{modules}\ \delta_{keratin} \sim 400$ sec (~7 min) for a fleet of $N_{trimbots} \sim 100{,}000$ digestion hairbots each with $n_{modules} \sim 2800$ digestion modules (Section 3.4.1) to consume all the dandruff flakes – assuming that dandruff (dried keratin-rich stratum corneum)[77] is sufficiently chemically similar to hairstalks to permit easy digestion by the hairbots.

---

[72] https://www.allure.com/story/razor-haircut-damage.

[73] Doll D, Luedi MM. New Attempt to Reach a Common Sense in Pilonidal Sinus Therapy. Dis Colon Rectum. 2019 Jun;62(6):e36-e38; https://boris.unibe.ch/130726/1/Doll%20Luedi_Pilonidal%20disease_DisColRect_letter_2019.pdf.

[74] In principle, such materials could be metabolized to produce energy, using oxygen drawn from the air.

[75] https://en.wikipedia.org/wiki/Dandruff#/media/File:Dandruff01.jpg.

[76] Anderson RL, Cassidy JM. Variation in physical dimensions and chemical composition of human stratum corneum. J Invest Dermatol. 1973 Jul;61(1):30-2; https://www.sciencedirect.com/science/article/pii/S0022202X15441089/pdf.

[77] https://en.wikipedia.org/wiki/Stratum_corneum.

Nanorobotic hairbots can also enable the removal of unwanted microbes and insects. In eyelashes, eyebrows, and in the hairs of the upper lip, the ears, and elsewhere on the body, dust mites measuring 150 μm x 300 μm or larger survive by chewing up dead skin cells. Epidermal-walking nanorobots must be able to identify mite surfaces to avoid climbing aboard them by mistake. Once identified, these insects can be torn apart and digested. Many other surface-dwelling ectoparasites and microfauna[78] similarly must be avoided or digested. Bacterial density over most of the body surface is quite low, ~10^3/cm^2; the count ranges from ~10^2/cm^2 on the palms and dorsa of the hands, up to 10^4-10^5/cm^2 on the hairy axilla, scalp, perineal regions, and beneath the distal end of the nail plate.[79]

After the daily cleaning cycle is completed, the scalp map should be updated if significant time has elapsed since the previous mapping. Human scalp normally sheds λ_{loss} ~ 100 hairs/day,[80] so the map builds up λ_{loss} / N_{hairs} ~0.1% error/day which should not be permitted to accumulate excessively. For example, after just one month of inattention an accumulated ~3000 hairs will have fallen out and been replaced with new hairstalks that might have grown as much as 30 g_{hair} ~ 1 cm in length and are completely unaccounted for in the scalp map.

On average, one hairshaft somewhere on the scalp falls out every $t_{hairshed}$ ~ t_{day} / λ_{loss} ~ 864 sec. Thus there is a crude probability of ($t_{scanscalp}$ + 2$t_{scanhair}$) / $t_{hairshed}$ ~ 1.6% that at least one hair of the N_{hairs} = 100,000 hairstalks being scanned during scalp mapping (Section 3.1) will fall out with a nanorobot attached to it, a probability of t_{cuts} / $t_{hairshed}$ ~ 21% that a hair being trimmed using the mincing protocol (Section 3.4.2) will fall out with a nanorobot attached to it, and an expectation that t_{digest} / $t_{hairshed}$ ~ 1 hair being trimmed using the digestion protocol (Section 3.4.1) will fall out with a nanorobot attached to it. In other words, the user can expect to lose ~1 hairbot per day, a negligible loss that is easily replaced from onboard inventory. Operationally, any hairbot that discovers it's been lost to shedding should be programmed to permanently shut down, immediately upon detecting the event. These robots should also be programmed not to digest non-human hair fibers such as wool in sweaters, polyester in shag carpets, or fur on pets.

3.6 Facial and Other Hair Trimming

Users may desire to trim or coif the hair in a few non-scalp regions of the human body.

---

[78] Knutson RM. Furtive Fauna: A Field Guide to the Creatures Who Live on You. Penguin Books, 1992; https://www.amazon.com/dp/0140153780/.

[79] Hunt TK, Dunphy JE. Fundamentals of Wound Management, Appleton-Century-Crofts, New York, 1979.

[80] Murphrey MB, Agarwal S, Zito PM. Anatomy, Hair. StatPearls [Internet], National Library of Medicine, NIH,14 Aug 2023; https://www.ncbi.nlm.nih.gov/books/NBK513312/.

Specifically, there are **~25,000** facial hairs in full beards[81] on men, plus **~420** eyelash hairs and **~600** eyebrow hairs per eye.[82] Programmed hairbots can execute microprecision trims that eliminate the need for frequent facial shaving[83] or for cosmetic eyebrow-plucking and shaping.[84] Facial hairs can have somewhat more irregular shapes, as shown by the image (left)[85] showing the cross-sectional profiles of multiple hairs taken from the center of the mustache of a Caucasian male.

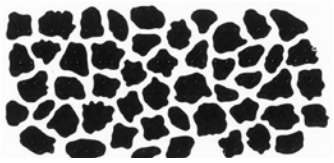

There are 10-40 hairs/cm^2 in the armpits, decreasing slowly with age.[86] Assuming ~30 cm^2 per armpit, the typical person has **~1500** axillary hairs.[87] Hairbots can keep the underarms clear of hair if this is desired by the user.[88]

The average density of human pubic hair[89] is 6-32 hairs/cm^2. Assuming ~80 cm^2 per pubis, each person has **500-2000** pubic hairs. The availability of hairbots to nanorobotically depilate the pubis in precise aesthetic patterns would spare interested users from the painful experience of bikini waxing,[90] while straightened, coifed,[91] frosted, or brightly colored pubic hair would become conveniently available.

---

[81] https://en.wikipedia.org/wiki/Beard.

[82] Amazing numbers in biology, Rainer Flindt, Springer 2006, pp. 212 table 4.2.2. See also: "Number of hairs on human head", Bionumbers, Harvard Univ.; https://bionumbers.hms.harvard.edu/bionumber.aspx?id=101509.

[83] https://en.wikipedia.org/wiki/Shaving.
[84] https://en.wikipedia.org/wiki/Eyebrow#Cosmetic_modification.

[85] Hess WM, Seegmiller RE, Gardner JS, Allen JV, Barendregt S. Human hair morphology: a scanning electron microscopy study on a male Caucasoid and a computerized classification of regional differences. Scanning Microsc. 1990 Jun;4(2):375-86, Figure 26; https://digitalcommons.usu.edu/cgi/viewcontent.cgi?article=2022&context=microscopy.

[86] Pecoraro V, Astore I, Barman JM. Growth rate and hair density of the human axilla. A. Comparative study of normal males and females and pregnant and post-partum females. J Invest Dermatol. 1971 May;56(5):362-5; https://core.ac.uk/download/pdf/82759802.pdf.

[87] https://en.wikipedia.org/wiki/Underarm_hair.
[88] https://en.wikipedia.org/wiki/Underarm_hair#Impact_of_hair_removal.

[89] Astore IP, Pecoraro V, Pecoraro EG. The normal trichogram of pubic hair. Br J Dermatol. 1979 Oct;101(4):441-5; https://pubmed.ncbi.nlm.nih.gov/508610/.

[90] https://en.wikipedia.org/wiki/Bikini_waxing.
[91] http://www.seaofstories.com/download/InteriorPages_Sample_HipSnip_24_8_9.pdf.

The thigh and calf regions[92] of the human leg have ~18 follicles/cm^2. Assuming a relevant skin area of ~2000 cm^2 per leg, each person has **~72,000** leg hairs on both legs. The availability of hairbots to depilate the legs would eliminate the unpleasant aspects of leg shaving,[93] waxing,[94] or electrolysis.[95] Some users might also wish to depilate a much smaller number of arm hairs.

The sum of the above haircounts is an additional $N_{morehairs}$ ~ 100,000 hairs, which would roughly double the number of N_{hairs} ~ 100,000 hairstalks already needing to be serviced by the existing hairbot fleet.

3.7 Nanorobot Detectability and Persistence

Will nanorobots residing or moving in the hair be physically detectable, either by the user or by outside observers?

Here we examine if hairbots traversing the skin will produce tickling or crawling sensations (Section 3.7.1), be visible to the naked eye of the user or bystanders (Section 3.7.2), be detectable by touch if the user or someone else touches the hair when nanorobots are present (Section 3.7.3), and be secure against dislodgement from the hair by external forces such as wind or human touch (Section 3.7.4).

3.7.1 Tickling or Crawling Sensations

Tickling or crawling sensations attributable to isolated nanorobots traversing the skin are unlikely. Everyday human experience tells us that skin-crawling ~2-mm ants are readily detected, whereas ambulating ≥100 μm mites are not.

Absolute epidermal minimum pressure stimulus thresholds, as measured by a laboratory esthesiometer,[96] range from a low of 2000 N/m^2 at the tongue- and finger-tip, up to 12,000 N/m^2 on the back of the hand, 26,000 N/m^2 on abdomen, 48,000 N/m^2 on the loin, and a high of 250,000 N/m^2 on the thickest part of the sole of the foot.[97] By comparison, the weight of a V_{robot} ~ 150,000 μm^3 nanorobot, if distributed across an $A_{contact} = (50\ \mu m)^2 = 2500\ \mu m^2$ contact surface, is only $M_{robot}\ g / A_{contact}$ ~ 1 N/m^2, quite undetectable on the skin, taking $M_{robot} = \rho_{robot}\ V_{robot}$ ~ 0.3 μg with mean robot density ρ_{robot} ~ 2 gm/cm^3.

---

[92] Otberg N, Richter H, Schaefer H, Blume-Peytavi U, Sterry W, Lademann J. Variations of hair follicle size and distribution in different body sites. J Invest Dermatol. 2004 Jan;122(1):14-9; https://www.sciencedirect.com/science/article/pii/S0022202X15306291.

[93] https://en.wikipedia.org/wiki/Leg_shaving.
[94] https://en.wikipedia.org/wiki/Waxing.
[95] https://en.wikipedia.org/wiki/Electrology.
[96] https://en.wikipedia.org/wiki/Esthesiometer.

[97] Woodworth RS, Schlosberg H. Experimental Psychology, Revised Edition, Holt, Rinehart & Winston, New York, 1954.

At a velocity of v_{bot} = 10 cm/sec, the inertial force required to propel an L_{robot} = 50 μm nanorobot of mean density ρ_{robot} ~ 2 gm/cm^3 is $F_{inertial} \sim \rho_{robot}\ v_{bot}^2\ L_{robot}^2$ ~ 50 nN.[98] This additional force, if distributed over 5 footpads each of area 10 μm x 10 μm = 100 μm^2, gives a shear pressure of ~100 N/m^2 across all contact surfaces, also undetectable.

Finally, skin sensor frequency response is typically << 1000 Hz,[99] whereas a skin walking hairbot may employ ν_{leg} ~ 1000 Hz leg motions (Section 3.1), well exceeding the maximum frequency response of human skin sensors. The ~2500/cm^2 of low-threshold mechanoreceptors in the scalp[100] can detect hair deflection stimuli as light as **0.5-2 mN** of force.[101] A hairbot with the power density P_D ~ 0.032 MW/L of a microbivore[102] and volume V_{robot} ~ 150,000 μm^3 would have a total robot power of P_{robot} ~ 4.8 μW which, even if wholly applied to producing motion at v_{bot} ~ 10 cm/sec, could only generate a force as high as $F_{bot} \sim P_{robot}/v_{bot}$ ~ **0.05 mN** – an order of magnitude below the threshold of detection for human tactile sensors in the skin and hair.

3.7.2 Visibility of Nanorobots on Hairstalks

Are nanorobots in the 50-100 μm size range, parked or traversing human hair strands, visible to the human naked eye? After all, typical household dust mites,[103] due to their small size (200-300 μm in length) and translucent bodies, are barely visible to the unaided human eye.

Ideally, the upper limit on robot size should normally be just below the lower limit of human visual acuity at maximum contrast (e.g., black particles against a solid white background). Normal "20/20" or "6/6" acuity corresponds to distinguishing black-on-white contours 1.75 mm apart at a distance of 6 meters,[104] or about 1 minute of arc. If the minimum distance that a human eye can focus (i.e., the maximum accommodation distance)[105] is d_{accomm} = 6.5 cm from the eye of a young person, then the minimum distinguishable size would be (6.5 cm / 6 m) (1750 μm) = **19 μm**.

---

[98] Freitas RA Jr. Nanomedicine, Volume I: Basic Capabilities, Landes Bioscience, Georgetown TX, 1999, Section 9.4.2.1, "Reynolds Number"; http://www.nanomedicine.com/NMI/9.4.2.1.htm.

[99] Freitas RA Jr. Nanomedicine, Volume I: Basic Capabilities, Landes Bioscience, Georgetown TX, 1999, Table 7.3, "Tactile Receptors in the Human Skin"; http://www.nanomedicine.com/NMI/Tables/7.3.jpg.

[100] https://www.renefurterer.com/en-ca/tips/scalp/the-physiology-of-the-scalp.

[101] Handler A, Ginty DD. The mechanosensory neurons of touch and their mechanisms of activation. Nat Rev Neurosci. 2021 Sep;22(9):521-537; https://www.ncbi.nlm.nih.gov/pmc/articles/PMC8485761/.

[102] Freitas RA Jr. Energy Density. IMM Report No. 50, 25 June 2019; Chapter 1, "Introduction"; http://www.imm.org/Reports/rep050.pdf.

[103] https://en.wikipedia.org/wiki/House_dust_mite.
[104] https://en.wikipedia.org/wiki/Visual_acuity#Definition.
[105] https://en.wikipedia.org/wiki/Accommodation_(vertebrate_eye).

The resolution of the human eye is constrained by the diffraction limit[106] which can be approximated by $\theta_{object} \approx 1.22\ \lambda_{light} / D_{pupil} = 1.2\text{-}4.3 \times 10^{-4}$ rad = 0.41-1.5 arcmin, where θ_{object} is the angular size of the object under scrutiny, the wavelength of visible light is λ_{light} = 400-700 nm, and the diameter of the human eye pupil aperture (as regulated by the iris) under normal daytime lighting conditions is D_{pupil} = 2-4 mm.[107] This corresponds to a minimum visible object size of $x_{visible} = d_{accomm}\ \theta_{object}$ = **8-28 µm** (at 400-700 nm wavelengths) for a young child with excellent visual acuity with d_{accomm} = 6.5 cm, or $x_{visible}$ = **30-108 µm** for normal adult eyes with d_{accomm} = 25 cm for comfortable viewing.[108] Also note that incoming light must strike two separate cone cells in the human eye in order for the brain to register separate pixels; cones in the densest center of the fovea centralis are spaced about x_{cone} = 2 µm apart[109] and the diameter of the human eye in the front-to-back direction is $D_{eyeball}$ ~ 24 mm,[110] hence by simple geometry $\theta_{object} \sim x_{cone} / D_{eyeball} = 8.3 \times 10^{-5}$ rad, giving $x_{visible} = d_{accomm}\ \theta_{object}$ = **21 µm** for normal adult eyes with d_{accomm} ~ 25 cm (at age 45)[111] in normal daytime lighting conditions.

Of course, dark-adapted rod cells in human eyes can detect individual photons of light,[112] and the naked human eye can see objects of any size that glow (emit light),[113] or objects as small as **10 µm** that scatter enough light (e.g., bubbles or transparent particles that scatter sunlight)[114] to trigger the eye's detector cells. Notes one author: "Light visible from the star Deneb covers a minuscule fraction of your visual field (its 'angular diameter' is 0.0024 arcsec) – a light-emitting object, seen as the same size when 15 cm from your face, would be 1.75 nanometers wide. What is limited is the eye's resolution: how close two objects can become before they blur into one. At absolute best, humans can resolve two lines about 0.01 degrees apart: a **26 µm** gap, if positioned 15 cm from your face. In practice, objects **40 µm** wide (the width of a fine human hair) are just distinguishable by good eyes, objects **20 µm** wide are not." [115]

We conclude that nanorobots resident in human hair should exhibit no externally visible features larger than ~20 µm in any dimension with high visual contrast relative to their surroundings if they are to remain "invisible" to human eyes under normal daytime lighting conditions. The hairbots described earlier have dimensions in the 50-100 µm size range, so maintaining optical

---

[106] http://hosting.astro.cornell.edu/academics/courses/astro201/diff_limit.htm.
[107] https://en.wikipedia.org/wiki/Pupil#Effect_of_light.
[108] https://www.quora.com/Vision-eyesight-What-is-the-smallest-thing-a-human-eye-can-see-and-why.
[109] https://en.wikipedia.org/wiki/Fovea_centralis.
[110] https://en.wikipedia.org/wiki/Human_eye#Size.
[111] https://zenodo.org/records/1529034/files/article.pdf.

[112] Tinsley JN, Molodtsov MI, Prevedel R, Wartmann D, Espigulé-Pons J, Lauwers M, Vaziri A. Direct detection of a single photon by humans. Nat Commun. 2016 Jul 19;7:12172; https://www.ncbi.nlm.nih.gov/pmc/articles/PMC4960318/. See also: https://www.nature.com/news/people-can-sense-single-photons-1.20282.

[113] The human brain will only register a detection event 4-10 times out of 100 photon impacts on a photoreceptor cell. https://www.quora.com/Vision-eyesight-What-is-the-smallest-thing-a-human-eye-can-see-and-why and http://math.ucr.edu/home/baez/physics/Quantum/see_a_photon.html.

[114] https://www.me.psu.edu/cimbala/me405/Lectures/Slides_Particles.pdf.
[115] https://www.sciencefocus.com/the-human-body/how-small-can-the-naked-eye-see/.

invisibility requires that nanorobot exterior surfaces should display no high-contrast patches (relative to the color of the user's hair) that are larger than ~20 μm. This can be accomplished via chromatic modification[116] of key portions of the nanorobots' outermost surfaces.[117]

For example, frequency-selective absorbers or emitters can be placed in patches below thin transparent diamondoid windows on the robot surface. Active manipulation of covershades to block or expose these windows permits rapid modulation of chromatic surface characteristics. One such colorant material is sapphire, which can be manufactured in a full spectrum of blues, pinks, yellows, oranges, teals, lavenders, greens, grays, whites, and all intermediate hues. More colors with greater intensity exist with sapphires than with almost any other mineral. This broad color palette is achieved by replacing aluminum atoms with ~0.1% iron atoms and ~0.01% titanium atoms. Rubies, also corundum crystals, achieve their vivid reds by replacing a few aluminum atoms with atoms of chromium. A wide variety of organic colorants such as rhodopsin, fluorescein, carotenoids, luciferins, or engineered porphyrins might also be used. A basic color palette should ensure that hairbot color sufficiently matches the user's hair color to ensure static invisibility of the nanorobots. Another important design consideration is photochemical stability, especially for nanodevices that must operate in open sunlight or near other sources of ultraviolet (UV) radiation. To avoid photochemical damage, such devices may require a UV-opaque surface or components purposely designed for photochemical stability.

Color may also be created and dynamically manipulated by embedding micron-scale light-emitting solid-state lasers in the surface. For a surface to appear a certain color, embedded monochromatic optical lasers must emit light of sufficient brightness to compete with other illuminated surfaces that may be present in the visual field. The required intensity[118] is probably ~1 watt/m^2 or ~1 pW/μm^2 – a feasible energy emission budget for micron-scale nanorobots. Even decades ago, Shen[119] had constructed 0.86-μm thick three-color electrically-tunable organic light-emitting devices[120] which generated ~0.5 pW/μm^2 with ~1% energy efficiency; red-only LEDs had achieved efficiencies up to 16%,[121] and larger diode lasers had achieved up to 60%-66%

---

[116] Freitas RA Jr. Nanomedicine, Volume I: Basic Capabilities, Landes Bioscience, Georgetown TX, 1999, Section 5.3.7, "Chromatic Modification"; http://www.nanomedicine.com/NMI/5.3.7.htm.

[117] Hairbots could also be designed with a longer and thinner body, running parallel to the hairstalk, to assist in maintaining invisibility.

[118] Freitas RA Jr. Nanomedicine, Volume I: Basic Capabilities, Landes Bioscience, Georgetown TX, 1999, Section 4.9.4, "Optical Macrosensing"; http://www.nanomedicine.com/NMI/4.9.4.htm.

[119] Shen Z, Burrows PE, Bulovic V, Forrest SR, Thompson ME. Three-color, tunable, organic light-emitting devices. Science 1997 Jun 27; 276(5321):2009-2011; https://citeseerx.ist.psu.edu/document?repid=rep1&type=pdf&doi=eb87ac0c9885152aae197c873582017e0d3a74f4.

[120] Sheats JR, Antoniadis H, Hueschen M, Leonard W, Miller J, Moon R, Roitman D, Stocking A. Organic Electroluminescent Devices. Science. 1996 Aug 16;273(5277):884-8; https://pubmed.ncbi.nlm.nih.gov/8688062/.

[121] Morkoç H, Mohammad SN. High-luminosity blue and blue-green gallium nitride light-emitting diodes. Science. 1995 Jan 6;267(5194):51-5; https://pubmed.ncbi.nlm.nih.gov/17840057/.

efficiencies.[122] Conventional organic light-emitting devices (OLEDs) using small organic molecules can have high brightness (2-4 pW/μm^2), lifetimes of >4000 hours, and can be made with a wide range of emission colors in a ~300 nm thick sandwich,[123] with white-light organic electroluminescent devices ~100 nm thick producing ~3 pW/μm^2 at 15 volts,[124] typically with 0.1%-1% energy efficiency.[125]

One additional consideration is the existence of separate visual acuity limits for otherwise visible objects that are in lateral motion across the field of view. In one experiment,[126] moving objects were foveally detected when they displaced 0.68 arcmin (near the human visual limit) at an angular velocity of $\theta_v \geq 0.001$ rad/sec, implying a maximum velocity limit on the locomotion of nanorobots seeking to remain unnoticed of $v_{visible} = d_{accomm}\ \theta_v =$ **0.25 mm/sec** at the closest viewing distance of $d_{accomm} = 25$ cm for normal adults. As another example, visual fixation[127] on a scene is interrupted by frequent saccades of the human eye, and a saccade in response to an unexpected stimulus normally takes $t_{initsac} \sim 200$ ms to initiate.[128] If object motion must be detected during the period of pre-saccade fixation, then an $x_{visible} = 20$ μm motion at a viewing distance of $d_{accomm} = 25$ cm represents a $\theta_{object} = x_{visible} / d_{accomm} = 8 \times 10^{-5}$ rad angular displacement, giving an angular velocity of $\theta_v = \theta_{object} / t_{initsac} = 4 \times 10^{-4}$ rad/sec during the 200 ms period of pre-saccade fixation and $v_{visible} = d_{accomm}\ \theta_v = x_{visible} / t_{initsac} =$ **0.10 mm/sec** at the closest viewing distance of $d_{accomm} = 25$ cm for normal adults. Further research is needed to confirm whether nanorobots with static invisibility might become visible when they move too fast.

---

[122] Welch D, Craig R, Streifer W, Scifres D. High reliability, high power, single mode laser diodes. Electronics Lett. 1990 Aug 30;26(18):1481-1482; https://www.infona.pl/resource/bwmeta1.element.ieee-art-000000058105. Botez D, Mawst LJ, Bhattacharya A, Lopez J, Li J, Kuech TF, Iakovlev VP, Suruceanu GI, Caliman A, Syrbu AV. 66% CW wallplug efficiency from Al-free 0.98 micron-emitting diode lasers. Electronics Lett. 1996 Oct 10;32(21):2012-2013; https://digital-library.theiet.org/content/journals/10.1049/el_19961300.

[123] Aziz H, Popovic ZD, Hu NX, Hor AM, Xu G. Degradation mechanism of small molecule-based organic light-emitting devices. Science. 1999 Mar 19;283(5409):1900-2; https://pubmed.ncbi.nlm.nih.gov/10082460/.

[124] Kido J, Kimura M, Nagai K. Multilayer white light-emitting organic electroluminescent device. Science. 1995 Mar 3;267(5202):1332-4; http://fuuu.be/polytech/LANGH300/LED/Multilayer%20White%20Light-Emitting%20Organic%20Electroluminescent%20Device.pdf.

[125] Granström M, Berggren M, Inganäs O. Micrometer- and nanometer-sized polymeric light-emitting diodes. Science. 1995 Mar 10;267(5203):1479-81; https://pubmed.ncbi.nlm.nih.gov/17743547/.

[126] Lappin JS, Tadin D, Nyquist JB, Corn AL. Spatial and temporal limits of motion perception across variations in speed, eccentricity, and low vision. J Vis. 2009 Jan 22;9(1):30.1-14; https://jov.arvojournals.org/arvo/content_public/journal/jov/932855/jov-9-1-30.pdf.

[127] https://en.wikipedia.org/wiki/Fixation_(visual).

[128] https://en.wikipedia.org/wiki/Saccade#Timing_and_kinematics.

3.7.3 Can Nanorobots be Detected by Touch?

If you run your hand through hair that has nanorobots on it, could you feel them as little bumps? The spatial resolution of touch (human tactile sensitivity) on the skin is most sensitive on fingertips and is often cited as ~2 mm,[129] given the ~1 mm separation between receptor field centers, though careful studies of the interactions of tactile neurons with dermal papillary ridges (i.e., fingerprints) suggest a subfield sensitivity as low as ~400 μm.[130]

The author acquired a calibrated set of diamond grit particles from Crystalite Corp.[131] and observed that when rubbed between thumb and forefinger (one of the most touch-sensitive areas of the human body), 25 μm particles feel entirely smooth to the touch, 44 μm particles give at most the slightest hint of roughness, and 60 μm particles feel only slightly gritty. This is consistent with the neuronal thresholds for pressure and edge detection SA I type receptors (Merkel's cells and tactile disks) of 60-100 μm on the human hand, though in special cases dislocations as small as 10 μm can be detected.[132] The palms are much less sensitive than the fingertips, having almost ten times fewer receptors/cm^2.

The conclusion is that the presence of ~50 μm hairbots in human hair may be just barely detectable by the human hand or fingers but should not feel unpleasantly gritty to the touch.

3.7.4 Nanorobot Dislodgement

If wind or water blows through the hair, or if fingers, combs or brushes are dragged through a coiffure, will nanorobots present on the hairstalks be dislodged?

Wind traveling at hurricane speeds[133] of v_{wind} = 33 m/sec (~74 mph) consisting of 273 K sea level air of density ρ_{air} = 1.29 kg/m^3 that encounters a hairbot of frontal area πR_{robot}^2 applies a dislodgement force of $F_{wind} \sim \pi R_{robot}^2 \rho_{air} v_{wind}^2$ = **2.76 μN**. Water of density ρ_{water} = 1 gm/cm^3 that flows through a hairbot-laden coiffure at the fastest Olympic swimming speed[134] of v_{swim} = 2.29 m/sec would apply a dislodgement force of $F_{swim} \sim \pi R_{robot}^2 \rho_{water} v_{swim}^2$ = **10.3 μN**. Water

---

[129] Sherman WR, Craig AB. Understanding Virtual Reality. Morgan Kaufmann, 2nd Edition, 2019; https://www.amazon.com/Understanding-Virtual-Reality-Interface-Application/dp/0128183993.

[130] Jarocka E, Pruszynski JA, Johansson RS. Human Touch Receptors Are Sensitive to Spatial Details on the Scale of Single Fingerprint Ridges. J Neurosci. 2021 Apr 21;41(16):3622-3634; https://www.ncbi.nlm.nih.gov/pmc/articles/PMC8055081/.

[131] Crystalite Corp.; https://www.abrasive-tech.com/.

[132] Johansson RS, Vallbo AB. Tactile sensory coding in the glabrous skin of the human hand. Trends Neurosci. 1983 Jan; 6(1):27-32; https://www.cns.nyu.edu/~bijan/courses/sm10/Readings/Johansson1983.pdf.

[133] https://www.nhc.noaa.gov/aboutsshws.php.
[134] https://hypertextbook.com/facts/2000/NoahKalkstein.shtml.

blown at hurricane speed in a storm could apply episodic dislodgement forces as large as $F_{hurricane} \sim \pi R_{robot}^2 \rho_{water} v_{wind}^2$ = **2140 μN**.

A hand of area $A_{palm} \sim 100$ cm^2 that presses down on the coiffure with a modest force of $W_{hand} \sim 10$ N (~1 kg) applies a dislodgement force of $F_{hand} \sim \pi R_{robot}^2 W_{hand} / A_{palm}$ = **1.96 μN**. A similar force of $W_{finger} = 10$ N applied between thumb and forefinger of contact area $A_{contact} \sim 5$ cm^2 could raise the dislodgement force to $F_{fingers} \sim \pi R_{robot}^2 W_{finger} / A_{contact}$ = **39.3 μN**.

If a hairbrush with ~1000 bristles contacts $n_{haircontact} \sim 5{,}000$ individual hairs as it is dragged through a coiffure applying a total force of $W_{hairbrush} \sim 1$ N, well below the $W_{pain} \sim 10$ N threshold of pain for tangled hair as determined experimentally using a sensorized robotic hairbrush,[135] then the dislodgement force applied to a robot on each hair is at most $F_{brush} \sim W_{hairbrush} / n_{haircontact}$ = **200 μN**.

It has previously been estimated that hairbot arms can generate a towing force of $F_{robot} \sim$ **10 μN** (Section 4.2) and a cutting force of $F_{min} \sim$ **540 μN** (Section 3.4.2). Applying a dislodgement-resisting hairstalk-clasping force up to $F_{grip} \sim$ **2000 μN** over an $x_{grip} = 25$ μm clasping distance requires an energy of $E_{grip} = x_{grip} F_{grip} \sim 0.05$ μJ. This amount of energy can be stored in an efficient diamondoid flywheel battery[136] of maximum energy density $E_d \sim 90$ MJ/L (9×10^{10} J/m^3) and onboard battery volume $V_{battery} = E_{grip} / E_d \sim 0.56$ μm^3 ($<< V_{robot} \sim 150{,}000$ μm^3), most of which can be recovered and recycled using an efficient regenerative energy recovery system.[137]

The upper limit of nanorobot clasping force is driven by the need to avoid crushing the hairstalk: If two hairbot arms of length $L_{robotarm} \sim 100$ μm and diameter $D_{robotarm} = 2R_{robotarm} = 10$ μm must restrict the grasping pressure they can apply in clinging to the hairstalk to the $Y_{stress} = 109$ MPa yield stress of human hair,[138] then the maximum grasping force they can be allowed to apply is $F_{grasp} \sim L_{robotarm} \ D_{robotarm} \ Y_{stress}$ = **100,000 μN**.

The above estimates suggest that nanorobots can be designed to provide sufficient grasping force to avoid dislodgement by reasonably anticipated external forces (such as wind gusts, ocean swimming, or vigorous water rinsing with detergents) without damaging the hairstalks.

---

[135] Hughes J, Plumb-Reyes T, Charles N, Mahadeven L, Rus D. Detangling hair using feedback-driven robotic brushing. Proceedings of the 4th IEEE International Conference on Soft Robotics (RoboSoft), 2021, pp. 487-494; https://par.nsf.gov/servlets/purl/10294692.

[136] Freitas RA Jr. Energy Density. IMM Report No. 50, 25 June 2019; Section 5.3.2, "Rotational Motion"; http://www.imm.org/Reports/rep050.pdf.

[137] https://en.wikipedia.org/wiki/Regenerative_braking#KERS_flywheel.

[138] Kunchi C, Venkateshan KC, Reddy ND, Adusumalli RB. Correlation between Mechanical and Thermal Properties of Human Hair. Int J Trichology. 2018 Sep-Oct;10(5):204-210; https://www.ncbi.nlm.nih.gov/pmc/articles/PMC6290292/.

4. Nanorobotic Hair Extension

If the user chooses a coiffure that requires some or all of their hair to be longer than its present length, then hair extensions made of chemically similar keratinous materials may be added to the existing hairstalks to lengthen them. After the desired coiffure has been selected (Section 3.3), the user's personal computer calculates the number and length of all the hair extension strands that must be added to each of the existing N_{hairs} = 100,000 hairstalks currently anchored to the user's scalp. For hairstalks that are too short, a small desktop nanofactory called a "hair mill" (Section 4.1) that is optimized for hair fabrication is used to manufacture up to $N_{strands}$ ~ 100,000 synthetic extension strands. Each strand is numbered with a specific length such that when bonded to the existing hairstalk the combined result will be the correct length for the selected coiffure. In the standard extension protocol, hairbots drag each extension strand to the apex of the target natural hairstalk (Section 4.2) and then permanently attach the new synthetic strand to the existing hairstalk (Section 4.3), thus extending the hairstalk to the desired length.

For each existing hairstalk that requires lengthening, the cross-sectional face of the terminal apex should be preworked by the methods described in Section 3.4 to be sufficiently microscopically flat or otherwise appropriately featured to allow facile joining with the engineered attachment face of the extension strand that has been fabricated by the hair mill. In the case where an existing hairstalk has a damaged terminus (Section 4.4), the trunk should be trimmed back to the nearest fully intact section with the synthetic extension strand extended sufficiently to recover the desired post-attachment hair length.

4.1 Hair Mill

Consider the worst-case challenge of adding L_{strand} = 30 cm of length to every hairstalk on the scalp. This will require the fabrication of up to $V_{AllStrands} = (\pi/4)\, d_{hairstalk}^2\, L_{strand}\, N_{strands}$ = 151 cm^3 of synthetic hair of mass $M_{AllStrands} = \rho_{hair}\, V_{AllStrands}$ ~ 199 gm, taking the density of dry human hair as ρ_{hair} ~ 1.32 gm/cm^3.

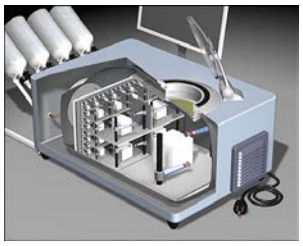

The classical desktop **nanofactory**[139] (image, right) is estimated to have a volume of $V_{nanofactory}$ ~ 50 L and to produce $m_{product}$ ~ 1 kg/hr of atomically-precise nonbiological products with a power draw of $P_{nanofactory}$ ~ 1300 W. Similarly, a **cell mill**[140] that produces $m_{product}$ ~ 1 kg/hr of atomically-precise biological products that are fully

---

[139] Drexler KE. Nanosystems: Molecular Machinery, Manufacturing, and Computation. John Wiley & Sons, New York, 1992, Section 14.4.3; https://www.amazon.com/dp/0471575186/. Freitas RA Jr., Merkle RC. Kinematic Self-Replicating Machines. Landes Bioscience, Georgetown, TX, 2004; http://www.MolecularAssembler.com/KSRM.htm.

[140] Freitas RA Jr. Cryostasis Revival: The Recovery of Cryonics Patients through Nanomedicine. Alcor Life Extension Foundation, Scottsdale AZ, 2022; Appendix D "Cell Mills"; https://www.alcor.org/cryostasis-revival/.

biocompatible with the user's body is estimated to have a volume of $V_{hairmill}$ ~ 100 L with a power draw of $P_{hairmill}$ ~ 5000 W.

Fabricating non-living hair strands is intermediate in complexity between manufacturing nonbiological products and manufacturing the full range of human biological materials. Therefore, an exemplar "hair mill" – a nanofactory specialized for efficient keratinous molecular manufacturing – might require $t_{synthhair}$ ~ 10,000 sec (~3 hr) to manufacture $N_{strands}$ ~ 100,000 synthetic hairstalk extension strands of total mass $M_{AllStrands}$ ~ 199 gm with a device volume of $V_{hairmill} = (M_{AllStrands} / m_{product}\ t_{synthhair})\ [(V_{nanofactory} + V_{hairmill}) / 2]$ ~ 5 L – a box ~17.1 cm (6.7 inches) on a side – while consuming $P_{hairmill} \sim (M_{AllStrands} / m_{product}\ t_{synthhair})\ [(P_{nanofactory} + P_{hairmill}) / 2]$ ~ 209 W of power. Several replaceable "toner cartridges" each containing a few fluid ounces of simple chemicals must be plugged into the hair mill to provide the basic molecular feedstock needed to fabricate the synthetic hair extensions, which can be manufactured with virtually any curl or color pattern.

Note that the choice of L_{strand} = 30 cm of length and $N_{strands}$ ~ 100,000 in this example is entirely arbitrary. Fabricating a lesser number of shorter hair strands would require less time, and vice versa. Similarly, using a larger hair mill would allow the same amount of hair to be produced faster, or more hair to be produced in the same amount of time. Also, the hair mill should be able to manufacture hair extensions of any desired length (image, right),[141] making possible a reenactment of the famous German legend of Rapunzel[142] with her ~20 meter long hair.[143]

The hair mill appliance should also include a comfortable chair and headrest attachment that can cradle the seated user's head during the hair extension procedure. This attachment must include a hair transfer mechanism that allows individual numbered extension strands fabricated by the hair mill to be efficiently presented to the hairbots that are performing the extension procedure at the user's scalp.

4.2 Standard Extension Protocol

A synthetic hair extension strand L_{strand} = 30 cm long and $d_{hairstalk}$ = 80 μm in diameter has a volume of $V_{strand} = (\pi/4)\ d_{hairstalk}^{\ 2}\ L_{strand}$ = 1510 x 10^6 μm^3 and mass $M_{strand} = V_{strand}\ \rho_{hair}$ = 1.99 x 10^{-6} kg and strand weight $W_{strand} = M_{strand}\ g$ = 6.51 x 10^{-6} N = **19.5 μN**. The force required to drag the aforementioned strand of hair horizontally across a dry scalp covered with dry hair may be crudely estimated as $F_{drag} \sim \mu_{drag}\ W_{strand}$ = **7.83 μN**, provisionally taking the hair-on-hair

---

[141] https://en.wikipedia.org/wiki/Hair#/media/File:Marianne_Ernst,_Long_hair_model.jpg.
[142] https://en.wikipedia.org/wiki/Rapunzel.

[143] The 2024 world record for the longest human hair was held by Xie Qiuping from China, whose hair had reached 5.6 meters after 31 years of uninterrupted growth; https://www.hairknowhow.com/longest-hair.

coefficient of friction as $\mu_{drag} \sim 0.4$.[144] (For comparison, the skin-on-skin[145] and hair-on-hair[146] coefficients of friction have been reported as 0.3-0.7 and 0.3-0.5, respectively, under dry conditions.) A hairbot robot with available towing power $P_{robot} \sim 10{,}000$ pW that travels at $v_{bot} \sim 1$ mm/sec can apply a towing force of $F_{robot} \sim P_{robot} / v_{bot} \sim$ **10 μN**. The apparent power density of the hairbot robot during strand towing is $P_{robot} / V_{robot} \sim$ **8×10^{-5} MW/L**, not much more than a passenger car (1.5×10^{-5} MW/L) or a mature desktop nanofactory (2.6×10^{-5} MW/L), well below the 10^{-1}-10^{-3} MW/L range estimated for medical nanorobots, and well within the 10^{-3}-10^{-7} MW/L range of biological cells.[147] (As an additional scaling validation, note that telescoping nanorobotic manipulators 30 nm wide and 100 nm in length may dissipate ~**1 MW/L** in continuous operation at a ~1 cm/sec arm speed.[148] The equivalent of ~10,000 such manipulators could apply the requisite ~**10 μN** of force but would have a collective volume of only ~1 $\mu m^3 << V_{robot}$.)

Is it reasonable to suggest that one hairbot of mass $M_{robot} = \rho_{robot} V_{robot} \sim 0.3$ μg, taking mean robot density as $\rho_{robot} \sim 2$ gm/cm^3, can tow a single synthetic hair extension strand of mass $M_{strand} = 1990$ μg which is $\gamma_{hairbot} = M_{strand} / M_{robot} \sim 6600$ times the weight of the robot? The cross-sectional area of muscles in animals (or actuators in robots) and other structures that can transport a weight scales as $\sim L^2$ and the mass that produces the weight to be transported scales as $\sim L^3$, so the amount of weight a device can carry scales very roughly as ~L, the characteristic size of the system.[149]

Thus an ant of length $L_{ant} \sim 1$ cm carrying $\gamma_{ant} \sim 30$ times its own weight (image, left)[150] is equivalent to an $L_{human} \sim 180$ cm (6 ft) tall ~70 kg human carrying $\gamma_{ant} (L_{ant} / L_{human}) \sim 18\%$ of their own weight, or ~12

---

[144] Synthetic keratinous hair strands can be manufactured by hair mills to have unusually smooth external surfaces that minimize the coefficient of friction.

[145] Chen CY, Yu CA, Hong TF, Chung YL, Li WL. Contact and frictional properties of stratum corneum of human skin. Biosurf Biotribol. 2015 Mar; 1(1):62-70; https://core.ac.uk/download/pdf/82484139.pdf.

[146] Chevalier NR. Hair-on-hair static friction coefficient can be determined by tying a knot. Colloids Surf B Biointerfaces. 2017 Nov 1;159:924-928; http://nicochevalier.net/wp-content/uploads/2017/09/2017-NChevalier-Hair-on-Hair-Friction.pdf.

[147] Freitas RA Jr. Energy Density. IMM Report No. 50, 25 June 2019; Table 3 "Power Density of Natural Systems"; http://www.imm.org/Reports/rep050.pdf.

[148] Freitas RA Jr., Nanomedicine, Volume I: Basic Capabilities, Landes Bioscience, Georgetown, TX, 1999, Section 9.3.1.4, "Telescoping Manipulators"; http://www.nanomedicine.com/NMI/9.3.1.4.htm. Drexler KE. Nanosystems: Molecular Machinery, Manufacturing, and Computation, John Wiley & Sons, New York, 1992, pp. 406-7; http://e-drexler.com/d/09/00/Drexler_MIT_dissertation.pdf.

[149] https://en.wikipedia.org/wiki/Square%E2%80%93cube_law.
[150] https://www.terminix.com/ants/behavior/how-much-can-an-ant-lift/.

kg (26 lbs) – the typical weight of a backpack for a multi-day hiking trip.[151] Similarly, an $L_{robot} \sim 2R_{robot} = 50$ μm long nanorobot carrying $\gamma_{hairbot}$ times its own weight is also equivalent to a human carrying $\gamma_{hairbot}$ (L_{robot} / L_{human}) ~ 18% of their own weight, or about 12 kg (~26 lbs). This seems quite reasonable, even conservative.

4.3 Attaching the Hair Extensions

After dragging the extension strand to the end of its assigned hairstalk on the scalp, the principle task of the multi-armed hairbot is to securely mate the engineered attachment face of the extension strand of area $A_{attachment} \sim (\pi/4)\ d_{hairstalk}^{\ 2} \sim 5000\ \mu m^2$ to the prepared face of the terminal apex of the hairstalk that requires lengthening, assumed to be essentially identical in area and shape. The interface must provide at least as much resistance to breakage by tensile forces as natural hair, and the surfaces to be mated should be prepared consistent with the chosen adhesion method, of which at least four have been identified, as follows:

(1) **Adhesive Bonding.** The hairbot could apply to the flat mating faces a biocompatible adhesive that can strongly bond keratin while not adding significant bulk. Cyanoacrylate-based glues[152] are biocompatible when used on the skin or for closing wounds in place of sutures, and have found use in eyelash[153] and other hair[154] extension procedures, but fiber or other additives might be required for hairbot use to ensure suitable flexibility and durability of the bond under typical long-term conditions to which hair is subjected such as washing, brushing, and environmental exposure. Silicone-based adhesives are also used in medical devices, applications involving biocompatible skin contact, and adhesives for hairpieces,[155] thus might provide a flexible bond more suitable for hair that must withstand bending and flexing. Protein-based adhesives can bond to the keratin in human hair – e.g., keratin glues[156] formulated to provide a strong, long-lasting attachment while also being gentle on the hair and scalp – and other keratin-derived adhesives such as hoof glue[157] are used as a coating to stiffen and strengthen cordage on chair backs and seats (though unsuitable for hairbots because it is water-soluble). The hairbot would need to include an internal reservoir of unactivated adhesive material and a means for evenly distributing and activating it on site, of volume $V_{adhesive} \sim x_{adhesive}\ A_{attachment} \sim 25{,}000\ \mu m^3 \sim 20\%\ V_{robot}$, assuming an adhesive thickness of $x_{adhesive} \sim 5$ μm between the two attachment faces.

---

[151] A common rule of thumb used in the hiking community is the 20% body weight rule, which suggests that your pack should weigh no more than 20% of your body weight; https://longwhitegypsy.com/backpacking-weight-calculator/.

[152] https://en.wikipedia.org/wiki/Cyanoacrylate.
[153] https://www.wholesalelashextensions.com/blank-5/cyanoacrylate-in-eyelash-glue-why-do-some-clients-develop-an-allergy.

[154] Skaryd P, Skaryd N. Method of elongating hair. US Patent 5,082,010, 21 Jan 1992; https://patents.google.com/patent/US5082010A/en. Spann CH. Hair extension and thickening process. US Patent 5,868,145, 9 Feb 1999; https://patents.google.com/patent/US5868145A/en.

[155] https://www.amazon.com/dp/B08K1B3M.
[156] https://www.amazon.com/dp/B07WN1LGPH.
[157] https://en.wikipedia.org/wiki/Hoof_glue.

(2) **Polymerization.** Covalent cross-linking of the keratin molecules on either side of the interface might be initiated and accelerated by chemical or enzymatic means, effectively "welding" the hairs at a molecular level. For example, mild oxidizing agents such as iodine, hydrogen peroxide, and dimethyl sulfoxide can promote the formation of disulfide bonds between the cysteine residues in keratin.[158] Enzymes such as protein disulfide isomerase (PDI) can facilitate disulfide bond formation.[159] The manufacture of extra-cysteine-rich keratin extension strands could further increase polymerizability.

(3) **Mechanical Interlocking.** Similar to the principles of Velcro[160] in fabric engineering and dovetail joints[161] in woodworking, or drywall anchors[162] and molly bolts[163] in construction, microscale or even molecular-scale[164] features could be designed and embedded in both attachment faces to facilitate a permanent mechanical interlock that cannot easily be pulled apart.

(4) **Ultrasonic Welding.** Ultrasonic vibrations could be applied to the interface to generate rapid highly localized heating that melts and fuses the two faces together. The energy required to melt a keratin interface zone of depth x_{melt} = 1 μm starting from room temperature T_{room} ~ 300 K is $E_{melt} \sim [\Delta H_{dryhair} + (T_{melt} - T_{room}) C_{keratin}] \rho_{hair} x_{melt} A_{attachment}$ = 0.304 μJ, taking hair density ρ_{hair} ~ 1.32 gm/cm^3 and $A_{attachment}$ = 5000 μm^2, a dry-hair keratin melting point of T_{melt} = 478 K and dry-hair melting enthalpy $\Delta H_{dryhair}$ = 16.2 J/gm,[165] and the heat capacity of dry virgin human hair as $C_{keratin}$ ~ 2.5 J/gm-K.[166] An ultrasound-generating hairbot producing a power output of $P_{ultrasound}$ ~ 1.01 μW equal to the P_{digest} ~ 1.01 μW power output of the hairbots executing the digestion protocol (Section 3.4.1) would suffice to melt the keratin interface zone in ~1 sec assuming ~30% efficiency in producing and absorbing the ultrasound in the keratin.

To summarize the attachment scenario: a single robot tows an extension strand up to the apex of its targeted too-short hairstalk in ~100 sec, then returns emptyhanded to the scalp in another ~100 sec after spending another ~100 sec to securely attach the extension strand to the existing

---

[158] Fass D, Thorpe C. Chemistry and Enzymology of Disulfide Cross-Linking in Proteins. Chem Rev. 2018 Feb 14;118(3):1169-1198; https://www.ncbi.nlm.nih.gov/pmc/articles/PMC5808910/.

[159] https://en.wikipedia.org/wiki/Protein_disulfide-isomerase.
[160] https://en.wikipedia.org/wiki/Velcro.
[161] https://en.wikipedia.org/wiki/Dovetail_joint.
[162] https://en.wikipedia.org/wiki/Drywall_anchor.
[163] https://en.wikipedia.org/wiki/Molly_(fastener).
[164] https://chemistry.illinois.edu/news/2022-02-09/molecular-velcro-enables-tissues-sense-react-mechanical-force.

[165] Cao J, Leroy F. Depression of the melting temperature by moisture for alpha-form crystallites in human hair keratin. Biopolymers. 2005 Jan;77(1):38-43; https://pubmed.ncbi.nlm.nih.gov/15578677/.

[166] Pires-Oliveira R, Oliveira FG, Batista TS, Joekes I. Specific heat capacity of cosmetically treated human hair. 22nd IFSCC Conference 2013, Windsor Barra Hotel, Rio de Janeiro, Brazil 30th October to 1st November, 2013; https://www.researchgate.net/profile/Rafael-Pires-Oliveira/publication/266454223_Specific_heat_capacity_of_cosmetically_treated_human_hair/links/5432a77d0cf225bddcc7c38a/Specific-heat-capacity-of-cosmetically-treated-human-hair.pdf.

hairshaft apex in the manner described above and then to verify the integrity of the attachment. In this case the total install time for all extension strands is $t_{install}$ ~ 300 sec (5 min) assuming the hairbots execute all extension operations simultaneously and all extension strands have already been manufactured in the hair mill. The energy consumption for each robot is $E_{install} = P_{robot}\ t_{install}$ = 3 μJ and the fleet energy consumption is $E_{fleet} = N_{trimbots}\ E_{install}$ = 0.3 J, with a fleet power consumption of $P_{fleet} = N_{trimbots}\ P_{robot}$ = 0.001 W assuming $N_{trimbots}$ = 100,000 robots, one for each hairstalk on the scalp.

4.4 Trichoptilosis Protocol

A special situation arises in cases where hairstalks exhibit "split ends" or trichoptilosis[167] (images, right)[168] near their apex, normally caused by thermal, chemical, or mechanical stress.

In this circumstance, the hair trimming protocol (Section 3.4) must be applied first, cutting the hairstalk back to the longest remaining intact structure after the split ends are removed, thus creating a new (shorter) base length. The standard hair extension protocol (Section 4.2) is then applied to the edited hairstalk in the second pass, extending the trunk of undamaged hair to the desired length.

---

[167] https://en.wikipedia.org/wiki/Trichoptilosis.

[168] Photo credits: https://upload.wikimedia.org/wikipedia/commons/c/c5/Spliss2.jpg and https://upload.wikimedia.org/wikipedia/commons/e/e1/Spliss1.jpg.

5. Nanorobotic Coiffure Maintenance

A coiffure (aka. hairstyle, hairdo, or haircut)[169] refers to the macroscale styling of hair, usually on the human head (image, right)[170] but sometimes on the face or body. The fashioning of hair is considered an aspect of personal grooming, beauty, fashion, and cosmetics, although practical, cultural, and popular considerations also influence some hairstyles. Selection of a particular coiffure is an individual choice with social and cultural implications[171] that often reflects a person's gender, religion, marital status, occupation, social class, life cycle (e.g., child, adolescent/coming-of-age, adult, retired, elder, etc.), balancing of asymmetrical facial features,[172] or historical[173] and cultural[174] preferences, with one source listing 105 short and long hairstyles.[175] Further discussion of the personal choice of coiffure is outside the scope of this paper.

Hairstyles are commonly created by arranging hair in a certain way, traditionally using combs, brushes, blow-driers, gels, sprays, or other products – a labor-intensive process often called hairdressing. A traditional hairdressing session might include some or all of the following steps: (1) washing the hair, (2) cutting the hair, (3) brushing and combing to detangle and orient hair strands in a uniform direction, (4) drying the hair, (5) coloring the hair, (6) curling or straightening the hair, (7) braiding[176] and up-dos (arranging the hair so it is carried high on the head),[177] (8) weaves (adding fullness by clipping, gluing, or sewing additional human or synthetic hair into the hairbody),[178] and (9) application of aerosol adhesives (e.g., hairspray),[179] hair mousse,[180] or similar products[181] to add body and to hold the hair in place against external disturbances such as body movements or wind gusts. These traditional barbering or beauty shop methods require intervention by a paid professional, consume considerable time and effort, and normally provide only a static result. With hairbots, coiffures can be quickly reprogrammed and physically implemented, then perfectly and continuously maintained thereafter until the user decides to change it.

The main task of coiffure hairbots is to establish and maintain the physical arrangement of the hairstalks in a specific 3D physical pattern representing the user's desired coiffure. This offers a new level of coiffure control that present-day haircuts do not provide. Here we assume that a

---

[169] https://en.wikipedia.org/wiki/Hairstyle.
[170] https://upload.wikimedia.org/wikipedia/commons/b/ba/Farrah_Fawcett_1977.JPG.
[171] https://en.wikipedia.org/wiki/Hairstyle#Social_and_cultural_implications.
[172] https://en.wikipedia.org/wiki/Asymmetric_cut.
[173] https://en.wikipedia.org/wiki/Hairstyle#Prehistory_and_history.
[174] https://en.wikipedia.org/wiki/Eponymous_hairstyle.
[175] https://en.wikipedia.org/wiki/List_of_hairstyles.
[176] https://en.wikipedia.org/wiki/Braid#Hair_braiding.
[177] https://en.wikipedia.org/wiki/Hairstyle#Braiding_and_updos.
[178] https://en.wikipedia.org/wiki/Artificial_hair_integrations.
[179] https://en.wikipedia.org/wiki/Hair_spray.
[180] https://en.wikipedia.org/wiki/Hair_mousse.
[181] https://en.wikipedia.org/wiki/Hairstyling_product.

particular coiffure has been selected by the user (Section 3.3) and the objective is to establish and continuously maintain the chosen hairstyle using nanorobotic hairbots. All hairstalks have already been trimmed (Section 3.4) or extended (Section 4) to the exactly correct lengths consistent with the chosen coiffure. What remains is to move all the hairs into their proper arrangement as defined by the Desired Coiffure Map, and then hold them there securely.

This task is accomplished first by mapping the current scalp hairbody to create the Current Coiffure Map (Section 5.1), then distributing both the Current Coiffure Map and the existing Desired Coiffure Map to all active hairbots in the coiffure maintenance system, including the hairstyling software application on the user's desktop computer or mobile device (Section 5.2). The user's computer compares the Current Coiffure Map to the Desired Coiffure Map and calculates the optimal deployment of nanorobotic activities that will allow converting the former map into the latter map, after which the instructions for performing this transition are downloaded into the hairbot population and the mechanical control framework of the desired coiffure using heavily robotized guidestalks and variable adhesion nodes is deployed (Section 5.3). The guidestalks and adhesion nodes are then manipulated to recruit all hairstalks into small hairgroups whose position and connectivity can be controlled by the guidestalks, completing the hairbody topology specified by the Desired Coiffure Map (Section 5.4). Subsequent dislocations of the coiffure caused by wind gusts, fingers drawn through the hair, or other external disruptions are quickly detected and reconfigured back to the desired state by the coiffure maintenance system (Section 5.5). Advanced coiffure modifications such as altering hairstalk color or curl patterns are discussed in Section 6.

5.1 Prepare Hairbody Map

The first step is to create a 3D map of the user's actual current scalp-based hairbody, which can then be compared to the Desired Coiffure Map to calculate any necessary remedial action.

We can create a hairstalk-centered map of the entire hairbody by assuming that hairbots can determine with some absolute 3D spatial resolution Δx_{hair} = 100 μm the xyz spatial position of the centroid[182] of individual ΔL_{hair} = 100 μm segments comprising each of N_{hair} = 100,000 hairstalks, with each hairstalk of maximum length $L_{hairstalk}$ = 30 cm. In this case, we have $N_{mappoints} = N_{hair} L_{hairstalk} / \Delta L_{hair} = 3 \times 10^8$ distinct hairbody map points that require $I_{hairbody} \sim N_{mappoints} [3\log(L_{hairstalk} / \Delta x_{hair}) / \log(2)] \sim 1 \times 10^{10}$ bits to describe. This hairbody map can be stored in $I_{hairbody} / i_{nano} = 1000\ \mu m^3$ of nanomechanical RAM onboard the hairbots, with the entire map accessible in $t_{hairbody} = I_{hairbody} / \tau_{nano} \sim 1$ sec, taking $i_{nano} = 10^7$ bits/μm^3 and $\tau_{nano} = 10^{10}$ bit/sec data access speed.[183]

---

[182] https://en.wikipedia.org/wiki/Centroid.

[183] Drexler KE. Nanosystems: Molecular Machinery, Manufacturing, and Computation, John Wiley & Sons, New York, 1992, Chapter 12 "Nanomechanical Computational Systems"; https://www.amazon.com/dp/0471575186/. Freitas RA Jr. Nanomedicine, Volume I: Basic Capabilities, Landes Bioscience, Georgetown TX, 1999, Section 10.2.1, "Nanomechanical Computers"; http://www.nanomedicine.com/NMI/10.2.1.htm.

How is this hairbody map assembled? The hairbots start with an accurate 3D spatial map of the A_{scalp} ~ 650 cm^2 scalp that specifies the 3D spatial position of the scalp and the location of the base of each hairstalk on that scalp to $x_{scanline}$ ~ 10 μm spatial resolution, representing an $I_{scalpmap}$ ~ 10^7 bit scalp map listing the names, locations, lengths, and other useful data for each of ~100,000 hairstalks (Section 3.1). This map may be regarded as relatively unchanging and fixed on the timescale of human coiffure-related events. Of course, the absolute spatial position of the scalp surface alters slightly as (1) cranial muscles move, (2) hairstalks are pulled by external forces, and (3) the skin covering the cranium flexes in response. But the average positions of hair follicles relative to the scalp surface change only very slowly,[184] allowing the scalp map to provide a stable foundation for further mapping.

The next step is to measure the angular deviations of each hairstalk to determine how the column curves through space. What is the minimum angular divergence from linear that we can measure on a hairstalk segment?[185] The hairbot has a body length of L_{robot} = 50 μm with at least two $L_{robotarm}$ ~ 100 μm arms that can be used as calipers[186] (image, left) to precisely measure the width of the hairstalk a distance ΔL_{hair} = 100 μm forward along the column. After determining the central axial direction of the column, the robot can move perpendicular to the axial direction along a circumferential path around the hairstalk, repeating the width measurements at several positions. The smallest measured forward width of a curving hair segment will occur twice, once at the convex peak and once at the concave peak of the curving hairstalk. The largest width measurements will occur ~90° around the normal-to-axial circle from the smallest width measurements, indicating the direction the hair is curving and by how much it deviates from the axial direction.

More specifically, a robot measuring arm consisting of a cylindrical rod of length $L_{robotarm}$ ~ 100 μm and radius $R_{robotarm}$ ~5 μm ($V_{robotarm}$ ~ 7900 μm^3) and Young's modulus of Y_{arm} ~ 10^{10} N/m^2 (vs. ~10^{12} N/m^2 for a solid diamond rod and an effective ~1.3 x 10^{10} N/m^2 for Drexler's 100 nm telescoping manipulator)[187] has a bending stiffness $k_s = 3\pi R_{robotarm}^4 Y_{arm} / 4 L_{robotarm}^3$ ~ 15 N/m. The thermally-excited positional uncertainty of a cylindrical robot arm is $\Delta w \sim (2k_B T e^{SNR} / k_s)^{1/2}$ ~ 3.5 nm, taking temperature T ~ 300 K, Boltzmann's constant k_B = 1.38 x 10^{-23} J/K, and a very conservative signal/noise ratio of SNR ~ 10. Under ideal circumstances, the **minimum** detectible angular divergence from the axial direction of a hairstalk segment of length ΔL_{hair} = 100 μm

---

[184] Araújo R, Fernandes M, Cavaco-Paulo A, Gomes A. Biology of human hair: know your hair to control it. Adv Biochem Eng Biotechnol. 2011;125:121-43; https://core.ac.uk/download/pdf/55616063.pdf.

[185] For the tightest curl of frizzy hair with a curl radius of r_{max} ~ 1 mm, the hairstalk completes one full 360° turn in a distance of $2\pi r_{max}$ = 6.28 mm, hence for one ΔL_{hair} = 100 μm segment of hairstalk the **maximum** angular divergence from linear that we must measure is $\Delta\theta_{max} = (360°) (\Delta L_{hair} / 2\pi r_{max})$ = **5.73°**.

[186] https://en.wikipedia.org/wiki/Calipers.

[187] Freitas RA Jr. Nanomedicine, Volume I: Basic Capabilities, Landes Bioscience, Georgetown TX, 1999, Section 9.3.1.4, "Telescoping Manipulators"; http://www.nanomedicine.com/NMI/9.3.1.4.htm.

linear is then $\Delta\theta_{min} \sim \sin^{-1}(\Delta w/\Delta L_{hair}) \sim$ **0.002°**. This would be equivalent to a maximum curvature angle of $\Delta\theta_{min}$ ($L_{hairstalk}$ / ΔL_{hair}) = 6° over the entire length of an $L_{hairstalk}$ = 30 cm hairstalk, or a maximum cumulative positional error of $\Delta x_{max} = \Delta w$ ($L_{hairstalk}$ / ΔL_{hair}) = 3000 Δw ~ 10.5 μm at the terminal segment of each hairstalk. Such an error would be roughly equivalent to the $x_{scanline}$ ~ 10 μm hairstalk spatial resolution on the scalp map (Section 3.1) and is well below the 3D spatial resolution Δx_{hair} = 100 μm of the xyz position of each hairstalk terminus in the hairbody map, as specified earlier. We assume that $N_{mapbots} \sim N_{trimbots} \sim$ 100,000 mapping hairbots will suffice for this purpose. Several factors may complicate these angular divergence measurements,[188] as follows:

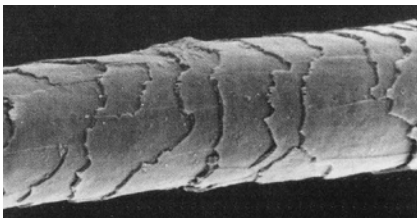

First, cuticle scales on the hair shaft overlap like roof shingles with a step thickness of 0.2-0.5 μm and a cuticle scale length of 30-100 μm (image, right),[189] so the calipers should measure angular deviation between identical positions on successive cuticle steps to minimize a potential measurement error of Δw_{cuti} ~ 0.2-0.5 μm that could otherwise increase the minimum detectible angular divergence ~100-fold to $\Delta\theta_{min,cuti} \sim \sin^{-1}(\Delta w_{cuti}/\Delta L_{hair}) \sim$ 0.1°-0.3°.

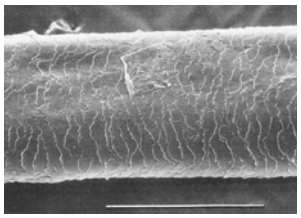

Second, bumps or other irregularities in the 1-10 μm size range (image, left; bump at upper left; 100 μm scale bar)[190] may occur on the cuticle-covered hair shaft, so the calipers must include sensor modalities that can detect and avoid (or compensate for) these anomalies when measurements are being taken to avoid increasing error by another factor of ~10-fold.

Third, human scalp hairs are narrower at the tip (image, right)[191] and increase to full diameter by the time they are 2.5-3 cm in length, a change that must included in the angular displacement calculations as the hairbot approaches the hairstalk terminus.

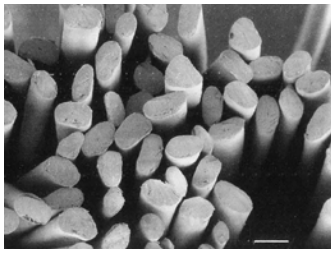

Fourth, human Caucasian terminal scalp hair is roughly oval to round in cross-section (image, left; 100 μm scale bar),[192] varying somewhat in shape and size, which must be accommodated by the hairbot's scanning algorithm.

Fifth, the central axis of wavy hair may oscillate around linear with a wavelength of 3-30 mm, creating a potential long-range periodic

---

[188] Hess WM, Seegmiller RE, Gardner JS, Allen JV, Barendregt S. Human hair morphology: a scanning electron microscopy study on a male Caucasoid and a computerized classification of regional differences. Scanning Microsc. 1990 Jun;4(2):375-86; https://digitalcommons.usu.edu/cgi/viewcontent.cgi?article=2022&context=microscopy.

[189] Hess *et al.*, Figure 1i.
[190] Hess *et al.*, Figure 10.
[191] Hess *et al.*, Figure 1a.
[192] Hess *et al.*, Figure 3.

error source that may be compensated by taking sufficient data points to quantify and subtract out the oscillation.

If necessary, curvature measurement accuracy may be improved by adding tactile sensors to better feel the bend and twist along the hairshaft's length, measuring the complex, multi-directional curvatures that might occur in highly curly or coiled hair types. Hairbots must be able to efficiently navigate the complex and unpredictable microenvironment of hair surfaces, overcoming obstacles and changing directions while maintaining stability.

5.2 Distribute and Update Map Data

For hairbots to take coordinated action, they must each have knowledge of the current actual positions of all the hairs and the ideal hairbody map that they are trying to maintain. To accomplish this, the data on the current positional state of each hairstalk collected by each hairbot must be merged with the data from all the other hairbots to create a Current Coiffure Map that is shared, along with a copy of the Desired Coiffure Map, with all active hairbots in the coiffure maintenance system and with the hairstyling software on the user's desktop computer or mobile device. The Current Coiffure Map may be updated as often as changes are detected. The Desired Coiffure Map is updated whenever the user changes the specifications of the desired coiffure.

If hairbots are stationed on each hairstalk for the duration of the coiffure maintenance period and continuously scan the hair in forward or reverse direction with equal facility, then whole-hairstalk positional data can be collected in $t_{CoifScan} = 2L_{hairstalk} / v_{bot} \sim 6$ sec, taking $L_{hairstalk} = 30$ cm and $v_{bot} \sim 10$ cm/sec during hairstalk scans. The user sets the frequency of scanning, with more frequent scans in cases where faster coiffure reactivity is desired at the cost of higher power usage. This assumes that each nanorobot must return to the base of its hairstalk at the scalp to report out its data. Additionally, the locations of all programmable reversible adhesion points throughout the hairbody (Section 5.4) provide supplemental 3D data to inform the estimated Current Coiffure Map.

Data is shared among hairbots by $N_{databots} = 100{,}000$ mobile databots that, when deployed, dwell exclusively on the scalp, with one assigned to each hairstalk. A descending hairbot, having just completed its scan, reaches the scalp and transfers its new data to the databot assigned to its hairstalk. In turn, the hairbot receives updated Current Coiffure Map data gathered from other hairbots along with any user-provided updates to the Desired Coiffure Map, then returns to its duties which include pre-programmed actions to be taken upon detecting differences between the two Maps that are relevant to its own hairstalk.

Databots circulate constantly on the scalp. After downloading data from a hairbot on its home hairstalk, each databot travels to its nearest neighbors on the scalp and exchanges data with those databots, updating the Current Coiffure Map with more recent data having later timestamps. The databot then returns to its home hairstalk and begins making the rounds again, continuously repeating the cycle. Net "bucket brigade" travel time across the entire scalp is $t_{min} \sim 2.5$ sec (Section 3.1). Data transfer time along an average line of $N_{hair}^{1/2} \sim 316$ robots where $f_{newdata} = 1\%$ of newer (i.e., later-timestamped) data is transferred during each exchange requires an additional $t_{transfer} = f_{newdata}\ t_{hairbody}\ N_{hair}^{1/2} \sim 3.2$ sec, so the time lag between a measurable change in the positioning of the hairs in a coiffure and all hairbots having full knowledge of it is $t_{latency} \sim t_{CoifScan} + t_{min} + t_{transfer} \sim 12$ sec. This may be considered the characteristic coiffure response time.

5.3 Deploy Guidestalks and Variable Adhesion Nodes

The user's personal computer or mobile device compares the Current Coiffure Map to the Desired Coiffure Map and determines the optimal deployment of nanorobotic activities that will allow converting the former map into the latter map. The instructions for performing this transition are downloaded into the hairbot population.

The next step is to deploy the basic mechanical control framework of the coiffure. This is accomplished by coating a small number of hairstalks with a single cladding of hairbots called guide robots. Each such hairbot is in direct physical contact with its neighboring devices on the hairstalk via two or more robot arms through which retractile or compressive forces can be selectively applied. This allows the chain of robots to be operated as a unit in the manner of an independent tentacle manipulator composed of individual modular robots (e.g., image, left).[193] The choice of which hairstalks within the hairbody should be converted into guidestalks depends on the nature of the chosen coiffure and the vectors of mechanical support needed to establish and maintain it. If $f_{guidestalks}$ ~ 1% of all hairstalks are converted into guidestalks with robots located $L_{robotarm}$ ~ 100 μm apart along a hairstalk of maximum length $L_{hairstalk}$ = 30 cm, then there are $n_{guidestalks} = f_{guidestalks}\ N_{hair}$ = 1000 guidestalks in the coiffure, each having $n_{guidebots} = L_{hairstalk} / L_{robotarm}$ = 3000 guidebots on each guidestalk and a total of $N_{guidebots} = n_{guidebots}\ n_{guidestalks}$ = 3,000,000 guidebots in the coiffure. As hairs grows out, guide robots must be inserted into the chain near the base to maintain continuity, or extracted from the apex if the hair length must be trimmed. The mean distance between guidestalks on the scalp is $(A_{scalp} / n_{guidestalks})^{1/2}$ ~ **0.8 cm**.

Additionally, a small number of hairbots are locked together in a ring around the base of each guidestalk to provide secure anchorage and to provide adequate leverage for the forces the guidestalks must apply to maintain the desired coiffure. The circumference of the base of a typical scalp hairstalk is $\pi d_{hairstalk}$ ~ 250 μm, but we will assume a hexagonal geometry of six anchor robots located ~100 μm apart to accommodate a larger maximum hair base circumference for hairstalks up to twice the normal diameter, requiring $N_{anchorbots} = 6\ n_{guidestalks}$ = 6000 anchor hairbots. These devices may need to establish additional adhesion to scalp dermal tissues or cells[194] if needed to support the forces necessary to establish and maintain the desired coiffure.

A third population of hairbots will serve as programmable adhesion nodes in the coiffure. These node robots can ascend or descend a hairstalk and park at a particular location, while physically grasping (a) an adjacent patch of hairstalk, (b) a node robot on an adjacent hairstalk, or (c) a guide robot on an adjacent guidestalk. These nodes provide moveable "sticky points" between neighboring hairs to enable the creation and maintenance of particular groupings of hairs in

---

[193] Yang J, Codd-Downey R, Dymond P, Xu J, Jenkin M. Planning Practical Paths for Tentacle Robots. Proc. 5th Intl. Conf. Agents and Artif Intelligence (ICAART-2013), pp. 128-137; https://www.scitepress.org/papers/2013/42635/42635.pdf.

[194] Freitas RA Jr. Nanomedicine, Volume I: Basic Capabilities, Landes Bioscience, Georgetown TX, 1999, Section 9.4.4.3, "Anchoring and Dislodgement Forces"; http://www.nanomedicine.com/NMI/9.4.4.3.htm.

specific desired patterns. Node robots can move along their home hairstalk while attached either to a point on an adjacent hairstalk or to a node robot parked or walking along an adjacent hairstalk. A minimum coiffure topological feature size of ~**1 cm** requires positioning node robots x_{node} = 1 cm apart along each hairstalk, which will involve up to $n_{nodebots} = L_{hairstalk} / x_{node}$ = 30 robots per hairstalk and a total of $N_{nodebots} = n_{nodebots} N_{hair}$ = 3,000,000 nodebots in the coiffure.

5.4 Execute Desired Coiffure

After the guide robots are deployed and assembled into guidestalks and a foundation of anchor robots is secured around the base of each strand, an appropriate distribution of node robots is deployed onto all hairstalks to await contact. Using serpentine motions, each guidestalk is swept in a wavy pattern intended to bring it into close contact with the $n_{hairgroup} = (1 – f_{guidestalks}) N_{hair} / n_{guidestalks}$ ~ 99 unmodified hairstalks that have been assigned to one of the ~1000 hairgroups controlled by each guidestalk. As it moves, each guidestalk encounters and secures a few adhesion points to the nearest hairstalks in the hairgroup, either directly to the hairstalk or to nodebots already positioned on those hairstalks. Adherent nodebots can slide up and down their assigned hairstalk to straighten the adherent stalk and to relieve mechanical tension caused by hairstalk bending. As the search pattern continues, more and more hairstalks are recruited into the hairgroup and adhere via nodebots that reversibly attach either to nodebots on adjacent hairstalks or directly to adjacent hairstalks. By the end of the accretion process, each guidestalk is surrounded by a bundle of $n_{hairgroup}$ ~ 99 hairstalks with multiple connection points between them, forming a completed hairgroup. Such hairgroup bundles might average 1-2 mm in width.

To complete the coiffure, all guidestalks are repositioned into the configurations that best match the topology of the Desired Coiffure Map. Control signals can be transmitted almost instantly from the base to the tip of a guidestalk through the linked robots. Nodebots are mobile and can drag one hairstalk relative to an adjacent hairstalk, both to relieve tension and to reposition each hairstalk within a hairgroup as uniformly as possible around each guidestalk to best disguise the borders of the hairgroups. Adhesion points can also be established between hairgroups, effectively actualizing such traditional techniques as teasing and backcombing[195] but with minimal damage to hair integrity. Note that the adhesion points mediated by the nodebots can be strong or weak, fixed-length or extensible, or programmed to release when disruptive external forces exceeding a preset threshold are encountered (e.g., fingers running through the hair, or a wind gust). Nanorobots in contact could also be programmed to modify their grip at a specific time, or in response to defined external circumstances or sensor readings (e.g., stress, light, sound, etc.), or even at the direct spoken command (Section 6.6) of the user.

The entire coiffure maintenance system thus consists of $N_{coiffurebots} = N_{mapbots} + N_{databots} + N_{guidebots} + N_{anchorbots} + N_{nodebots}$ ~ 6,206,000 hairbots of volume $V_{coiffurebots} = V_{robot} N_{coiffurebots}$ ~ 0.93 cm^3 – small enough to fit inside a modest-sized decorative earring (image, right).[196] Assuming P_{robot} ~ 10,000 pW for each of the hairbots, the continuous power draw of the entire coiffure fleet during

[195] https://en.wikipedia.org/wiki/Backcombing.
[196] https://www.mondi.nyc/products/champagne-white-diamond-cube-shaped-earrings.

coiffure setup is $P_{coiffurebots} = N_{coiffurebots}\ P_{robot} \sim 62$ mW. If establishing the coiffure takes $t_{coiffure} \sim 25\ t_{latency} \sim 300$ sec (5 min),[197] then the total energy requirement is $E_{coiffurebots} = t_{coiffure}\ P_{coiffurebots} = 18.6$ J, or $E_{Cbot} = E_{coiffurebots} / N_{coiffurebots} = 3$ μJ per nanorobot. Enough energy for $n_{coif} \sim 100$ coiffure reconfigurations can be stored onboard each hairbot in an efficient diamondoid flywheel battery[198] of energy density $E_d \sim 90$ MJ/L and volume $V_{battery} = n_{coif}\ E_{Cbot} / E_d \sim 3300\ \mu m^3$ (<< $V_{robot} \sim 150{,}000\ \mu m^3$). Ambient illumination might only provide enough energy for one or two coiffure reconfigurations per day (e.g., 30 J/day; Section 3.4.1), so a wireless external power supply or a small recharging station for the earrings similar to those employed for modern-day hearing aids[199] will be required to keep the batteries fully charged. Alternatively, a second earring worn on the other ear as a pair (image, left) could provide enough stored power to operate all hairbot fleets virtually indefinitely.[200]

5.5 Subsequent Coiffure Disruptions

An important component of the Desired Coiffure Map is the description of how the hairbody is supposed to move under a variety of external perturbations. For example, the user may want their hair to swish around in a particular way when they shake their head back and forth, or fan out in a particular pattern when wind blows through the hair at various angles. Or they may wish for their hairgroups to separate in a particular way when human fingers are passed through the hairbody, allowing hair movement to feel natural to the touch and only later restoring its previous form, perhaps after some defined period of time has passed or some specific sensory stimulus (e.g., light, sound, vibration, scent) is applied. These passive behaviors can to some degree be programmed by judicious selection of the number and pattern of adhesion points, along with their strength and response to specific external force vectors.

If the user's hair has become mussed and misplaced, the coiffure maintenance system can perform a whole-hairbody remapping in $t_{latency} \sim 12$ sec, followed by a complete coiffure reconfiguration cycle requiring at most $t_{coiffure} \sim 300$ sec (but possibly much less if most hairstalks remain in their correct locations). If we have enough energy for $n_{coif} \sim 100$ coiffure reconfigurations, and each one takes $t_{coiffure} \sim 300$ sec, then we could actively manage a coiffure that was suffering continuous disruption for $n_{coif}\ t_{coiffure} \sim 30{,}000$ sec (~8 hours) before the onboard batteries would be completely drained.

Alternatively, the user could present a continuously changing coiffure for a similar period of time at theatrical performances, parties, or other social events.

---

[197] Elaborate braiding might take a little longer.

[198] Freitas RA Jr. Energy Density. IMM Report No. 50, 25 June 2019; Section 5.3.2, "Rotational Motion"; http://www.imm.org/Reports/rep050.pdf.

[199] https://www.amazon.com/s?k=hearing+aid+charger.

[200] As an alternative to guidestalks, the strandbots used in bionic hair (Section 8) can probably manipulate large hairgroups much faster, e.g., at speeds of ~0.5 m/sec.

The coiffure maintenance system must include protocols for testing and detecting failed or malfunctioning hairbots, especially those comprising the guidestalks, and replacing these hairbots with functional robots from inventory in the nanorobot storage vessel (e.g., the earrings).

On average one guidestalk might be lost every $N_{hair}\ t_{hairshed} / n_{guidestalks} \sim 1$ day because one hairshaft falls out of the scalp every $t_{hairshed} \sim 864$ sec (Section 3.5), though the presence of anchorbots at the base of each guidestalk might slow the attrition. Typically 87%-90% of hair follicles are in active growth (anagen phase) for 2-5 years and are solidly attached; in the catagen phase (2-4 weeks, 2%-3% of all follicles), the hair bulb separates from the feeding blood vessels, moves toward the upper epidermis, and growth ceases; and in the telogen phase (~3 months, 10% of all follicles), hair is held on the head only by the skin and separates at the slightest impact. The coiffure maintenance system must be able to detect that the underlying hairstalk is ready to depilate,[201] permitting the safe recall of the resident guide robots on that hairstalk and directing their migration onto an adjacent hairstalk in the same hairgroup. This creates a new guidestalk for the same hairgroup without significant loss of nanorobots, thus maintaining the integrity of the coiffure while allowing the distressed hairstalk to be safely jettisoned from the scalp. Ideally, guidestalks would be built atop hairstalks that are still in anagen phase and likely to remain so for a long time.

Nodebots can be used either to corral and restrain frizzy hair (i.e., hairs that stand up or curl independently, creating a fuzzy or irregular texture),[202] or to enhance frizziness if that is desired by the user.

---

[201] https://rejuvenatehairtransplant.com/blog/hair-structure/.
[202] https://en.wikipedia.org/wiki/Frizz.

6. Altering Hairstalk Color and Curl

A hairstalk (image, right)[203] consists of three components. On the outer surface is the **cuticle**, composed of 8-10 layers of flat overlapping translucent cells that are essentially transparent, like window glass, and arranged like roof tiles. Underneath the cuticle is the **cortex**, consisting of long, tightly packed keratin spindles and also the melanin granules (pigment packets) that give hair its color. At the center is the **medulla**, a porous lipid-rich structure with large voids containing air, water, and oils.

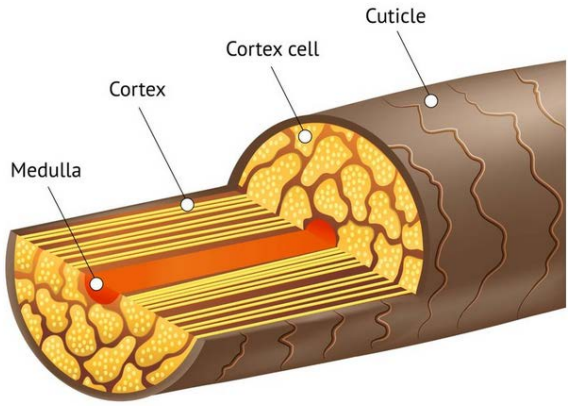

If melanin pigment is completely removed or bleached from the cortex, the clear hair appears white, gray or silvery, depending on the lighting, the angle of viewing, and the thickness and consistency of the lipid coating on the cuticle. Light blond hair retains a small amount of pigment in the cortex, whereas dark blond, brown, red, and black hair get their color from increasing amounts of black-brown eumelanin or reddish-brown/reddish-yellow pheomelanin in the cortex.[204] These melanins are embedded between keratin spindles in the form of $d_{granule}$ = 200-800 nm diameter granules comprising $f_{melanin}$ ~ 1% of dark-colored human hair by weight.[205] Blond hair has a number density of $n_{blond} \sim 6.0 \times 10^{-5}$ granules/μm^3 (~0.0015 granules/μm^2), vs. $n_{brown} \sim 1.2 \times 10^{-3}$ granules/μm^3 (~0.011 granules/μm^2) for brown hair and $n_{black} \sim 1.3 \times 10^{-3}$ granules/μm^3 (~0.012 granules/μm^2) for black hair,[206] assuming uniform spatial distribution in the cortex, for granules of volume 0.008-0.51 μm^3. The melanin volume inside an $L_{hairstalk}$ = 30 cm long dark-colored hairstalk of volume $V_{hairstalk} = (\pi/4)\, d_{hairstalk}^2\, L_{hairstalk}$ = 2.51 mm^3 might be as high as $V_{melaninHair} \sim f_{melanin}\, V_{hairstalk}\, \rho_{hair} / \rho_{melanin}$ = 0.019 mm^3, in which case the volume of all melanin in an entire head of such long hair would be $V_{melaninHead} = V_{melaninHair}\, N_{hairs} \sim 1.9\ cm^3$.

6.1 Bleachbots

Traditional permanent hair color lightening uses contact with ammonia to temporarily open pores in the cuticle layer which permits an oxidizing agent such as hydrogen peroxide to enter the

---

[203] https://www.hairknowhow.com/know-your-hair-structure.
[204] https://en.wikipedia.org/wiki/Human_hair_color.
[205] https://www.hairscientists.org/hair-pigmentation.

[206] Roldan-Kalil J, Zueva L, Alves J, Tsytsarev V, Sanabria P, Inyushin M. Amount of Melanin Granules in Human Hair Defines the Absorption and Conversion to Heat of Light Energy in the Visible Spectrum. Photochem Photobiol. 2023 Jul-Aug;99(4):1092-1096; https://www.ncbi.nlm.nih.gov/pmc/articles/PMC10199145/.

cortex and bleach the melanin pigments in the hair.[207] Applied to black hair, the color will change to brown, red, orange, orange-yellow, yellow, and finally pale yellow over the course of a typical 30-45 min (1800-2700 sec) exposure[208] to ~60 ml of a ~9% solution of hydrogen peroxide[209] and ~2 ml of a ~5% ammonia solution that is "used in the smallest amount possible to minimize excess keratin damage and scalp irritation."[210] (In laboratory experiments under ideal conditions, a solution of 1% ammonia and 1% hydrogen peroxide bleaches eumelanin to colorless in ~30 min.[211]) Assuming a full head of very long hair, $V_{melaninHead} \sim 1.9$ cm^3 of melanin is bleached by ~60 ml of ~9% H_2O_2, equivalent to $V_{H2O2Head} \sim 5.4$ cm^3 of pure liquid H_2O_2, and by ~2 ml of ~5% NH_3 solution, equivalent to $V_{NH3Head} \sim 0.1$ cm^3 of pure liquid NH_3.

By comparison, the melanin generated during just one day's growth of a single hairstalk has a volume of $V_{melaninDay} = (\pi/4)\, d_{hairstalk}^2\, g_{hair}\, f_{melanin}\, \rho_{hair} / \rho_{melanin} \sim 14{,}000$ μm^3/day taking hair growth rate $g_{hair} \sim 350$ μm/day,[212] hair density $\rho_{hair} \sim 1.32$ gm/cm^3, and melanin density $\rho_{melanin} \sim 1.7$ gm/cm^3. This can be bleached by the application of an estimated $V_{H2O2Day} \sim (V_{melaninDay} / V_{melaninHead})\, V_{H2O2Head} \sim 39{,}800$ μm^3/day of H_2O_2 and $V_{NH3Day} \sim (V_{melaninDay} / V_{melaninHead})\, V_{NH3Head} \sim 737$ μm^3/day of NH_3, or $M_{H2O2Day} = \rho_{H2O2}\, V_{H2O2Day} \sim 0.0577$ μg/day of H_2O_2 and H_2O_2 and $M_{NH3Day} = \rho_{NH3}\, V_{NH3Day} \sim 0.000503$ μg/day of NH_3, taking $\rho_{H2O2} = 1.45$ gm/cm^3 for pure liquid hydrogen peroxide[213] and $\rho_{NH3} = 0.6819$ gm/cm^3 for pure liquid ammonia.[214]

Thus to fully bleach the daily new growth of the hairstalk to which it is assigned, a single bleachbot nanorobot must deliver $M_{bleach} = M_{H2O2Day} + M_{NH3Day} = 0.0582$ μg/day of bleach molecules of average molecular weight $MW_{bleach} = (MW_{H2O2}\, M_{H2O2Day} + MW_{NH3}\, M_{NH3Day}) / M_{bleach} = 33.9$ gm/mole, taking $MW_{H2O2} = 34$ gm/mole and $MW_{NH3} = 17$ gm/mole.

---

[207] Ammonia: (1) swells the hair fibers allowing oxidants into the cortex where melanin is found; (2) creates an alkaline pH which is necessary for deprotonation of H_2O_2 (pKa = 11.65) and generation of the perhydroxyl anion, believed to be an important oxidant of melanin; and (3) during melanin bleaching has the key role (and particular to ammonia over other bases) of rupturing the melanosomal membrane leading to release of 30-50 nm melanin nanoparticles. Smith RAW, Garrett B, Naqvi KR, Fülöp A, Godfrey SP, Marsh JM, Chechik V. Mechanistic insights into the bleaching of melanin by alkaline hydrogen peroxide. Free Radic Biol Med. 2017 Jul;108:110-117; https://eprints.whiterose.ac.uk/114603/1/Melanin_Paper_v35_RS.docx.

[208] https://en.wikipedia.org/wiki/Hair_coloring#Permanent_synthetic_dyes.
[209] https://en.wikipedia.org/wiki/Hair_bleaching#Using_bleaching_agents.

[210] Draelos ZD. Hair Care: An Illustrated Dermatologic Handbook, CRC Press, 2004, p. 132; https://www.amazon.com/dp/1841841943.

[211] Prem P, Dube KJ, Madison SA, Bartolone J. New insights into the physicochemical effects of ammonia/peroxide bleaching of hair and Sepia melanins. J Cosmet Sci. 2003 Jul-Aug;54(4):395-409; https://pubmed.ncbi.nlm.nih.gov/14528391/.

[212] Murphrey MB, Agarwal S, Zito PM. Anatomy, Hair. StatPearls [Internet], National Library of Medicine, NIH,14 Aug 2023; https://www.ncbi.nlm.nih.gov/books/NBK513312/.

[213] https://en.wikipedia.org/wiki/Hydrogen_peroxide.
[214] https://en.wikipedia.org/wiki/Ammonia.

A nanorobotic chemical synthesis module for manufacturing simple molecules was scaled to produce $\gamma_{molecules} = 10^5$ molecules/sec or $m_{synthmodule} = \gamma_{molecules}\ MW_{bleach} / N_A = 5.63 \times 10^{-12}$ μg/sec of bleach molecules with a nanomachinery system volume of $V_{synthmodule} \sim 0.001\ \mu m^3$ and power draw $P_{synthmodule} \sim 0.094$ pW.[215] Quickly performing the synthesis of the bleach needed for 1 day of coloration activities in $t_{bleachsynth} \sim 900$ sec (15 min) requires each bleachbot to include $N_{synthmodules} = M_{bleach} / t_{bleachsynth}\ m_{synthmodule} = 11.5 \times 10^6$ synthesis modules of total volume $V_{synth} = V_{synthmodule}\ N_{synthmodules} = 11{,}500\ \mu m^3$ and power draw $P_{synth} = P_{synthmodule}\ N_{synthmodules} = 1.08$ μW.

Of the three elements required to synthesize the H_2O_2 and NH_3 bleach mixture, oxygen and nitrogen are plentiful in the air, and hydrogen (the scarcest of the three elements) is also available from the air in the form of water. The required $m_{bleachH} \sim (MW_{H2} / MW_{bleach})\ M_{bleach} = 0.00343$ μg/day of hydrogen ($MW_{H2} = 2$ gm/mole) can be sourced from atmospheric water vapor ($MW_{H2O} = 18$ gm/mole) which is present in 20 °C air at a concentration of $c_{H2O} = 5.2\ gm/m^3$ at a typical relative humidity[216] of 30% (range: 1.7 gm/m^3 at 10% humidity to 15.6 gm/m^3 at 90% humidity). This requires extracting $m_{H2O} = (2\ MW_{H2O} / MW_{H2})\ m_{bleachH} \sim 0.0617$ μg/day of water from $V_{Hsource} = m_{H2O} / c_{H2O} \sim 0.0119\ cm^3$/day of air.

A previous analysis[217] concluded that CO_2 could be extracted from the atmosphere by sorting rotors[218] at the rate of $\kappa_{CO2} \sim 1$ tonne/day at an energy cost of $P_{extract} = 13{,}900$ W using $M_{extract} = 0.0316$ kg of sorting rotors. CO_2 and H_2O require similar-sized binding sites[219] and water vapor is ~10 times more abundant in air than CO_2,[220] so setting $\kappa_{H2O} = \kappa_{CO2} \sim 10^6$ gm/day for rotor-based atmospheric H_2O extraction seems very conservative. Thus the mass of sorting rotors on a single bleachbot needed to extract the required $m_{H2O} \sim 0.0617$ μg/day of water from the air while operating the pumps for only $t_{rotors} \sim 900$ sec (15 min) during each day is $M_{rotors} = (m_{H2O} / \kappa_{H2O})\ M_{extract}\ (t_{day} / t_{rotors}) = 1.87 \times 10^{-13}$ kg of sorting rotors of volume $V_{rotors} = M_{rotors} / \rho_{robot} = 93.6\ \mu m^3$ ($<< V_{robot} \sim 150{,}000\ \mu m^3$), taking mean robot density $\rho_{robot} \sim 2\ gm/cm^3$, and power consumption $P_{rotors} = (m_{H2O} / \kappa_{H2O})\ P_{extract}\ (t_{day} / t_{rotors}) = 0.823$ μW, only a few times larger than digestion power consumption of $P_{digest} \sim 0.336$ μW (Section 3.4.1). In this case, there are $N_{rotors} = V_{rotors}$ /

---

[215] Freitas RA Jr. Cryostasis Revival: The Recovery of Cryonics Patients through Nanomedicine. Alcor Life Extension Foundation, Scottsdale AZ, 2022; Section D.1.1.2, "Molecular Manufacturing of Generic Organics"; https://www.alcor.org/cryostasis-revival/.

[216] https://en.wikipedia.org/wiki/Humidity#Relative_humidity.

[217] Freitas RA Jr. The Nanofactory Solution to Global Climate Change: Atmospheric Carbon Capture. IMM Report No. 45, Dec 2015; http://www.imm.org/Reports/rep045.pdf.

[218] Freitas RA Jr. Nanomedicine, Volume I: Basic Capabilities, Landes Bioscience, Georgetown TX, 1999, Section 3.4.2, "Sorting Rotors"; http://www.nanomedicine.com/NMI/3.4.2.htm.

[219] Freitas RA Jr. Cryostasis Revival: The Recovery of Cryonics Patients through Nanomedicine. Alcor Life Extension Foundation, Scottsdale AZ, 2022; Section H.1, "Binding Site Design for Carbon Dioxide Molecules" (CO_2) and Section H.2, "Binding Sites for Other Simple Molecules" (O_2, N_2, H_2O); https://www.alcor.org/cryostasis-revival/.

[220] Taking 5.2 gm/m^3 at 20 °C air with 30% relative humidity, atmospheric concentrations are ~4300 ppm for H_2O vs. ~400 ppm for CO_2.

$V_{onerotor}$ = 6.82 x 10^7 sorting rotors each of volume $V_{onerotor}$ = 7 nm x 14 nm x 14 nm = 1372 nm^3, with a total absorptive surface area (facing into the airflow extraction tunnel) of $A_{rotors} = A_{onerotor} N_{rotors}$ = 6680 μm^2, taking $A_{onerotor}$ = 7 nm x 14 nm = 98 nm^2.

Airflow velocity through an onboard cylindrical extraction tunnel of radius r_{tunnel} = 3 μm, cross-sectional area $A_{tunnel} = \pi r_{tunnel}^2$ = 28.3 μm^2, and length $L_{tunnel} = A_{rotors} / 2\pi r_{tunnel}$ = 354 μm is $v_{airflow} = (V_{Hsource} / A_{tunnel}) (t_{day} / t_{airflow})$ ~ 46.7 cm/sec while pumping the air for only $t_{airflow}$ ~ 900 sec (15 min) during each day, using an extraction tunnel of volume $V_{tunnel} = A_{tunnel} L_{tunnel}$ = 10,000 μm^3 (< V_{robot} ~ 150,000 μm^3). This velocity implies a pressure drop of $\Delta p_{air} = 8 \eta_{air} L_{tunnel} v_{airflow} / r_{tunnel}^2$ = 2660 N/m^2 = 0.0263 atm with a modest Poiseuille power dissipation of $P_{flow} = \pi r_{tunnel}^4 \Delta p_{air}^2 / 8 \eta_{air} L_{tunnel}$ = 0.0351 μW,[221] taking absolute viscosity η_{air} = 1.813 x 10^{-5} Pa-sec for air at 20 °C and 1 atm.[222] This assumes a 100% efficient water extraction process with ~4300 ppm H_2O at the input end and ~0 ppm H_2O at the output end of an extraction tunnel externally packed with V_{rotors} = 93.6 μm^3 of sorting rotors and incorporates baffles, airflow pumps, and other atomically-precise structures. Incomplete extraction will require more rotors to compensate.

An additional energy cost of $\Delta H_{f\text{-}H2O}$ = 242 kJ/mole must be applied to separate water vapor into its constituent elements and $\Delta H_{f\text{-}O}$ = 249 kJ/mole must be applied to split molecular oxygen into monatomic oxygen; $\Delta H_{f\text{-}H2O2}$ = 191 kJ/mole can be recovered when these elements are exoergically recombined into liquid hydrogen peroxide.[223] This implies an additional power requirement of $P_{chem} \sim (\Delta H_{f\text{-}H2O} + \Delta H_{f\text{-}O} - \Delta H_{f\text{-}H2O2}) (M_{bleach} / MW_{bleach}) / t_{chem}$ = 0.572 μW, assuming a chemical processing time of t_{chem} = 900 sec (15 min). Note that the ammonia/peroxide bleaching combination was used in the above scaling analysis solely for computational convenience. Other more gentle bleaching mixtures are sometimes used in modern cosmetology, and other oxidizers are known to be stronger melanin bleaching agents than hydrogen peroxide, such as peroxyacetic acid (CH_2COOOH).[224] Of course, bleaching chemicals can also damage keratin and make hair brittle, although organic chemicals such as bis-aminopropyl diglycol dimaleate and ceramides are known to restore the health of bleached hair.[225] Other simple chemicals or nanorobotic activities might be developed to rebuild the full integrity of bleach-damaged keratinous hair. The total power draw during chemical synthesis and the deployment and retraction of tenting (see below) is $P_{synth} + P_{flow} + P_{chem} \sim 2.51$ μW/robot.

Bleachbot nanorobots need three additional features not present in previous hairbot designs:

(1) **Coiled Extraction Tunnel.** If the robots are to produce their own bleach molecules, they must pass humid ambient air past an array of sorting rotors lining the walls of an extraction tunnel that is $2r_{tunnel}$ = 6 μm in diameter and L_{tunnel} = 354 μm in length. The V_{tunnel} = 10,000 μm^3 volume of the extraction tunnel is mostly hollow space and could easily fit entirely inside a bleachbot of volume V_{robot} ~ 150,000 μm^3. However, the diameter of the robot body is only D_{robot} = 50 μm so the tunnel must be gently coiled through ~2 complete loops internally if located near

---

[221] Freitas RA Jr. Nanomedicine, Volume I: Basic Capabilities, Landes Bioscience, Georgetown TX, 1999, Section 9.2.5, "Pipe Flow"; http://www.nanomedicine.com/NMI/9.2.5.htm.

[222] https://www.engineeringtoolbox.com/air-absolute-kinematic-viscosity-d_601.html.
[223] https://en.wikipedia.org/wiki/Standard_enthalpy_of_formation#Inorganic_substances.
[224] https://en.wikipedia.org/wiki/Peracetic_acid.
[225] https://www.webmd.com/beauty/what-to-know-about-hair-bleach.

the bleachbot's perimeter. The layer of sorting rotors embedded in the extraction tunnel wall add only $[r_{tunnel}^2 + (V_{rotors} / \pi L_{tunnel})]^{1/2} - r_{tunnel}$ = 14 nm to the r_{tunnel} = 3 μm tunnel radius.

(2) **Tenting Capability.** The bleachbot must be able to deploy and retract a roughly toroidal watertight tent around the hairstalk circumference to minimize leakage of bleaching chemicals. Once deployed, chemicals can be released into the tent and allowed to diffuse through the cuticle and into the hairstalk cortex to perform the bleaching function. Afterwards, any remaining chemicals can be extracted by sorting rotors and the tent retracted. The tent walls may be composed of multiwalled graphene, diamondoid metamorphic surfaces,[226] or other leakproof materials. Tentings are limited by the minimum of 30-45 min requiring to complete a diffusion-limited bleaching or dyeing cycle. Considering the likely setup overhead for each tenting, we should allow $t_{tenting}$ ~ 80 min for each full tenting cycle, giving a maximum of $n_{tent} \sim t_{day} / t_{tenting}$ = 18 tentings/day that could be theoretically possible. Assuming just one tenting per day, bleaching each g_{hair} ~ 350 μm/day of new growth will take 80 min, not 15 min. Modeling the tent itself as a hollow cylindrical annular volume of inner diameter $d_{hairstalk}$ = 80 μm, radial depth z_{tent}, and length (running down the hairstalk) of $L_{tent} = g_{hair}\ t_{day}$ = 350 μm, then the tent wall materials have a solid volume of $V_{tentwalls} = x_{wall}\ A_{wall}$ = **928 μm^3** (<< V_{robot} ~ 150,000 μm^3) when stowed, taking x_{wall} = 10 nm and $A_{wall} = 2\pi\ d_{hairstalk}\ z_{tent} + \pi\ L_{tent}\ (d_{hairstalk} + 2z_{tent})$ = 92,800 μm^2 and $z_{tent} \sim V_{tent} / A_{surf}$ = **1.8 μm**, where the hairstalk surface area covered by the tent is $A_{surf} = \pi d_{hairstalk}\ L_{tent}$ = 88,000 μm^2, the deployed tent interior volume $V_{tent} = k_{bleach}\ V_{bleach}$ = 160,000 μm^3 per tenting with spare volume multiplier k_{bleach} = 4, and the liquid volume of bleach to be released into the tent is $V_{bleach} = M_{bleach} / \rho_{bleach}$ ~ 40,000 μm^3 per tenting, taking M_{bleach} = 0.0582 μg/day and $\rho_{bleach} \sim \rho_{H2O2}$ = 1.45 gm/cm^3. Design details of the tent and its mechanisms of deployment,[227] retraction, pumping, and seal maintenance are beyond the scope of this simple scaling study.

(3) **Cuticle Lipid Sequestration and Recoating.** Bleaching chemicals can strip away the natural fatty acids coating the hair shaft. This x_{lipid} ~ 0.9 nm thick lipid coating is present in the amount of $V_{lipid} \sim \pi\ d_{hairstalk}\ g_{hair}\ x_{lipid}$ ~ 79.2 μm^3 (only ~0.2% V_{bleach}) and $m_{lipid} \sim V_{lipid}\ \rho_{lipid}$ ~ 7.13 x 10^{-5} μg in every 350 μm of natural hairstalk, assuming long-chain fatty acid density ρ_{lipid} ~ 0.9 gm/cm^3 for anteiso-18-methyleicosanoic acid or "18-MEA" ($C_{21}H_{42}O_2$), an unusual branched chain fatty acid that represents 70% of cuticle-coating lipids, with the remainder consisting mostly of stearic and palmitic acids, all covalently linked to the cuticle surface.[228] It should be possible to include a bleachbot subprogram that either sequesters or manufactures the small required amount of 18-MEA and other fatty acids prior to the release of the bleaching agents, then reapplies the materials to the hairstalk after the bleaching process is completed and all bleach chemicals have been extracted from the hairstalk segment under the tent, restoring full integrity to the hairstalk cuticle.

---

[226] Freitas RA Jr. Nanomedicine, Volume I: Basic Capabilities, Landes Bioscience, Georgetown TX, 1999, Section 5.3, "Metamorphic Surfaces"; http://www.nanomedicine.com/NMI/5.3.htm.

[227] If bleachbots have only ~100 μm reach, in one approach the robot would advance to the far end of its target segment, attach the tent, then retreat down the segment as it unfurls and secures the tent, finally sealing the tent upon reaching the 350 μm mark. The procedure would be reversed during tent retraction.

[228] Rogers GE. Known and Unknown Features of Hair Cuticle Structure: A Brief Review. Cosmetics 2019;6(2):32; https://www.mdpi.com/2079-9284/6/2/32.

6.2 Dyebots

Once the melanin has been fully bleached, creating a "blank canvas," a variety of permanent plant-derived[229] or synthetic[230] dyes can be applied by dye-producing nanorobots to diffuse any desired color back into the cortex (image, right).[231] There are many compilations of known organic dyes, including books[232] and an online list with 333 entries.[233] The selections shown in the table below contain only C, H, O, and N, so all colors should be synthesizable using similar chemical processing modules as described earlier for hydrogen peroxide and ammonia. If the same chemical leaching method used by the bleachbots was followed for introducing dye molecules into the hair, the molecular weight of hair coloring dyes would have to be low enough to permit facile diffusion into the hairstalk cortex under the influence of ammonia. Also, the dyes could not be water-soluble so that the hair would remain colorfast when wetted.

Henna[234]	**Curcumin**[235]	**Berberine**[236]	**Vat Green 1**[237]	**Indigo**[238]	**Eumelanin**[239]
red	orange	yellow	green	blue	black
$C_{10}H_6O_3$	$C_{21}H_{20}O_6$	$C_{20}H_{18}NO_4$	$C_{36}H_{20}O_4$	$C_{16}H_{10}N_2O_2$	$C_{25}H_9N_3O_{13}$
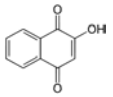	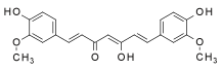	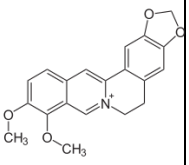	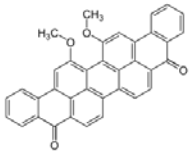	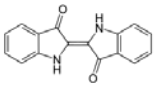	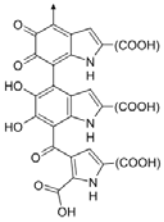

How much dye must the dyebot manufacture onboard? The melanin generated by the growth of one hairstalk in one day is $V_{melaninDay} \sim 14{,}000\ \mu m^3$/day or $M_{melaninDay} \sim \rho_{melanin}\ V_{melaninDay} \sim 0.0238$ µg/day, taking $\rho_{melanin} \sim 1.7\ gm/cm^3$. Assuming that one chemical synthesis module of volume $V_{synthmodule} \sim 0.001\ \mu m^3$ and power draw $P_{synthmodule} \sim 0.094$ pW (Section 6.1) could produce $m_{dyemodule} \sim m_{synthmodule} = 5.63 \times 10^{-12}$ µg/sec of melanin-like dye, manufacturing the daily amount of such dye ($M_{melaninDay}$) in $t_{dyesynth} = 900$ sec (15 min) every day would require the synthesis unit of each dyebot to incorporate $N_{dyemodules} = (M_{melaninDay} / m_{dyemodule})\ (t_{day} / t_{dyesynth}) = 4.70 \times 10^6$

---

[229] https://en.wikipedia.org/wiki/Hair_coloring#Plant-based_dyes.
[230] https://en.wikipedia.org/wiki/Hair_coloring#Synthetic_dyes.
[231] https://hairmotive.com/crazy-hairstyles/ ("44. Short Spikes Hairstyle").

[232] Awwad N, Samanta AK, Algarni HM. Chemistry and Technology of Natural and Synthetic Dyes and Pigments. Intechopen, 2020; https://www.amazon.com/dp/1789859972/.

[233] https://en.wikipedia.org/wiki/List_of_dyes.
[234] https://en.wikipedia.org/wiki/Lawsone.
[235] https://en.wikipedia.org/wiki/Curcumin.
[236] https://en.wikipedia.org/wiki/Berberine.
[237] https://en.wikipedia.org/wiki/Vat_Green_1.
[238] https://en.wikipedia.org/wiki/Indigo_dye.
[239] https://en.wikipedia.org/wiki/Melanin#Eumelanin.

onboard dye synthesis modules of volume $V_{dyemodules} = V_{synthmodule}\ N_{dyemodules} = 4700\ \mu m^3$ (<< $V_{robot} \sim 150{,}000\ \mu m^3$) and power draw $P_{dyesynth} = P_{synthmodule}\ N_{dyemodules} = 0.442\ \mu W$.

Fortunately, it is possible to introduce dyes consisting of small, medium or large molecules, even including fairly sizeable granules of packed pigment (all of which could be manufactured by the hairbots), using specialized dyebots that can avoid the diffusion-based limitations suffered by the bleachbots, by the following means.

Hairstalks consist of dried dead cells that are tightly packed together and are largely devoid of water. Dry human hair of density $\rho_{hair} \sim 1.32\ gm/cm^3$ can absorb another $0.40\ gm/cm^3$ of water.[240] These water molecules penetrate the hair shaft through 3-100 nm diameter pores in the cuticle and are absorbed by the cortical cells, where they bond with the keratin proteins, enabling the hair to absorb moisture and swell. The small size of these pores facilitates the capillary action that draws water into the hair, allowing for hydration and the transport of water molecules deep into the cortex. The swelling is uniform throughout the hair's structure and does not form localized aqueous pools.

This is important because while micron-scale nanorobots should operate well even in a cluttered aqueous environment, they cannot "swim" inside a hairstalk because the water absorption process does not typically create navigable water-filled pools with diameters in the 1-10 micron range. The absorption process is more about water molecules diffusing into the microstructure of the hair fiber rather than forming discrete pools. That's why hairbots cannot easily extract multitudes of melanin granules scattered randomly throughout existing hairshafts, thus demanding the use of slower diffusion-based methods as exemplified by the bleachbots (Section 6.1). However, this limitation does not apply to the *insertion* of melanin pigment granules *into* a hairshaft in a specified pattern. To accomplish this, nanorobots don't need to navigate inside the hairshaft. They only need to be able to reach inside the hairshaft with an injector mechanism that can directly release pigment granules of a color, size, number, and spatial distribution that is consistent with the user's desires. No tenting is needed because injected materials are delivered to specific locations and are not expected or allowed to diffuse randomly to their destination.

If we inject new pigment molecules or granules of density $\rho_{dye} \sim \rho_{melanin} \sim 1.7\ gm/cm^3$ and absolute viscosity $\eta_{dye} \sim 2$ Pa-sec[241] into a previously-bleached $g_{hair}\ t_{day} = 350\ \mu m$ segment of hairstalk using a nanorobot injector needle of radius $r_{injector} = 0.5\ \mu m$ and length $L_{injector} = 50\ \mu m$ with a pumping pressure differential of $\Delta p_{dye} = 1$ atm $= 1\ .01 \times 10^5\ N/m^2$ over a daily pumping duty cycle lasting $t_{dyepump} \sim t_{dyesynth} = 900$ sec, then the power draw of Poiseuille pipe flow[242] is $P_{dyeflow} = \pi\ r_{injector}^4\ \Delta p_{dye}^2 / 8\ \eta_{dye}\ L_{injector} = 2.50\ \mu W$ and the volumetric dye flow rate is $V_{dyeflow} =$

---

[240] Zimmerley M, Lin CY, Oertel DC, Marsh JM, Ward JL, Potma EO. Quantitative detection of chemical compounds in human hair with coherent anti-Stokes Raman scattering microscopy. J Biomed Opt. 2009 Jul-Aug;14(4):044019; https://www.ncbi.nlm.nih.gov/pmc/articles/PMC2872558/.

[241] Compare: $\eta \sim 3$ Pa-sec for lacquer with 25% pigments at 20 °C and $\eta \sim 0.55$-2.20 Pa-sec for printer's inks at 40 °C; https://oilviscositychart.com/learn/viscosity-list.php.

[242] Freitas RA Jr. Nanomedicine, Volume I: Basic Capabilities, Landes Bioscience, Georgetown TX, 1999, Section 9.2.5, "Pipe Flow"; http://www.nanomedicine.com/NMI/9.2.5.htm.

$\pi\ r_{injector}^4\ \Delta p_{dye} / 8\ \eta_{dye}\ L_{injector} = 24.8\ \mu m^3/sec$, or $M_{dyeflow} = \rho_{dye}\ V_{dyeflow}\ t_{dyesynth} \sim 0.0380\ \mu g/day$, roughly equal to the $M_{melaninDay} \sim 0.0238\ \mu g/day$ manufacturing rate calculated earlier.

6.3 Hair Coloration Scenarios

Bleachbots and dyebots can be applied in a variety of hair coloration scenarios. For instance, the modest fleet of hairbots as previously described could colorize just the roots as they grow out (Section 6.3.1) or could provide frosting of hairtips or highlights that gradually replace the entire hairbody color (Section 6.3.2). The entire hairbody could be recolorized by nanorobots with a larger fleet of hairbots deployed using a home hairstyling appliance (Section 6.3.3), or hair mills could be used to replace the entire natural hairbody down to the roots with the new colors in just a few minutes' installation time, thereafter continuously colorizing the roots as they grow out using hairbots (Section 6.3.4). Hair color could also be permanently altered at the roots via chromosome replacement therapy applied to hair follicle cells using chromallocytes (Section 6.3.5).

Users with gray or white hair have already lost their hair melanin, thus can skip the bleaching treatment (Section 6.1) and proceed immediately to dyeing (Section 6.2) using one of the coloration scenarios described below.

6.3.1 Colorized New Growth

In one scenario, the coloration process is executed every day only on new hair growth. The recolored hair grows out slowly over several years as the hair naturally grows by ~365 $g_{hair} \sim 12.8$ cm/year, or $t_{convert} = L_{hairstalk} / g_{hair} \sim 857$ days for full grow-out of newly colorized hair of maximum length. This method is probably the least aesthetically desirable by today's cosmetic standards because of the long period of time that large sections of the old hair color and the new hair color would be simultaneously visible. However, the possibility that "showing roots" could become a desired fashion statement sometime in the future cannot be ruled out.[243]

6.3.2 Highlighting

Rather than applying new color from the roots of all the hairs, hairbots could be used to alter the color of just a few hairstalks, starting from the terminus of the hairstalk and moving downward some distance toward the scalp, producing results similar to conventional frosting[244] or highlighting.[245]

Using fleets of bleachbots (Section 6.1) and dyebots (Section 6.2) that could colorize $g_{hair} \sim 350$ μm/day of $N_{hair} = 100{,}000$ hairstalks, we could alternatively process $N_{hair}/100 = 1\%$ of all

---

[243] https://www.dailymail.co.uk/femail/article-11462665/Showing-roots-used-no-no-stars-paying-fortune-painted-on.html and https://www.refinery29.com/en-us/visible-roots-hair-trend.
[244] https://en.wikipedia.org/wiki/Frosted_tips.
[245] https://en.wikipedia.org/wiki/Hair_highlighting.

hairstalks with new color over 100 g_{hair} ~ 3.5 cm/day (~1.4 inches) from their tips. Each day the same hairs could be colorized another 3.5 cm, or a different 1% of all hairstalks could receive the new frosting.

Alternatively, the same hairbot fleets could colorize $N_{highlight} = g_{hair} N_{hair} / L_{hairstalk}$ ~ 117 hairstalks/day with the new color from root to tip. Every day, the robots could convert another $f_{highlight} = N_{highlight} / N_{hair}$ ~ 0.12% of the hair to the new color, slowly adding whole-hairstalk highlights in selected locations, or even gradually transitioning the entire hairbody from the old color to the new color in $t_{convert} = f_{highlight}^{-1}$ = 2.35 years.

6.3.3 Whole-Hairbody Coloration Appliance

Bleachbots and dyebots could perform coloration of all N_{hairs} = 100,000 scalp hairs over their entire $L_{hairstalk}$ = 30 cm length. Each coloration nanorobot has been scaled to recolor g_{hair} ~ 350 μm/day of hairstalk during a brief duty cycle of ~ $t_{bleachsynth}$ ~ t_{rotors} ~ $t_{airflow}$ ~ t_{chem} ~ $t_{dyesynth}$ ~ 900 sec (15 min) per day of simultaneous onboard activity (Section 6.1). However, the maximum speed of nanorobot-mediated colorization is limited by the tenting cycle time of $t_{tenting}$ ~ 80 min. In the previous analyses, the coloration hairbot fleet was assumed to comprise one nanorobot per hairstalk, or $N_{hairbots} = N_{hair}$ = 100,000 robots. Simultaneously processing the full length of all hairstalks in a total coloration time of $t_{coloration} \sim t_{tenting}$ ~ 80 min would require a much larger fleet of $N_{colorbots} = (L_{hairstalk} / g_{hair}) N_{hairbots} = 85.7 \times 10^6$ robots with a fleet volume of $V_{colorbots} = V_{robot} N_{colorbots}$ = 12.9 cm^3 and a fleet power requirement of $P_{colorbots} = (P_{synth} + P_{rotors} + P_{flow} + P_{chem} + P_{dyesynth}) N_{colorbots}$ = (2.95 μW/robot) $N_{colorbots}$ ~ 253 W, taking P_{synth} = 1.08 μW, P_{rotors} = 0.823 μW, P_{flow} = 0.0351 μW, P_{chem} = 0.572 μW, and $P_{dyesynth}$ = 0.442 μW (Section 6.1), giving a quite reasonable nanorobot power density of ~0.02 MW/L.[246] During this high-intensity coloration process, there are $n_{colorbots/stalk} = L_{hairstalk} / g_{hair}$ ~ 857 robots positioned on each $L_{hairstalk}$ = 30 cm hairstalk, spaced ~ 350 μm apart, of total robot mass $m_{colorbots/stalk} = n_{colorbots/stalk} M_{robot}$ ~ 257 μg which is ~13% of the hairstalk mass of $M_{hairstalk} = (\pi/4) d_{hairstalk}^2 L_{hairstalk} \rho_{hair}$ ~ 1990 μg, taking M_{robot} ~ 0.3 μg, $L_{hairstalk}$ = 30 cm, and ρ_{hair} ~ 1.32 gm/cm^3.

The significant extra mass, volume, and power requirements for a hairbot fleet able to fully colorize the entire hairmass in $t_{coloration}$ ~ 80 min suggest that this fleet should be deployed and managed using the headrest attachment appliance on the hair mill (Section 4.1). The $P_{colorbots}$ ~ 255 W power requirement can readily be provided by house wall current or other convenient external energy source, and the appliance can easily deploy additional functions such as relipidization and hydration to offset the harmful effects of bleach on the cortex and cuticle of natural keratinous hair. The headrest attachment could also execute the daily hair trimming task in a few minutes (Section 3.4.2) for people who are willing to forgo the convenience of on-body nanorobot storage vessels or who prefer not to wear earrings, and could also expedite coiffure deployment and maintenance (Section 5). Further design elaborations of the appliance are beyond the scope of this paper.

---

[246] We could get away with a fleet of only $N_{colorbots} = (L_{hairstalk} / g_{hair}) (t_{tenting} / t_{day}) N_{hairbots}$ = 4.76 million hairbots if we were willing to let the coloration process take all day to complete.

6.3.4 Rehairing with Colorized New Growth

In another scenario, existing hair is trimmed (Section 3.4) back to the roots, hair extensions with the new color are manufactured in $t_{synthhair}$ ~ 3 hours of machine time by the hair mill (Section 4.1) and immediately attached to the root hairstalks in $t_{install}$ ~ **5 min** of user time (Section 4.3), after which the new growth need only be recolorized daily as the hairstalks grow out. The result is aesthetically desirable because the user's hair is almost instantly transformed into the new colors (image, right),[247] and the new color is continuously maintained thereafter so the person never "shows roots" as is common after conventional hair coloration processes. It should be reiterated that the manufactured hairstalks can be as molecularly identical to the user's natural hair as desired. In this sense, it is "real hair", but with the new desired color or coloration pattern. Rehairing is probably the most aesthetically desirable and by far the fastest method of any option available to the user.

6.3.5 Genetically Modified Follicular Cells

Since excessive bleaching can damage keratin and make hair brittle, an alternative solution would inject chromallocyte[248] nanorobots into all of the active follicular generative cells in the scalp and install replacement chromosomes inside the cell nuclei containing genes that code for the desired color of hair, assuming the desired color is available naturally. If not, it may still be possible to bioengineer the genes to produce unnatural hair colors by inducing cells to manufacture, for example, a non-melanin substitute dye.[249] After the DNA substitution, hair of the new color would grow out naturally at the usual g_{hair} ~ 350 μm/day rate. In this scenario, it would be optimal to remove the existing hairbody down to the roots and manufacture extension replacement hair that is biochemically identical to the original hair, but having the new color (Section 6.3.4). The new color would be expressed in the new growth from the gene-modified follicular cells, perfectly matching the rehairing materials. One minor inconvenience: to change hair color again, the user would have to re-engineer their follicular genes once more, then apply chromallocytes to perform another replacement in all relevant cells in the scalp.

The color of hair is primarily determined by the amount and type of melanin synthesized by melanocytes in the hair follicles. Different hair color phenotypes arise primarily as a result of varying ratios of these two pigments in the human population. Regulatory DNA is believed to be

---

[247] https://hairmotive.com/crazy-hairstyles/ ("25. Peacock Tail Hairstyle").

[248] Freitas RA Jr. The Ideal Gene Delivery Vector: Chromallocytes, Cell Repair Nanorobots for Chromosome Replacement Therapy. J. Evol. Technol. 2007 Jun;16:1-97; http://jetpress.org/v16/freitas.pdf.

[249] Saito N, Zhao M, Li L, Baranov E, Yang M, Ohta Y, Katsuoka K, Penman S, Hoffman RM. High efficiency genetic modification of hair follicles and growing hair shafts. Proc Natl Acad Sci U S A. 2002 Oct 1;99(20):13120-4; https://www.ncbi.nlm.nih.gov/pmc/articles/pmid/12232045/.

closely involved in human pigmentation,[250] and one study[251] identified 13 DNA variations across 11 different genes that could be used to predict hair color. A few of these genes include:

- **MC1R (Melanocortin 1 Receptor).**[252] This gene plays a crucial role in determining whether the melanin produced is eumelanin (black or brown) or pheomelanin (red or yellow). Variants in MC1R can lead to red hair and fair skin that tans poorly.

- **TYR (Tyrosinase).**[253] Tyrosinase is an enzyme essential for the production of melanin. Mutations in this gene can cause albinism, a condition characterized by a lack of pigment in hair, skin, and eyes.

- **OCA2 (Oculocutaneous Albinism II).**[254] This gene affects the melanosome, the organelle in cells that synthesizes and stores melanin. Variations in this gene can influence the lightness or darkness of hair color.

- **SLC24A5 (Solute Carrier Family 24 Member 5).**[255] This gene contributes to pigmentation in humans and variations in it are associated with skin and hair color diversity.

- **SLC45A2 (Solute Carrier Family 45 Member 2).**[256] This gene is also involved in pigmentation and mutations here can lead to a reduction in melanin, affecting hair, skin, and eye color.

- **KITLG (KIT Ligand).**[257] This gene is involved in the development and function of melanocytes. Differences can influence hair color variation, particularly in lighter hair.

---

[250] Pennisi E. The Genetics of Blond Hair. Science Adviser, 1 Jun 2014; https://www.science.org/content/article/genetics-blond-hair.

[251] Branicki W, Liu F, van Duijn K, Draus-Barini J, Pośpiech E, Walsh S, Kupiec T, Wojas-Pelc A, Kayser M. Model-based prediction of human hair color using DNA variants. Hum Genet. 2011 Apr;129(4):443-54; https://www.ncbi.nlm.nih.gov/pmc/articles/PMC3057002/.

[252] Ji RL, Tao YX. Melanocortin-1 receptor mutations and pigmentation: Insights from large animals. Prog Mol Biol Transl Sci. 2022;189(1):179-213; https://pubmed.ncbi.nlm.nih.gov/35595349/. See also: https://en.wikipedia.org/wiki/Melanocortin_1_receptor.

[253] Lai X, Wichers HJ, Soler-Lopez M, Dijkstra BW. Structure and Function of Human Tyrosinase and Tyrosinase-Related Proteins. Chemistry. 2018 Jan 2;24(1):47-55; https://research.rug.nl/files/77300451/Lai_et_al_2018_Chemistry_A_European_Journal.pdf.. See also: https://en.wikipedia.org/wiki/Tyrosinase.

[254] https://en.wikipedia.org/wiki/P_protein.
[255] https://en.wikipedia.org/wiki/Sodium/potassium/calcium_exchanger_5.
[256] https://en.wikipedia.org/wiki/Membrane-associated_transporter_protein.
[257] https://en.wikipedia.org/wiki/Stem_cell_factor.

In general, eumelanin determines the darkness of the hair color[258] – more of the black subtype of eumelanin leads to blacker hair, while more of the brown subtype of eumelanin produces browner hair.[259] All human hair has some amount of both pigments; >95% of melanin content in black and brown hair is eumelanin. Pheomelanin has higher concentrations in blond and red hair, representing about one-third of total melanin content. Strawberry blond color occurs when there is no black eumelanin; pure blond occurs when there is small amounts of brown eumelanin with no black eumelanin.[260]

6.4 Altering Hairstalk Curl Pattern

There are four commonly recognized curl patterns in human hair: straight, wavy, curly, and kinky.[261] The cross-sectional shape of the hair shaft is believed to determine the curliness of the individual's hair (image, right).[262] A very round shaft allows for fewer disulfide bonds to be present in the hair strand, placing these bonds directly in line with one another, resulting in straight hair. The flatter the hair shaft becomes, the curlier hair gets, because the shape allows more cysteines to come into contact with each other, resulting in a bent shape that, with every additional disulfide bond, becomes curlier in form.

Disulfide bond disruption and formation are known to be associated with changes of hair shape.[263] The presence of disulfide bonds in cysteine residues of the hair keratin protein determines the maintenance of the shape of the hair, and can be altered by perming or relaxing.[264] Perming adds curls to hair – traditionally, by wrapping the hair around rods and then applying a chemical treatment.[265] Relaxing removes curls, straightening hair. For example, alkaline reducing agents, when in contact with the cortex, break and rearrange the disulfide bonds,

---

[258] Farthmann B, Schmitz S, Krasagakis K, Orfanos CE. Photoprotection by Total Melanin Content and Pigment Phenotype (Eumelanin, Pheomelanin) in Human Melanoma Cell Lines. In: Altmeyer P, Hoffmann K, Stücker M, eds. Skin Cancer and UV Radiation. Springer, Berlin, Heidelberg, 1997; https://link.springer.com/chapter/10.1007/978-3-642-60771-4_21.

[259] Schlessinger DI, Anoruo M, Schlessinger J. Biochemistry, Melanin. 2023 May 1. In: StatPearls [Internet]. Treasure Island (FL): StatPearls Publishing; 2024 Jan–. PMID: 29083759.

[260] https://en.wikipedia.org/wiki/Human_hair_color#Genetics_and_biochemistry_of_hair_color.
[261] https://en.wikipedia.org/wiki/Hair#Texture.
[262] https://www.bio.davidson.edu/courses/genomics/2011/Piper/Background.html.

[263] Robbins CR. Chemical and Physical Behavior of Human Hair. Springer, Berlin, 4th Ed., 2002.

[264] Cruz CF, Martins M, Egipto J, Osório H, Ribeiro A, Cavaco-Paulo A. Changing the shape of hair with keratin peptides. Roy Soc Chem. 2017;7:51581-51592; https://pubs.rsc.org/en/content/articlepdf/2017/ra/c7ra10461h.

[265] https://www.wikihow.com/Perm-Your-Hair.

stretching the spiral coil of keratin molecules.[266] Chemical relaxers provide permanent hair straightening, sometimes using sodium hydroxide (caustic lye) or non-caustic relaxers such as ammonium thioglycolate that selectively weakens the hair's cystine bonds without disrupting the entire protein and causes less protein loss than hydroxides. Peptides can also be used as substitutes for the alkaline agents and thio-relaxers that are commonly used for hair straightening.[267]

Similar to coloration, each hairstalk could be treated by hairbots with the appropriate chemical agents commonly used to perm or relax hair, and chromallocytes could be employed to alter the genetic code of the follicular germinative cells.[268] The implementation details and performance of hairbots performing curl pattern alteration will be similar to those for robots performing color alterations (Section 6.3). Hair curling or straightening could be applied on a whole-hairbody or just a partial hairbody basis (in patches or patterns) to produce interesting combinations or juxtapositioning effects.

6.5 Thinning Hair or Baldness

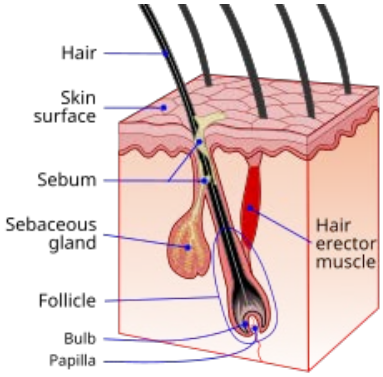

The human hair follicle is programmed to produce ~25 hairs,[269] which corresponds to the number of hair cycles an individual has in their lifetime. If the user still has some hair left, there will be a mixture of live hair follicles (image, right)[270] whose bulbs are still producing hair strands and degenerate or dead hair follicles that are no longer producing any hair.

To replace the **dead hair follicles**, chromallocytes[271] bearing new chromosomes encoding the DNA of a young healthy follicle cell are sent into the scalp to find live subdermal skin cells and inject the new chromosomes into the nuclei of those live cells, effectively transforming them into new live follicular cells from which healthy hair strands soon will begin to grow.[272]

---

[266] Gavazzoni Dias MF. Hair cosmetics: an overview. Int J Trichology. 2015 Jan-Mar;7(1):2-15; https://www.ncbi.nlm.nih.gov/pmc/articles/pmid/25878443/.

[267] Cruz CF, Martins M, Egipto J, Osório H, Ribeiro A, Cavaco-Paulo A. Changing the shape of hair with keratin peptides. Roy Soc Chem. 2017;7:51581-51592; https://pubs.rsc.org/en/content/articlepdf/2017/ra/c7ra10461h.

[268] Westgate GE, Ginger RS, Green MR. The biology and genetics of curly hair. Exp Dermatol. 2017 Jun;26(6):483-490 ; https://onlinelibrary.wiley.com/doi/pdf/10.1111/exd.13347.

[269] https://www.renefurterer.com/en-ca/tips/scalp/the-physiology-of-the-scalp.
[270] https://en.wikipedia.org/wiki/Hair_follicle

[271] Freitas RA Jr. The Ideal Gene Delivery Vector: Chromallocytes, Cell Repair Nanorobots for Chromosome Replacement Therapy. J. Evol. Technol. 2007 Jun;16:1-97; http://jetpress.org/v16/freitas.pdf.

[272] Alternatively, a modified hair mill could manufacture new hair follicles containing cells with the user's coiffure-modified DNA, which can then be physically implanted into the scalp.

For the **live hair follicles**, chromallocytes are again employed to inject un-aged "young DNA" into their nuclei, allowing stronger hair strands of the desired color and texture to begin to be produced immediately by these rejuvenated vigorous cells. Synthetic hair of the desired type can be manufactured in the hair mill and attached to existing hair to lengthen it to conform to the desired coiffure, and also to new hair strands as they emerge from the germinative bulbs of follicle-transformed skin cells in the scalp. The existing hair will look better immediately and will become thicker over time as more of the new hair grows out.

If the user is completely bald with no remaining live hair follicles, the more time-consuming approach is to perform the aforementioned chromallocyte transformation of skin stem cells[273] into healthy follicular cells, followed by attachment of full-length synthetic hair manufactured in the hair mill to new hair as it grows out. The aging of the hair follicle is a key aspect of hair loss with age.[274] Hair follicle renewal is normally maintained by the stem cells associated with each follicle, with aging primed by a sustained cellular response to the DNA damage that accumulates in renewing stem cells as they get older.[275] Using chromallocytes to replace the chromosomes that have DNA damage with new chromosomes that lack this damage should rejuvenate the follicle stem cells, allowing hair production to resume.

A faster approach is to use the hair mill to generate full-length synthetic hair that's phenotypically matched to the user's original natural hair, then bond these new hair strands to permanent biocompatible hairstalk anchors securely embedded in the scalp. These anchors will eventually come loose as scalp dermis sheds over time, at which time they should be replaced or embedded deeper into the scalp tissue. This procedure immediately produces a head of full thick hair. As the synthetic hair gets worn or discolored over time, it can be trimmed, extended, recolored, retextured, or replaced by the methods described earlier in this paper. This is conceptually equivalent to installing a permanent toupée, wig, or other hairpiece made of the user's own hair.

It may also be theoretically possible to design, fabricate and install in the scalp multiple miniature hair mills (Section 4.1) called "minimills". The output of each minimill is just a single strand of engineered "natural" hair of any desired length. Each strand remains anchored to its minimill, which in turn is securely anchored to the scalp, preserving the physical integrity of the hairbody under stress. The mean distance between natural scalp follicles is $(A_{scalp} / N_{hairs})^{1/2} \sim 800$ μm. If minimills are $L_{minimill} \sim 500$ μm in diameter, then each one extrudes hair at a rate of $v_{extrude} \sim L_{strand} L_{minimill}^{3} N_{hair} / V_{hairmill} t_{synthhair} = 0.65$ cm/day, with $N_{minimill} = 100{,}000$ minimills over the

---

[273] Garza LA, Yang CC, Zhao T, Blatt HB, Lee M, He H, Stanton DC, Carrasco L, Spiegel JH, Tobias JW, Cotsarelis G. Bald scalp in men with androgenetic alopecia retains hair follicle stem cells but lacks CD200-rich and CD34-positive hair follicle progenitor cells. J Clin Invest. 2011 Feb;121(2):613-22; https://www.ncbi.nlm.nih.gov/pmc/articles/pmid/21206086/.

[274] Lei M, Chuong CM. STEM CELLS. Aging, alopecia, and stem cells. Science. 2016 Feb 5;351(6273):559-60; https://www.science.org/doi/abs/10.1126/science.aaf1635.

[275] Matsumura H, Mohri Y, Binh NT, Morinaga H, Fukuda M, Ito M, Kurata S, Hoeijmakers J, Nishimura EK. Hair follicle aging is driven by transepidermal elimination of stem cells via COL17A1 proteolysis. Science. 2016 Feb 5;351(6273):aad4395; https://pubmed.ncbi.nlm.nih.gov/26912707/. Wang L, Siegenthaler JA, Dowell RD, Yi R. Foxc1 reinforces quiescence in self-renewing hair follicle stem cells. Science. 2016 Feb 5;351(6273):613-7; https://www.ncbi.nlm.nih.gov/pmc/articles/pmid/26912704/.

entire scalp drawing $P_{minimill} \sim L_{minimill}^3 N_{minimill} P_{hairmill} / V_{hairmill} = 0.523$ W of continuous power that could be provided by a necklace or hairstyle accessory (Section 7) or by other means. Hair that is fabricated by minimills will grow out to 30 cm length in ~46 days, or can keep growing longer if desired. The user can control color, curl, and surface features of the fabricated hair as it grows out, and can download a new pattern into the minimills at any time. Biocompatibility of the tissue-embedded minimill nanomachines must be maintained,[276] and some provision must be made for replacement of individual minimills when they eventually suffer mechanical or control failure.

Minimills could also be programmed to extrude animal furs[277] – like mink, sable, alpaca, or rabbit – from the human scalp. Mammalian fur typically involves two separate coats: (1) a soft thick undercoat of shorter wavy or curly "down hairs" (70-90% of hair density) that provides warmth, and (2) an outer waterproofing coat of oily mostly-straight guard hairs (10-30% of hair density) that have the most pigmentation and gloss.[278] There may be 200-1800/cm^2 guard hair follicles and 800-7200/cm^2 down hair follicles on animal skin, considerably more than the 200-300/cm^2 hair density on human scalp, potentially placing guard hair follicles as close as ~240 μm and down hair follicles as close as ~120 μm on the skin.

If a user wishes to grow animal down hair and we shrink the minimill diameter from 500 μm to ~100 μm to retain comparable spacing on the scalp, hair volume production is reduced by a factor of $(500/100)^3 \sim 125$. However, hypoallergenic alpaca down fibers are just ~18 μm in diameter,[279] reducing the volume per unit length by a factor of ~20 compared to ~80 μm diameter human hair. Thus the net loss in length productivity for the smaller minimills is only a factor of 6, reducing $v_{extrude}$ from ~0.65 cm/day to ~0.11 cm/day for alpaca down hair continuously fabricated on a human scalp. Production of animal guard hair should have an extrusion rate closer to the earlier estimate for human hair.

For the cosmetically adventurous, one final alternative might be to fully embrace the bald coiffure and make a defiant cosmetic statement by installing a programmable dermal display on the otherwise bare scalp. The dermal display could exhibit virtually any image desired by the user, including colors, textures, photos, faces (image, right),[280] words, graphic designs, or even creative images or videos of hair.

---

[276] Freitas RA Jr. Nanomedicine, Volume IIA: Biocompatibility, Landes Bioscience, Georgetown TX, 2003, Section 15.5.1, "Mechanical Interaction with Human Integument"; http://www.nanomedicine.com/NMIIA/15.5.1.htm.

[277] https://en.wikipedia.org/wiki/List_of_types_of_fur#Mink, https://en.wikipedia.org/wiki/Animal_fiber.
[278] https://en.wikipedia.org/wiki/Fur.
[279] https://en.wikipedia.org/wiki/Alpaca_fiber.
[280] https://www.boredpanda.com/hair-art-roberto-perez-rob-the-original/.

The original description of the concept by the author published in 1999[281] envisioned a tattoo-like programmable display embedded in the skin on the back of the hand (e.g., images at left and right; artist Gina Miller)[282] that report results to the patient or user from nanorobots collecting medical data inside the body. Following the original scaling analysis, covering the entire A_{scalp} ~ 650 cm^2 scalp area would require embedding ~65 billion dermal display nanorobots each measuring ~1 μm^3 in volume and each consuming ~10 pW of power while generating visible photons of desired colors at a comfortable visible intensity of ~1 pW/μm^2 or ~1 W/m^2, for a total power draw of the entire display of ~0.65 W when operated continuously on the bare scalp.[283]

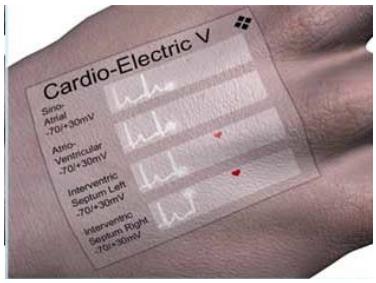

6.6 Special Effects: Visible, Audible, Olfactible, and Tactile

Hair colors and color patterns are not restricted to the natural color palette that might traditionally be available in for synthetic keratinous hair. Virtually any hue of any color can be used. Even more impressively, coloration patterns are limited only by the user's imagination. Simple patterns might include concentric stripes (like the tails of raccoons or ring-tailed lemurs; image, left)[284] or helical barber-pole stripes, individually on every hair, with visual feature sizes ranging from centimeter down to micron scale. Longitudinal bleach features such as stripes running axially down the hairstalk, or features combining both circumferential and longitudinal extent such as circular spots, are also possible using asymmetrical or partitioned tenting.

Lines or dots of various shapes and sizes below the $x_{visible}$ ~ 20 μm maximum limit of human eye resolution (Section 3.7.2) could be used to create Moiré patterns (image, right)[285] or artistic pointillist[286] motifs in the hairbody displaying images of people, places, animals, words or numbers, or creative designs. Bleached hairstalks can receive submicron patches of dyes inserted by

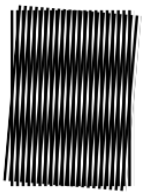

---

[281] Freitas RA Jr. Nanomedicine, Volume I: Basic Capabilities, Landes Bioscience, Georgetown TX, 1999, Section 7.4.6.7, "Macroscale Outmessaging Transducers"; http://www.nanomedicine.com/NMI/7.4.6.7.htm#p3.

[282] http://nanogirl.com/museumfuture1/dermaldisplay.html. See video narrated by the author at http://nanogirl.com/museumfuture1/freitastalk.html.

[283] Surplus power could be supplied by nanorobotic (e.g., flywheel) batteries installed in earrings. A wireless external power supply or a small recharging station for the earrings similar to those employed for modern-day hearing aids can keep the batteries fully charged (Section 5.4).

[284] https://en.wikipedia.org/wiki/Ring-tailed_lemur.
[285] https://en.wikipedia.org/wiki/Moir%C3%A9_pattern.
[286] https://en.wikipedia.org/wiki/Pointillism.

dyebot injectors (Section 6.2), allowing different colors to be embedded on different sides of the hairstalk, or in patterns at least as small as the $r_{injector}$ = 0.5 μm dyebot injector radius.[287]

Many other special effects are possible. For example, nanorobots permanently resident in the hair could emit white or colored light, adding the appearance of visibly coruscating glitter randomly dispersed throughout the hairbody. Up to ~100,000 points of light could form static or dynamic visual patterns, such as: (1) alternating all reds, then all greens, at Christmastime (image, right);[288] (2) synchronized waves of light washing from one side of the head to the other, or emanating radially from a center point somewhere on the scalp; (3) a shifting band of color surrounding just the face; (4) different patterns of different colors (e.g., a happy face when blue lights are on, or an angry face when red lights are on) superimposed on the same hairbody, alternately flashing at various frequencies or upon command; and so forth. Temporal synchronization of resident hairbots for precision optical timing can be provided by good onboard clocks[289] and periodic recalibration by roving databots (Section 5.2).

As another example, hairbots could manufacture and emit tiny amounts of fragrant chemicals, allowing the user to walk around in a cloud of perfume all the time,[290] wherever they go. Working at capacity, a synthesis unit similar to the dyebot's (Section 6.2) with 4.70 x 10^6 onboard chemical synthesis modules could produce perfume at a maximum rate of $m_{perfume} \sim M_{melaninDay} / t_{perfumesynth} \sim 2.64 \times 10^{-5}$ μg/sec, or $M_{perfume} = N_{perfumebots}\ m_{perfume} \sim 2.64$ μg/sec for a population of $N_{perfumebots}$ = 100,000 nanorobots all simultaneously emitting the same scent throughout the hairbody, taking $t_{perfumesynth}$ = 900 sec (15 min). Several common perfume ingredients can be detected by the human nose at air concentrations as low as 2-6 ppb for vanillin,[291] 3 ppb for musk ketone,[292] and 8-38 ppb for limonene (citrus scent),[293] so the emitted

---

[287] Features below the human visual limit of ~20 μm down to the λ = 0.4-0.7 μm wavelengths of visible light might be able to create unusual interference patterns, diffraction gratings, or other specialized optical effects in the hairbody.

[288] https://hairmotive.com/crazy-hairstyles/ ("41. Christmas Balls Hairstyle").

[289] Freitas RA Jr. Nanomedicine, Volume I: Basic Capabilities, Landes Bioscience, Georgetown TX, 1999, Section 10.1, "Nanochronometry"; http://www.nanomedicine.com/NMI/10.1.htm.

[290] Skin-applied perfumes typically last only 2-6 hours; https://en.wikipedia.org/wiki/Perfume#Applying_fragrances.

[291] de-la-Fuente-Blanco A, Ferreira V. Gas Chromatography Olfactometry (GC-O) for the (Semi)Quantitative Screening of Wine Aroma. Foods. 2020 Dec 18;9(12):1892; https://www.ncbi.nlm.nih.gov/pmc/articles/pmid/33353150/.

[292] Ahmed L, Zhang Y, Block E, Buehl M, Corr MJ, Cormanich RA, Gundala S, Matsunami H, O'Hagan D, Ozbil M, Pan Y, Sekharan S, Ten N, Wang M, Yang M, Zhang Q, Zhang R, Batista VS, Zhuang H. Molecular mechanism of activation of human musk receptors OR5AN1 and OR1A1 by (*R*)-muscone and

perfumes might be detectable in a volume of air around the hairbody of $V_{scent} \sim M_{perfume}\ t_{disperse} / c_{perfume}\ \rho_{air} \sim 2.05\ m^3$, with a radius of detectability around the perfume-emitting head of $R_{detectable} = [R_{head}^3 + (3V_{scent} / 4\pi)]^{1/3} \sim 0.788$ m (~2.6 ft), taking $\rho_{air} = 1.29\ kg/m^3$, human head radius $R_{head} = C_{head} / 2\pi = 8.9$ cm assuming human head circumference $C_{head} \sim 56$ cm,[294] the detectable perfume concentration as $c_{perfume} \sim 100$ ppb $= 100 \times 10^{-9}$, and assuming that emitted scents linger in the air for $t_{disperse} \sim 100$ sec before being dispersed by wind or body movements. Since perfume molecules are being manufactured in real time, the user could vary the scent of the perfume cloud on timescales measured in seconds, allowing the scent to serve an olfactory communications purpose.

As yet another example, a fleet of hairbots could be operated as an audio speaker, producing sounds that can be heard by human ears. A minimum acoustic output power of $P_{whisper} \sim 0.1$ microwatt is required to produce an audible whisper, and $P_{speech} \sim 10$ microwatts is the estimated source power for conversational speech as it originates at the vocal cords.[295] Obtaining the minimum necessary whisper-level audible acoustic output power requires a robot input power of $P_{in} \sim (1.525 \times 10^5)\ P_{whisper} = 0.0153$ W, for a hairbot-mounted cylindrical piston of radius 16 μm vibrating at 3000 Hz in air with density $1.29\ kg/m^3$, sound velocity 331.4 m/sec, and viscosity 0.018×10^{-3} kg/m-sec.[296] This amounts to a per-robot power draw of $P_{speakerbot} \sim P_{in} / N_{speakerbots} = 0.153$ μW/robot for $N_{speakerbots} = 100{,}000$ "speaking" nanorobots all simultaneously emitting the same whisper sounds throughout the hairbody, or ~15.3 μW/robot to generate sounds as loud as normal conversational speech. Talking hairbots could collectively issue stern spoken warnings or whisper "sweet nothings",[297] or could emit arbitrary low-volume sounds like the susurrations of gentle breezes moving through trees, the buzzing of bees, the crashing of waves on a rocky beach, or the quiet metronomic ticking of a mechanical clock.

Hairbots equipped with onboard acoustic pressure sensors[298] of similar size to the microspeakers could also hear and respond to verbal instructions spoken by the user using speech recognition

---

diverse other musk-smelling compounds. Proc Natl Acad Sci U S A. 2018 Apr 24;115(17):E3950-E3958; https://www.ncbi.nlm.nih.gov/pmc/articles/PMC5924878/.

[293] Cain WS, Schmidt R, Wolkoff P. Olfactory detection of ozone and D-limonene: reactants in indoor spaces. Indoor Air. 2007 Oct;17(5):337-47; https://pubmed.ncbi.nlm.nih.gov/17880630/. Nagata Y. Measurement of Odor Threshold by Triangle Odor Bag Method. Bulletin of Japan Environmental Sanitation Center 1990;17:77-89; https://www.env.go.jp/en/air/odor/measure/02_3_2.pdf.

[294] https://www.jasfashion.com.au/buying/buying-guides/head-n-hat-size-guide/.

[295] Freitas RA Jr. Nanomedicine, Volume I: Basic Capabilities, Landes Bioscience, Georgetown TX, 1999, Section 4.9.1.5, "Vocalizations"; http://www.nanomedicine.com/NMI/4.9.1.5.htm.

[296] Freitas RA Jr. Nanomedicine, Volume I: Basic Capabilities, Landes Bioscience, Georgetown TX, 1999, Section 7.2.2.1, "Acoustic Radiators", Eqn. 7.7; http://www.nanomedicine.com/NMI/7.2.2.1.htm.

[297] https://www.collinsdictionary.com/us/dictionary/english/sweet-nothings.

[298] Freitas RA Jr. Nanomedicine, Volume I: Basic Capabilities, Landes Bioscience, Georgetown TX, 1999, Section 4.9.1.6, "Environmental Sources"; http://www.nanomedicine.com/NMI/4.9.1.6.htm.

protocols,[299] identify particular speakers by voice biometrics or voice recognition,[300] and possibly enable improved forms of voice stress[301] and emotional prosody[302] analysis. Robots with such sensors could also hear and interpret arbitrary environmental sounds such as music, cash register noises, police sirens, or ultrasonic sounds too high in frequency for human hearing.

Finally, a network of nanorobots present in the hair could provide a pleasant scalp massage. A light touch applies ~1 N of force, so a gentle scalp massage might apply 3-15 N per finger, or require $F_{massage}$ ~ 30 N for a standardized scalp massage.[303] In principle, the individual hairbots comprising the coiffure maintenance system (Section 5.4) could provide a very gentle massage that moves at $v_{massage} \sim P_{coiffurebots} / F_{massage}$ ~ 2 mm/sec. Alternatively, bionic hair (Section 8) consisting of as few as $F_{massage} / F_{strandbot}$ ~ 1000 strandbots could deliver a more vigorous massage with undulating motions at speeds up to $v_{massage} \sim v_{strandbot}$ = 10 cm/sec (Section 8.2).

---

[299] http://en.wikipedia.org/wiki/Speech_recognition.
[300] http://en.wikipedia.org/wiki/Speaker_recognition.
[301] http://en.wikipedia.org/wiki/Voice_stress.
[302] https://en.wikipedia.org/wiki/Emotional_prosody.

[303] English RS Jr, Barazesh JM. Self-Assessments of Standardized Scalp Massages for Androgenic Alopecia: Survey Results. Dermatol Ther (Heidelb). 2019 Mar;9(1):167-178; https://www.ncbi.nlm.nih.gov/pmc/articles/PMC6380978/.

7. Aerial Hairbots and Hairflight

Properly designed nanorobots should be capable of controlled flight[304] and be able to transport payloads more massive than themselves. The leads to the concept of aerial hairbots, nanoflybots, or "**flybots**" – microscale nanorobots attached to every strand of hair on a human head that can tow those strands along arbitrary paths through the air (image, right),[305] enabling hairflight.

We can imagine being able to directly control the 3D physical movement of every single hair in real time, forming active kinematic or reactive patterns with the hair. Such patterns could reflect the user's emotional state, acting as hair emoticons[306] or hair emojis[307] surrounding the user's face, enhancing facial expressions or creating an emotionally expressive shape like a heart or funnel shape framing the face (image, left),[308] a halo above the head, or a linguistically recognizable shape such as a question mark or exclamation point. More playfully, the entire hairbody could be programmed to do a little dance, perhaps tying itself into complex knots[309] and then untying itself, or roiling like the undulating surface of a wind-tossed flag or ocean surface with scores of cresting waves, or seething like a nest of snakes on a Medusa[310] head. The effort may be crudely similar to recent lighting entertainment displays created by glowing radio-controlled aerial drones that are operated in a coordinated manner to draw 3D images in the night sky that are even better than fireworks. By 2024, drone fleets of up to 5000 robots had been fielded (image, right)[311], but the coordinated flybots used as aerial hairbots may number in the millions.

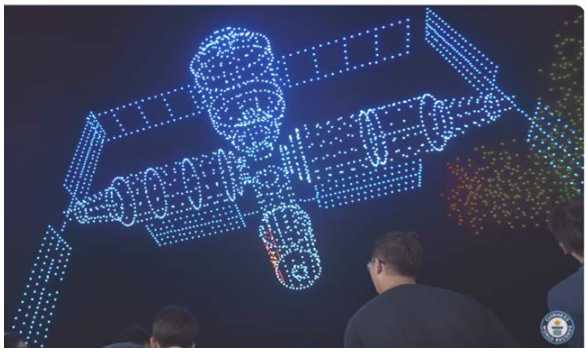

---

[304] Freitas RA Jr. Nanomedicine, Volume I: Basic Capabilities, Landes Bioscience, Georgetown TX, 1999, Section 9.5.3, "Nanoflight"; http://www.nanomedicine.com/NMI/9.5.3.htm.

[305] https://www.pinterest.com/pin/23221754315224106/.
[306] https://en.wikipedia.org/wiki/Emoticon.
[307] https://en.wikipedia.org/wiki/Emoji.
[308] https://www.pinterest.com/pin/573716440003722166/.
[309] https://en.wikipedia.org/wiki/Knot.
[310] https://en.wikipedia.org/wiki/Medusa.
[311] https://www.youtube.com/watch?app=desktop&v=44KvHwRHb3A.



Flybots are aerial hairbots that can attach to a single hairstalk and lift it into the air, making it possible to imbue otherwise difficult coiffures (above left,[312] middle,[313] right,[314] and below[315]) with real-time programmed hair motion and permitting fast reconfiguration of the coiffure on timescales on the order of ~1 sec. To satisfy all the performance requirements and technical constraints on hairflight, flybots probably must be slightly larger than the hairbots described elsewhere in this paper, here modeled as a cubical device L_{flybot} = 200 μm on a side, density ρ_{flybot} ~ 1 gm/cm^3, volume $V_{flybot} = L_{flybot}^3$ ~ 8 x 10^6 μm^3, and mass m_{flybot} ~ 8 μg.

The power requirements for robot motion in fluids is in part determined by the Reynolds number,[316] defined as the ratio of inertial forces (where mass and gravity have dominant effect) to viscous forces (where surface area and viscous drag are dominant) acting on the robot. Taking v_{flybot} ~ 10 cm/sec, air density ρ_{air} = 1.29 kg/m^3 and absolute viscosity η_{air} ~ 1.813 x 10^{-5} Pa-sec, the Reynolds number $N_R = F_{inertial} / F_{viscous} = \rho_{air} v_{flybot} L_{flybot} / \eta_{air}$ = **100** for ~2 cm inertial-dominated ~1 cm robots, **0.01** for viscous-dominated ~2 μm robots, and **1** for "transitional" ~200 μm robots whose behavior is not solidly in either camp. Since our flybots fall in the transitional regime, we will estimate the lift and power requirements for both viscous and inertial regimes, then conservatively choose the least favorable of the two to conclude our analysis.

In the **viscous regime**, the robot must generate enough force to drag a strand of hair through viscous air at the desired velocity. Here we assume that each hairstalk has one flybot attached to it for every $L_{hairsegment}$ = 1 cm of length, providing ~1 cm of "feature resolution" in the dynamic aerial coiffure, giving $n_{flybots}$ = 30 flybots on each $L_{hairstalk}$ = 30 cm long hairstalk of radius $r_{hairstalk} = d_{hairstalk} / 2$ = 40 μm. The drag force[317] is largest if the hairstalk is dragged through the air in a

---

[312] https://hairmotive.com/crazy-hairstyles/ ("46. Running Air Hairstyle").
[313] https://thewondrous.com/wp-content/uploads/2010/03/odd-haircuts08_display.jpg.
[314] https://hairmotive.com/crazy-hairstyles/ ("14. Lady Gaga Hat Hairstyle").
[315] https://hairmotive.com/crazy-hairstyles/ ("32. Classic Waves Hairstyle").
[316] https://en.wikipedia.org/wiki/Reynolds_number.

[317] Freitas RA Jr. Nanomedicine, Volume I: Basic Capabilities, Landes Bioscience, Georgetown TX, 1999, Section 9.4.2.4, "Force and Power Requirements"; http://www.nanomedicine.com/NMI/9.4.2.4.htm.

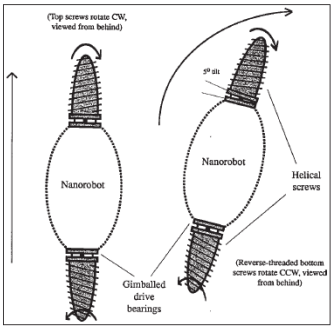

direction normal to its central axis, in which case the required force is $F_{dragN} = 8\pi\ \eta_{air}\ L_{hairsegment}\ v_{flybot} / [1 + \ln(L_{hairsegment}^2 / r_{hairstalk}^2)] = 4.56 \times 10^{-7}$ N. The output power requirement is then $P_{flybotOUT} = F_{dragN}\ v_{flybot} = 0.0456$ μW.[318] The drag force on the hair strand must be overcome by the flybot pushing on the hair. A simple microscale screw drive (schematic, left)[319] has been estimated to have a net mechanical efficiency of $e_{\%} \sim 27\%$, increasing the required nanorobot power input to $P_{flybotIN} = P_{flybotOUT} / e_{\%} \sim$ **0.169 μW**.

In the **inertial regime**, a hovering[320] flybot must produce $F_{lift} = m_{hairsegment}\ g = 6.51 \times 10^{-7}$ N of lift force to offset the downward pull of gravity at g = 9.81 m/sec^2, taking hair segment mass $m_{hairsegment} = \pi\ r_{hairstalk}^2\ L_{hairsegment}\ \rho_{hair} = 66.4$ μg, hair density $\rho_{hair} \sim 1.32$ gm/cm^3, and $L_{hairsegment} =$ 1 cm. To generate this lift, the flybot operating in the inertial regime could pump air out of an exhaust nozzle of aperture area $A_{nozzle} = (100\ \mu m)^2 = 10{,}000\ \mu m^2$ at a velocity v_{air} and a mass flow rate of $\mathscr{M}_{air}$ kg/sec, requiring a power consumption of $P_{pump} = 1/2\ \mathscr{M}_{air}\ v_{air}^2$ and generating a lifting force of $F_{pump} = P_{pump} / v_{air} = 1/2\ \mathscr{M}_{air}\ v_{air} = 1/2\ \dot{V}_{air}\ \rho_{air}\ v_{air} = F_{lift} = m_{hairsegment}\ g$, with volume flow rate $\dot{V}_{air} = \mathscr{M}_{air} / \rho_{air} = 2\ m_{hairsegment}\ g / v_{air}\ \rho_{air} = A_{nozzle}\ v_{air}$, hence $v_{air} = (2\ m_{hairsegment}\ g / A_{nozzle}\ \rho_{air})^{1/2} = 10$ m/sec and the required flybot hover power is $P_{hover} = F_{lift}\ v_{air} =$ **6.54 μW**. Since $P_{hover} >> P_{flybotIN}$, we adopt P_{hover} as our estimated flybot power requirement.

If 10% of flybot volume is reserved for flywheel energy storage at energy density $E_d = 90$ MJ/L,[321] then the onboard storage capacity of $E_{flybot} = 0.1\ V_{flybot}\ E_d = 0.072$ J gives a flight time on battery power alone of $t_{batteryflight} = E_{flybot} / P_{hover} = 11{,}000$ sec ~ **3 hours**. The entire flybot fleet, consisting of $N_{flybots} = n_{flybots}\ N_{hairs} = 3 \times 10^6$ flybots deployed onto $N_{hairs} \sim 100{,}000$ hairstalks, has a total volume $V_{AllFlybots} = N_{flybots}\ V_{flybot} \sim 24$ cm^3 (~ half the size of a 41 cm^3 golf ball), mass $M_{AllFlybots} = N_{flybots}\ m_{flybot} \sim 24$ gm (~0.8 oz), and power draw $P_{AllFlybots} = N_{flybots}\ P_{hover}$ ~ 20 W (~ a small light bulb).

---

[318] By comparison, the viscous drag force on the robot, treated as a squat cylinder, is $F_{bot} = 3.82 \times 10^{-9}$ N with drag power only $P_{bot} = 0.000382$ μW, only 0.8% of the drag power required to tow the hairstalk – or, in other words, negligible.

[319] Freitas RA Jr. Nanomedicine, Volume I: Basic Capabilities, Landes Bioscience, Georgetown TX, 1999, Section 9.4.2.5.2, "Inclined Plane"; http://www.nanomedicine.com/NMI/9.4.2.5.2.htm; Fig. 9.24, "Schematic of screw drive"; http://www.nanomedicine.com/NMI/Figures/9.24.jpg.

[320] Except at the highest airspeeds, hovering requires more power than forward flight, as shown in the standard power curves for helicopters; e.g., Harris J. Implications of the Power Curve on Single-engine Flight in a Twin-engine Helicopter. Helicopter Safety (Flight Safety Foundation) 1992 Mar/Apr;18(2); https://flightsafety.org/hs/hs_mar-apr92.pdf.

[321] Freitas RA Jr. Energy Density. IMM Report No. 50, 25 June 2019; Section 5.3.2, "Rotational Motion"; http://www.imm.org/Reports/rep050.pdf.

Users who wish to indefinitely extend nanorobot flight time (image, left)[322] beyond 3 hours can wear a necklace[323] or hairstyle accessory[324] that wirelessly broadcasts continuous radiofrequency (rf) power to the flybots. From previous work citing experimental results,[325] a $2r_{coil}$ = 14 cm diameter transmitter coil (about the diameter of the human neck) with 11 turns and a 10 volt peak driving voltage at 2 MHz with P_{coil} = 4 W power of rf energy has been demonstrated to deliver a received power density of $P_d \sim 10^6$ W/m^3 to a 400 μm diameter ferrite core receiver. Thus, in principle, $V_{AllFlybots} \sim 24$ cm^3 of flybots could receive $P_{rf} = V_{AllFlybots} P_d \sim 24$ W by this means. The aforementioned coil has an areal rf power density of $P_{coil} / \pi r_{coil}^2 = 260$ W/m^2, well below the allowable human occupational safety limit of 1000 W/m^2 for rf radiation at 2 MHz.[326]

Neighboring flybots arrayed on hairstalks can emit low-power electromagnetic (e.g., invisible infrared) or acoustic (e.g., inaudible ultrasound) signals that can be detected by each other over centimeter ranges. Starting from its baseline hairbody spatial position in the Current Coiffure Map, each robot can measure the changing angular deviations of adjacent devices as they fly, then calculate its new 3D position relative to its neighbors. Information exchange with roving databots (Section 5.2) allows periodic recalibration of the onboard estimated Aerial Coiffure Map to correct for the gradual accumulation of angular measurement errors. Hairstyling accessories such as headbands or barrettes (commonly employed simply to hold hair in place or to enhance its ornamental appearance) can be loaded with nanomachinery to provide supplemental mechanical, computational, or power resources that enable more rapid deployment and reconfiguration of the flybot fleet. For example, a 1 cm^3 cache of nanomachinery can hold nanocomputers capable of ~10^{24} bit/sec bursts of data processing[327] or can hold up to $E_d \sim 90 \times 10^9$ μW-sec of stored energy.

Interestingly, a ~2 cm^3 helium-filled balloon would be required to lift a single 1990 μg hairstalk.

---

[322] A small number of flybots would need to be placed at sub-millimeter intervals along a sufficient number of hairstalks to create the persistent horsehead hair-sculptures shown here; https://www.boredpanda.com/funny-hair-styles/ (#23).

[323] https://en.wikipedia.org/wiki/Necklace.
[324] https://en.wikipedia.org/wiki/Hair_clip.

[325] Freitas RA Jr. Nanomedicine, Volume I: Basic Capabilities, Landes Bioscience, Georgetown TX, 1999, Section 6.4.2, "Inductive and Radiofrequency Power Transmission"; http://www.nanomedicine.com/NMI/6.4.2.htm

[326] Cleveland RF Jr., Sylvar DM, Ulcek JL. Evaluating Compliance with FCC Guidelines for Human Exposure to Radiofrequency Electromagnetic Fields. OET Bulletin 65, Edition 97-01, Aug 1997, p. 67, Table 1. "Limits for Maximum Permissible Exposure (MPE)"; https://transition.fcc.gov/oet/info/documents/bulletins/oet65/oet65.pdf.

[327] Freitas RA Jr. Nanomedicine, Volume I: Basic Capabilities, Landes Bioscience, Georgetown TX, 1999, Section 10.2.1, "Nanomechanical Computers"; http://www.nanomedicine.com/NMI/10.2.1.htm.

8. Bionic Hair

For the most adventurous and technophilic fashionistas, bionic hair provides the most complete solution to the challenge of coiffure flexibility, maintenance, and control.

To install bionic hair, the user's N_{hairs} ~ 100,000 natural hairstalks are depilated to the base.[328] These are replaced[329] with a similar number of strands of artificial nanomechanical hair, which we will call "**strandbots**", entirely composed of strong diamondoid nanomachinery. Each such artificial hairstalk is essentially an independently controlled single robotic tentacle manipulator that incorporates:

(1) arbitrary programmable color variation (Section 3.7.2) along its entire length, including the ability to project images or video displays throughout the strandbody (i.e., the entire population of strandbots) such as the appearance of flapping flags or flickering flames;[330]

(2) a wider variety of visible,[331] audible, olfactible, and tactile special effects than are available using standalone hairbots (Section 6.6), partly due to increased onboard nanomachinery;

(3) rapid length control[332] of strandbots using telescoping segments[333] equipped with metamorphic surfaces;[334]

---

[328] As a conservative measure, the follicular bulb of each hair should be left in place, but chromallocytes should insert altered chromosomes into the nuclei of generative cells to place them in a continuous (but nanorobotically reversible) "telogen" or resting phase of the hair cycle, during which the hair follicle is dormant and growth of the hair shaft does not occur. Typically 10%-15% of all hairs on the body are in resting phase at any given time and can remain in this state for a variable amount of time – from a few weeks for eyelashes to nearly 1 year for scalp hair. Hoover E, Alhajj M,Flores JL. Physiology, Hair. StatPearls [Internet], National Library of Medicine, NIH, 30 Jul 2023; https://www.ncbi.nlm.nih.gov/books/NBK499948/. This retains reversibility in case the user ever wants to abandon the bionic hair and return to natural hair growth.

[329] In principle, natural hair could be left in place to continue to grow, with bionic hair strands installed in the interfolliclar spaces on the scalp. This would result in the presence of two independent coiffure systems with wholly different behaviors and maintenance requirements, the aesthetic and logistic complications of which are beyond the scope of this paper.

[330] It may be possible to create holographic displays using strandbots that can controllably radiate light of various visible frequencies with submicron feature sizes.

[331] For example, flecks or spots of color in geometric shapes (e.g., triangles, stars) could appear and disappear, or move around on the hairbody, forming visual patterns varying in time. Sensors on the strandbot surface could detect changes in room or skin temperature and alter color in response, or detect the elevated warmth or CO_2 content of a human breath blown across the hair, causing the hair to ripple in patterns of color like a wave of wind undulating across a field of wheat.

[332] Design constraints will dictate the maximum and minimum lengths that a telescoping strandbot can reversibly assume.



(4) internal nanomotors[335] to enable instantaneous flexing and large scale movement of microscale strandbot tentacles throughout 3D circumcranial space, with even more coiffure mobility and flexibility than is provided by flybots (Section 7), including fanciful dynamic representations of moving 3D objects such as creeping hands (above, left),[336] barking dogs (above, center),[337] or melodious musical instruments (above, right);[338]

(5) firm attachment to a strong scalp- or skull-embedded biocompatible nanomechanical anchor that provides sufficient dislodgement resistance when exposed to leverage forces transmitted through the artificial hairstalk, with secure links to nanocomputers and energy storage units;

(6) thermally conductive pathways and radiator surfaces sufficient to facilitate airflow-driven dissipation of excess heat;

(7) additional special optical effects available from modifying the non-keratinous strandbot surface, such as mirror hair (e.g., strandbots with perfectly reflective surfaces), iridescent hair (e.g., fixed-geometry diffraction gratings), or monocolor hair (e.g., variable-geometry diffraction gratings,[339] filters and photonic crystals,[340] or controlled structural coloration[341] as employed by various plants and animal species);

---

[333] Freitas RA Jr. Nanomedicine, Volume I: Basic Capabilities, Landes Bioscience, Georgetown TX, 1999, Section 5.3.2.3, "Telescoping Model"; http://www.nanomedicine.com/NMI/5.3.2.3.htm.

[334] Freitas RA Jr. Nanomedicine, Volume I: Basic Capabilities, Landes Bioscience, Georgetown TX, 1999, Section 5.3, "Metamorphic Surfaces"; http://www.nanomedicine.com/NMI/5.3.htm.

[335] Freitas RA Jr. Nanomedicine, Volume I: Basic Capabilities, Landes Bioscience, Georgetown TX, 1999, Section 6.3, "Power Conversion"; http://www.nanomedicine.com/NMI/6.3.htm.

[336] https://hairmotive.com/crazy-hairstyles/ ("34. Hands Hairstyle").
[337] https://hairmotive.com/crazy-hairstyles/ ("26. Funny Dog Wig Hairstyle").
[338] https://hairmotive.com/crazy-hairstyles/ ("27. The Violin Hairstyle").

[339] Creating a programmable monocolor strandbot surface would require selectively reflecting or diffracting light of only one wavelength (color) while minimizing the dispersion of other wavelengths, possibly by adjusting the spacing between the lines of the diffraction grating (e.g., grating periods and groove depths in the 0.3-0.7 μm range for visible light) on the strandbot surface to change the angles at which different wavelengths of light are diffracted. Precise design of the grating spacing can enhance the reflection of a specific wavelength while suppressing others, making the surface appear to be a single color. Rapid

(8) large numbers of onboard nanocomputers[342] throughout the artificial hairstalk and additional nanocomputers in the base of each device to provide continuous positional control and Coiffure Map updating using high-bandwidth hard datalinks[343] between all strandbots that are anchored to the scalp; and

(9) the ability to provide some measure of physical protection for the user's head.

A coiffure composed entirely of $N_{strandbots}$ = 100,000 strandbots – that is, the "strandbody" – having the same dimensions and numbers as natural hair would have a total solid volume of $V_{strandbody} = N_{strandbots}\ V_{strandbot}$ = **151 cm^3** and strandbody mass $M_{strandbody} = \rho_{strandbot}\ V_{strandbody}$ = 302 gm, taking strandbot volume $V_{strandbot} = \pi\ r_{strandbot}^2\ L_{strandbot}$ = 1.51 mm^3 and strandbot mass $m_{strandbot} = \rho_{strandbot}\ V_{strandbot}$ = 3020 μg, with $r_{strandbot} \sim d_{hairstalk} / 2$ = 40 μm, $L_{strandbot} \sim L_{hairstalk}$ = 30 cm, and $\rho_{strandbot}$ = 2 gm/cm^3.[344] Strandbots may be intricately patterned, extremely durable (if composed of diamondoid materials),[345] and manufactured using a specialized nanofactory having similar productivity and power requirements as the hair mill (Section 4.1).

---

variation among different monocolors in specific locations along the strandbot may be possible if grating angles and spacing are physically manipulated via a user-controlled metamorphic surface; Freitas RA Jr. Nanomedicine, Volume I: Basic Capabilities, Landes Bioscience, Georgetown TX, 1999, Section 5.3, "Metamorphic Surfaces"; http://www.nanomedicine.com/NMI/5.3.htm.

[340] A thin coating that acts as a bandpass filter would allow only a specific range of wavelengths to pass through or be reflected, effectively blocking all wavelengths outside of a desired band, resulting in the appearance of a single color. A narrowband reflective coating could be designed to reflect only the desired color while absorbing or transmitting other wavelengths. Photonic crystals with specific lattice parameters might be able to create a band gap for certain wavelengths, thereby allowing only a specific color to be reflected.

[341] https://en.wikipedia.org/wiki/Structural_coloration.

[342] Freitas RA Jr. Nanomedicine, Volume I: Basic Capabilities, Landes Bioscience, Georgetown TX, 1999, Section 10.2.1, "Nanomechanical Computers"; http://www.nanomedicine.com/NMI/10.2.1.htm.

[343] Freitas RA Jr. Nanomedicine, Volume I: Basic Capabilities, Landes Bioscience, Georgetown TX, 1999, Section 7.3.1, "Fiber Networks"; http://www.nanomedicine.com/NMI/7.3.1.htm.

[344] Each strand could instead be composed of a chain of mechanically linked flybots (Section 7) whose external shape and color were designed to closely mimic segments of the desired appearance of the hair, requiring a fleet of $N_{flyhair} \sim V_{strandbody} / V_{flybot} \sim 18.9 \times 10^6$ flybots. The flybots comprising the ~151 cm^3 flybody fleet could detach from the user's head at sleeptime and flitter into a tennis-ball-sized storage garage for recharging overnight, then re-emerge in the morning like a cloud of intelligent swarming gnats to reassemble itself into 100,000 flybot hairstrands on the user's head. Non-flying legged hairbots could perform a similar function, somewhat analogous to utility fog, but with lesser elegance.

[345] In principle, the synthetic hair could be made of almost any material from plastic to metal, fiber optic cables (https://www.science.org/doi/10.1126/science.ado5922), nanotubes, or even computronium (https://en.wikipedia.org/wiki/Computronium).

8.1 Strandbot Computation

It is difficult to estimate the exact processing and memory requirements to operate a strandbot. If we assume that an $L_{strandbot}$ = 30 cm device is operated in $x_{segment}$ = 100 μm distinct segments, then just specifying the name and xyz coordinates for $n_{segments} \sim L_{strandbot} / x_{segment}$ = 3000 segments to a spatial resolution of $x_{segment}$ would require ~4 log(3000) / log(2) ~ 46 bits. If we assume that $J_{strandbot} \sim 200$ bits can fully specify the position, color, configuration, and activity state of each strandbot segment, then a strandbot state map has $I_{state} = n_{segments} J_{strandbot}$ = 600,000 bits. Storing or recording $t_{hr} \sim 1$ hour of choreographed programmed actions with a time resolution of $t_{reso} \sim 1$ sec implies a requirement for $I_{strandstore} = I_{state} (t_{hr} / t_{reso}) \sim$ **2.16×10^9 bits of onboard data storage per strandbot**. If onboard nanocomputers must perform $n_{ops} \sim 1000$ operations on each bit of the state map to calculate each shift between states using 64-bit words, this implies a requirement for $\Omega_{strandcomp} = 64\ n_{ops}\ I_{state} \sim$ **38.4×10^9 bits/sec of onboard processing speed per strandbot**.

Mature diamondoid nanocomputers can achieve a storage density of $i_{nano} = 10^7$ bits/μm^3 with a $\tau_{nano} = 10^{10}$ bit/sec data access speed (Section 3.1) and a specific processing power of $U_{nano} \sim 10^{30}$ bit/sec-m^3.[346] Assigning 1% of the total strandbot hairbody volume to active nanocomputers ($V_{strandnanocomp}$ = 1.51 cm^3) would allow a maximum strandbody computational capacity of $\Omega_{strandbody} = U_{nano}\ V_{strandnanocomp} = 1.51 \times 10^{24}$ bits/sec at a power draw of $P_{strandbodyC} = \Omega_{strandbody}\ E_{Landauer300K}$ = 4340 W, or $\Omega_{strandbot} = \Omega_{strandbody} / N_{strandbots} = 1.51 \times 10^{19}$ bits/sec and $P_{strandbotC} = P_{strandbodyC} / N_{strandbots}$ = 43,400 μW for individual strandbots, for $E_{Landauer300K} \sim 2.87 \times 10^{-21}$ J/bit. Such high power requirements virtually ensure that full nanocomputer capacity will be used only rarely or in brief surges. Assigning another 1% of strandbody volume ($V_{strandnanomem}$ = 1.51 cm^3) to diamondoid computer memory would allow the strandbody to store $I_{strandbody} = i_{nano}\ V_{strandnanomem} = 1.51 \times 10^{19}$ bits, or $I_{strandbody} / N_{strandbots} = 1.51 \times 10^{14}$ bits per strandbot.

8.2 Strandbot Force and Power

If $f_{motor} \sim 10\%$ of the solid strandbot volume is assigned to actuator nanomachinery of volume $V_{actuator} = f_{motor}\ V_{strandbot}$ = 0.151 mm^3 having an active power density of $P_{d\text{-}actuators} \sim 0.02$ MW/L that may be typical for medical nanorobots,[347] then each strandbot could exert a maximum force up to $F_{strandbot} \sim P_{d\text{-}actuators}\ V_{actuator} / v_{strandbot} \sim 0.0302$ N when moved at a velocity of $v_{strandbot}$ = 10 cm/sec, consuming $P_{strandmotors} = P_{d\text{-}actuators}\ V_{actuator} \sim 3020$ μW of continuous motor power during this movement. Total strandbody mechanical power would then be $P_{strandbodyM} = N_{strandbots}\ P_{strandmotors}$ = 302 W.

---

[346] Assuming 1 GHz operation of a (400 nm)^3 CPU using 64-bit words: (64 bits/operation) (10^9 operations/sec) / (400 nm)^3 = 1 x 10^{30} bits/sec-m^3; Drexler KE. Nanosystems: Molecular Machinery, Manufacturing, and Computation, John Wiley & Sons, New York, 1992, Chapter 12 "Nanomechanical Computational Systems"; https://www.amazon.com/dp/0471575186/.

[347] e.g., respirocytes (~0.12 MW/L), microbivores (~0.032 MW/L), and chromallocytes (~0.0029 MW/L); Freitas RA Jr. Energy Density. IMM Report No. 50, 25 June 2019; Chapter 1, "Introduction"; http://www.imm.org/Reports/rep050.pdf.

Theoretically, a force of 0.0302 N should be enough to lift a single $m_{object} = F_{strandbot} / g \sim 3$ gm marble against the pull of gravity,[348] and then throw the marble at a velocity up to $v_{object} = (2 P_{strandmotors} x_{act} / m_{object})^{1/2} \sim 0.45$ m/sec, assuming the strandbot executes an $x_{act} = 10$ cm throwing arc, since marble kinetic energy $E_{object} = P_{strandmotors} x_{act} / v_{object} = 1/2 m_{object} v_{object}^2$. The key technical challenge will be to design a strandbot collective behavior protocol that avoids the classical mechanical limitations of bending stiffness and buckling forces on rods. For example, a solid diamond rod of radius $r_{strandbot} = 40$ μm and length $L_{strandbot} = 30$ cm with Young's modulus of $Y_{diamond} \sim 10^{12}$ N/m^2 is deflected d = 5 cm by a lateral force of only $F_{deflect} = 3\pi Y_{diamond} r_{strandbot}^4 d / 4 L_{strandbot}^3 = 11$ μN at the tip, and will buckle if a force of $F_{buckle} = \pi^3 Y_{diamond} r_{strandbot}^4 / 4 L_{strandbot}^2 = 0.0002$ N is applied coaxially at the tip.[349] But if a dozen strandbots bunch together into a tight cable with a collective radius of ~140 μm, the buckling force increases to 0.0302 N.

A 0.0302 N force would also be enough to raise up to $F_{strandbody} / M_{hairstalk} g \sim 1550$ natural hairstalks, each of length 30 cm and mass $M_{hairstalk} \sim 1990$ μg (Section 6.3.3), and maneuver them as a group at similar speed – suggesting a possible use for strandbots in place of guidestalks for the task of rapidly reconfiguring coiffures (Section 5.4). While these artificial mechanical hair strand robots are very strong, they'd still have to be 18-28 times stronger to rip a natural human hairstalk out of its follicle base in the scalp, a feat which requires an average of ~0.85 N (86.61 gm) for actively growing hair in anagen phase or ~0.53 N (53.69 gm) during the growth-dormant telogen phase when hairs are more weakly held,[350] and individual hairs can support a weight of ~1.6 N before breaking.[351] (Ripping the entire scalp off the skull may require up to 65,000 N.[352])

---

[348] If a single strandbot could lift 3 gm, this implies that 100,000 strandbots on a human scalp could lift ~300,000 gm = 300 kg. Even biological hair can could handle this stress, since the current world record for human "hair hanging" in 2024 was ~181 kg (126 kg of held weights plus ~55 kg of body weight)* and strandbots could be designed with even stronger scalp attachments that natural hair follicles. Amusingly, the 2024 world record for vehicular hair towing was 12,216 kg (26,932 lbs).**

* https://voyagedenver.com/interview/rising-stars-meet-stephanie-little-thunder-morphet-tepp-of-me-fort-collins-phantom-circus-denver/.

** https://www.hindustantimes.com/trending/woman-from-india-pulls-vehicle-by-hair-creates-world-record-watch-101641272530833.html.

[349] Freitas RA Jr. Nanomedicine, Volume I: Basic Capabilities, Landes Bioscience, Georgetown TX, 1999, Section 9.3.1.2, "Nanocilium Manipulators"; http://www.nanomedicine.com/NMI/9.3.1.2.htm.

[350] Muthuvel K, Chakravati S, Nair S. Assembling a Hand-Held Trichotillometer and Determination of Epilation Force in Normal Individuals. Indian Dermatol Online J. 2017 Mar-Apr;8(2):111-114; https://www.ncbi.nlm.nih.gov/pmc/articles/PMC5372430/.

[351] Hess WM, Seegmiller RE, Gardner JS, Allen JV, Barendregt S. Human hair morphology: a scanning electron microscopy study on a male Caucasoid and a computerized classification of regional differences. Scanning Microsc. 1990 Jun;4(2):375-86; https://digitalcommons.usu.edu/cgi/viewcontent.cgi?article=2022&context=microscopy.

[352] If the Warner-Bratzler shear force for cutting raw meat away from bone is $F_{meat} \sim 100$ N, then assuming a knife of contact width w ~ 1 mm and contact length L ~ 10 cm the shear stress for separating meat from bone is $\tau_{meat} = F_{meat} / w L \sim 10^6$ N/m^2 and the uniformly-applied force required to pull the scalp off the skull bone may be crudely estimated as $\tau_{meat} A_{scalp} \sim 65{,}000$ N (6630 kg).

Assuming energy can be stored aboard a strandbot in flywheel batteries having an energy density of E_d ~ 90 MJ/L,[353] then assigning 10% of the total strandbody solid volume ($V_{strandbattery}$ = 15.1 cm^3) to battery energy storage implies that the strandbody can store $E_{strandbody} = E_d\ V_{strandbattery}$ ~ 1.36 MJ,[354] or $E_{strandbot} = E_{strandbody} / N_{strandbots}$ ~ 13.6 J per strandbot.[355] That's enough energy to continuously operate the entire force-generating nanomachinery for $E_{strandbot} / P_{strandmotors}$ = 4500 sec (~1.3 hours).[356] It could operate the maximum number of active nanocomputers for a total of $E_{strandbot} / P_{strandbotC}$ = 313 sec of runtime. It could also operate the maximum number of active nanocomputers for $E_{strandbot} / P_{strandbotC}$ = 313 sec. If strandbody nanocomputer heat generation was held to the ~20 W power draw of the human brain, the strandbody would only be processing ~6.96 x 10^{21} bits/sec, or ~6.96 x 10^{16} bits/sec per strandbot, which it could do for ~68,000 sec (~19 hours). But strandbot nanocomputers that only needed to process $\Omega_{strandcomp}$ ~ 38.4 x 10^9 bits/sec could do so for $E_{strandbot} / \Omega_{strandcomp}\ E_{Landauer300K}$ ~ 1.23 x 10^{11} sec – in other words, indefinitely.

8.3 Defensive Hairbots

A human head of average mass m_{head} ~ 5 kg,[357] could potentially be protected from harm due to collisional impacts if the strandbot tentacle manipulators surrounding the head can act with sufficient speed and counterforce to neutralize the threat.

Consider a standing human who suddenly **falls to the ground** for some reason. If the head free-falls from a height h_{fall} = 2 meters to the ground and if the head is brought to a halt by impact with concrete floor due to the compression of scalp tissue of thickness x_{scalp} ~ 8 mm (occipital region) to 3 mm (forehead),[358] then the velocity at impact is $v_{impact} = (2\ g\ h_{fall})^{1/2}$ = 6.36 m/sec and the deceleration upon impact is $a_{floor} = v_{impact}^2 / 2\ x_{scalp}$ = 2450-6540 m/sec^2 = **250-667 gees** during an impact time of $t_{floor} = (2\ x_{scalp} / g)^{1/2}$ = 40-25 msec.

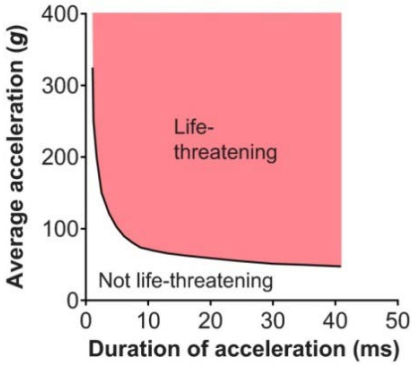

---

[353] Freitas RA Jr. Energy Density. IMM Report No. 50, 25 June 2019; Section 5.3.2, "Rotational Motion"; http://www.imm.org/Reports/rep050.pdf.

[354] This is roughly equivalent to the energy released by exploding 450 gm of gunpowder.

[355] External illumination falling on the strandbody could produce $P_{light} = \varepsilon_{light}\ A_x\ I_{light}$ = 0.13-48 W of power assuming external illumination levels of I_{light} = 10 W/m^2 (indoors) to 100 W/m^2 (outdoors) using photoelectric cells with ε_{light} ~ 20% efficiency and an exposed collector area between $A_x = A_{scalp}$ = 0.065 m^2 (minimum) and $A_x = 2\ r_{strandbot}\ L_{strandbot}\ N_{strandbots}$ = 2.4 m^2 (maximum).

[356] If the user flies only half of their bionic hairs, the energy store would last twice as long; and so forth.

[357] https://www.gwosteopathy.co.uk/much-head-weigh/.

[358] Hayman LA, Shukla V, Ly C, Taber KH. Clinical and imaging anatomy of the scalp. J Comput Assist Tomogr. 2003 May-Jun;27(3):454-9; https://pubmed.ncbi.nlm.nih.gov/12826816/. Seery GE. Surgical anatomy of the scalp. Dermatol Surg. 2002 Jul;28(7):581-7; https://pubmed.ncbi.nlm.nih.gov/12135510/.

The Wayne State Tolerance Curve (chart, above)[359] shows that an acceleration of this magnitude is potentially life-threatening.

However, if $L_{strandbot}$ = 30 cm long strandbots can interpose themselves between the falling head and the onrushing ground sufficiently fast to decelerate the head by applying a resistive force across a distance of x_{act} = 10 cm, then the deceleration experienced by the falling head drops to $a_{cushion} = v_{impact}^2 / 2\ x_{act}$ = 202 m/sec^2 = **20.6 gees** during an impact time of $t_{cushion} = (2\ x_{act} / g)^{1/2}$ = 143 msec, which is no longer life-threatening. (The same paper[360] mentions that the lowest measured NFL football deceleration observed to cause concussion injury is 48 gees.)

Dissipating the energy of impact $E_{head} \sim 1/2\ m_{head}\ v_{impact}^2$ = 101 J during the strandbot-cushioned $t_{cushion}$ = 143 msec deceleration time requires a resistive mechanical power expenditure of $P_{cushion} = E_{head} / t_{cushion}$ = 707 W. But the strandbots described in Section 8.2 have a deliverable mechanical power of only $P_{strandmotors} \sim$ 3020 μW/strandbot, so performing the cushioning maneuver would require $P_{cushion} / P_{strandmotors}$ = 234,000 of these strandbots, more than twice the number ($N_{strandbots}$ = 100,000) of available strandbots.

However, the potentially available onboard stored energy is $E_{strandbot} \sim$ 13.6 J/strandbot (Section 8.2), so in principle the cushioning maneuver could be performed by as few as $E_{head} / E_{strandbot} \sim 8$ "defensive strandbots" if these robots could be redesigned to enable a quicker release of the onboard energy store in the form of mechanical force during the $t_{cushion}$ = 143 msec deceleration time, in which case each defensive strandbot would be briefly producing $E_{strandbot} / t_{cushion}$ = 95.1 W. Such a high power level would generate unacceptable heating in just a few milliseconds. If we specify that diamondoid defensive strandbots must only rise ΔT = 20 K in temperature while performing the cushioning maneuver, then the maximum deployable mechanical power is $P_{strandbotMAX} = \Delta T\ C_{diamond}\ V_{strandbot} / t_{cushion}$ = 0.384 W per strandbot, taking the heat capacity of diamond as $C_{diamond}$ = 1.82 x 10^6 J/m^3-K. The $E_{discharge} = P_{strandbotMAX}\ t_{cushion}$ = 0.0549 J/strandbot discharge energy per event could be replenished by photoelectric cells that cover the entire strandbot surface in $t_{replace} \sim E_{discharge} / 2\ r_{strandbot}\ L_{strandbot}\ \varepsilon_{light}\ I_{light} \sim$ 110-1100 sec, taking ε_{light} = 20% and I_{light} = 100 W/m^2 (outdoors) to 10 W/m^2 (indoors).

In this case, $N_{cushion} = P_{cushion} / P_{strandbotMAX}$ = **1840 defensive strandbots** (~2% of all robots) could perform the **cushioning maneuver**, burning ~707 W during the ~143 msec action. The power density of a high-power defensive strandbot in this scenario would be a quite reasonable $P_{strandbotMAX} / V_{strandbot}$ = 0.254 MW/L, roughly comparable to the estimated 0.121 MW/L peak power density of the respirocyte medical nanorobot.[361] A similar number of defensive strandbots

---

[359] Namjoshi DR, Good C, Cheng WH, Panenka W, Richards D, Cripton PA, Wellington CL. Towards clinical management of traumatic brain injury: a review of models and mechanisms from a biomechanical perspective. Dis Model Mech. 2013 Nov;6(6):1325-38; https://www.ncbi.nlm.nih.gov/pmc/articles/pmid/24046354/.

[360] *ibid.*

[361] Freitas RA Jr. Exploratory Design in Medical Nanotechnology: A Mechanical Artificial Red Cell. Artif Cells Blood Subst Immobil Biotech. 1998;26:411-430; https://www.tandfonline.com/doi/pdf/10.3109/10731199809117682.

should provide comparable head protection during **car crashes**, where a 2.75 msec impact deceleration of a car traveling at 65 mph freeway speed could impose ~215 gees on passengers wearing a seatbelt or ~1076 gees on passengers without a seat belt.[362] An onboard displacement accelerometer ~1 μm in radius should detect local accelerations as small as 0.004 gees in a ~1 msec measurement time,[363] allowing rapid response to impacts.

As a more extreme example, a m_{bullet} ~ 1 gm **high-speed bullet** traveling at v_{bullet} ~ 1000 m/sec toward the user's head with $E_{bullet} = 1/2\ m_{bullet}\ v_{bullet}^2$ = 500 J of energy could potentially be stopped by the coordinated intervention of $E_{bullet} / t_{cushion}\ P_{strandbotMAX}$ = **9110 defensive strandbots**, burning ~3500 W during the ~143 msec action. This would require, among other things, the ability to detect the approach and trajectory of the bullet far enough away from the user's head to give the strandbot population enough time to appropriately reposition and intercept the projectile, halting or deflecting it before impact. An onboard displacement accelerometer[364] R_{accel} ~ 10 μm in radius should detect a local $a_{min} \sim (4\ k_B\ T / 3\pi\ \eta_{air}\ R_{accel}\ t_{meas}^3)^{1/2} \geq 1$ gee acceleration (due to initial contact with the incoming bullet) in a t_{meas} ~ 46.5 μsec measurement time for T ~ 300 K, during which time the bullet travels $v_{bullet}\ t_{meas}$ ~ 4.65 cm which is well within the detection and response range of fully extended $L_{strandbot}$ = 30 cm long strandbots. Similarly, a box-spring accelerometer[365] with a signal/noise ratio of SNR ~ $\ln(V_{Pt}^2\ \rho_{Pt}^2\ a_{min}^2 / 2\ k_B\ T\ k_s) \sim 2$ should detect $a_{min} \geq 1$ gee accelerations using a suspended V_{Pt} ~ 1180 μm^3 platinum reaction mass ($L_{Pt} \sim V_{Pt}^{1/3}$ ~ 10.6 μm) assuming supports with spring constant k_s ~ 1 N/m, taking platinum density ρ_{Pt} = 21.45 gm/cm^3; or alternatively, SNR ~ 5 for $a_{min} \geq 5$ gees. A modest number of high-power defensive strandbots could be interspersed amongst the much larger population of ~100,000 regular strandbots, adding a protective component to the coiffure.

In principle, prehensile hair could even throw bullets. For example, approximately $(m_{BB} / m_{object})\ (v_{BB} / v_{object})^2 \sim 3560$ defensive strandbots could throw a standard BB gun pellet of mass m_{BB} ~ 0.6 gm at the v_{BB} ~ 60 m/sec muzzle velocity of a BB air rifle, taking m_{object} ~ 3 gm and v_{object} ~ 0.45 m/sec from the earlier calculation (Section 8.2).

Defensive strandbots equipped with acoustic sensors could detect the onset of **painfully loud sound** and quickly block the user's external auditory canals to protect the tympanic cavities from damage. Strandbot optical sensors could detect the presence of **dangerously bright light** or laser illumination and quickly assemble a dense robotic mass over the eyes to prevent retinal damage. Further design of defensive strandbots and elaboration of their many possible applications is beyond the scope of this paper and must await future exploratory engineering research.

---

[362] https://www.omnicalculator.com/physics/car-crash-force.

[363] Freitas RA Jr. Nanomedicine, Volume I: Basic Capabilities, Landes Bioscience, Georgetown TX, 1999, Section 4.3.3.2, "Displacement Accelerometers"; http://www.nanomedicine.com/NMI/4.3.3.2.htm.

[364] Freitas RA Jr. Nanomedicine, Volume I: Basic Capabilities, Landes Bioscience, Georgetown TX, 1999, Section 4.3.3.2, "Displacement Accelerometers"; http://www.nanomedicine.com/NMI/4.3.3.2.htm.

[365] Freitas RA Jr. Nanomedicine, Volume I: Basic Capabilities, Landes Bioscience, Georgetown TX, 1999, Section 4.3.3.1, "Box-Spring Accelerometers"; http://www.nanomedicine.com/NMI/4.3.3.1.htm.

9. Conclusions

This paper presents the first technical analysis of the application of microscopic nanorobots to the cosmetological activities of haircutting and hairstyling, also known as hairdressing.[366]

For the **haircutting** activity, ~100,000 nanorobots called "hairbots" collectively drawing ~8.5 μW of power are deployed from an on-person storage vessel such as an earring and perform a comprehensive survey of the user's scalp (Section 3.1), recording both the surface topography and the size and position of each of the ~100,000 individual hairs on the human head in a deployment time of ~2.6 sec for the scalp, plus another ~11 sec for the nanorobots to ascend and descend each hairstalk, measuring each one's length with precision. The user's personal computer downloads and processes these measurements to create a ~10^7 bit scalp map (Section 3.2). After the user selects the desired coiffure (Section 3.3), the personal computer calculates the ideal length of each individual hair needed to achieve the selected style and creates a cut list indicating the exact amount that must be trimmed from each individual hairstalk. Hairbots then climb their assigned hairstalks and make the trim, using either a 900-sec (**15 min**) digestion protocol that creates a harmless odorless gaseous effluent with a fleet power draw of 33 mW (Section 3.4.1) or a 60-sec (**1 min**) mincing protocol that generates <20 μm odorless keratinous "dust" particle effluent with a fleet power draw of 1.3 mW (Section 3.4.2), removing each day's growth of new hair. (If more than one day's growth needs to be trimmed, the excess length can be minced off as a single cutting for external disposal.) The nanorobots will produce no tickling or crawling sensations, can be made invisible to the naked eye of the user or bystanders, won't be easily detectable by touch if the user or someone else touches the hair when nanorobots are present, and will be secure against dislodgement from the hair by external forces such as wind or human touch (Section 3.7).

A **hair extension** protocol should be followed for hairstalks that are too short and must be made longer. A small desktop nanofactory optimized for the molecular manufacture of "natural" human hair, called a "hair mill" (Section 4.1), having a volume of ~5 liters (a box half a foot wide) and drawing ~209 W of power is sized to be able to manufacture ~100,000 strands of 30-cm-long biochemically "natural" human hair in ~10,000 sec (~3 hrs) – or proportionally less time, to the extent that fewer or shorter strands are required. Hairbots collect the manufactured hair via a headrest attachment to the hair mill, then drag the extension strand of the proper length to their assigned hairstalk that is too short (Section 4.2) and then attach the strand by one of a variety of adhesion methods (Section 4.3), extending the individual hairstalk to the precisely desired length in a projected total install time of ~300 sec (~**5 min**).

With all individual hairs adjusted to the proper lengths, what remains for **coiffure deployment and maintenance** is to move all the hairs into their proper arrangement as defined by the desired coiffure and then hold them there securely. This is accomplished by mapping the current scalp hairbody to create a Current Coiffure Map (Section 5.1), then distributing the Current Coiffure Map and the existing Desired Coiffure Map to all active hairbots in the coiffure maintenance system, including the hairstyling software application on the user's desktop computer or mobile

---

[366] https://en.wikipedia.org/wiki/Hairdresser.

device (Section 5.2). The user's computer compares the Current Coiffure Map to the Desired Coiffure Map and calculates the optimal deployment of hairbots to convert the former map into the latter map. Coiffure control is mediated by ~1000 "guidestalks" which are individual hairstalks loaded with a contiguous chain of "guide" hairbots through which retractile or compressive forces can be selectively applied, allowing the coated hairstalk to be operated as a tentacle manipulator. The instructions for guidestalk deployment are downloaded into the hairbot population and the mechanical control framework of the desired coiffure using heavily robotized guidestalks and variable adhesion nodes (individual hairbots) is activated (Section 5.3). The guidestalks and adhesion nodes are manipulated to recruit all remaining hairstalks into ~1000 small hairgroups of ~100 hairs each, whose position and connectivity can be controlled by the guidestalks, completing the hairbody topology specified by the Desired Coiffure Map (Section 5.4). There are ~3 million guide robots and ~3 million node robots, drawing ~62 mW of power during a ~300 sec (**5 min**) coiffure deployment time. Subsequent dislocations of the coiffure caused by wind gusts, fingers drawn through the hair, or other disruptions are quickly detected and reconfigured back to the desired state by the coiffure maintenance system for up to ~8 hrs of continuous disruption (Section 5.5).

Hairstalk color alteration begins by deploying nanorobots called bleachbots (Section 6.1) that apply bleaching chemicals to tented sections of the hairstalk to break down the colored pigment to create color-free hair. The bleaching chemicals needed to process the melanin pigments in one day's growth of hair are synthesized onboard the hairbot in ~900 sec (15 min) using a nanorobotic chemical fabrication module that acquires the necessary carbon (C), hydrogen (H), oxygen (O), and nitrogen (N) atoms from the water, carbon dioxide, and nitrogen in the air, requiring a ~2.51 μW/robot power draw during chemical synthesis and the deployment and retraction of tenting. A second group of nanorobots called dyebots (Section 6.2) use injector needles to add pigments (also synthesized onboard) into the bleached hairstalks without the need for tenting. Bleachbots and dyebots can be applied in a variety of hair coloration scenarios. Specifically: A modest fleet of hairbots could colorize just the roots as they grow out (Section 6.3.1) or could provide frosting of hairtips or highlights that gradually replace the entire hairbody color (Section 6.3.2). The entire hairbody could be recolorized in ~80 min using a much larger ~26 cm^3 fleet of ~86 million hairbots deployed using a 253-watt home hairstyling appliance (Section 6.3.3), or hair mills could be used to replace the entire hairbody down to the roots with the new colors in just **~5 min** (assuming the hair mill has previously fabricated all the replacement hairs), thereafter continuously colorizing the roots as they grow out using the usual fleet of ~100,000 hairbots, once a day (Section 6.3.4). Such rehairing seems aesthetically desirable because the user's hair is almost instantly transformed into the new colors, and the new color is continuously maintained thereafter so the person never "shows roots" as is common after conventional hair coloration processes. Hair color could also be permanently altered at the roots via chromosome replacement therapy applied to hair follicle cells using chromallocytes (Section 6.3.5).

The **hairstalk curl pattern** can be altered by nanorobots applying chemical or genetic treatments (Section 6.4), and could be applied on a whole-hairbody or partial hairbody basis to produce interesting effects. **Thinning or balding hair** can be dealt with by (1) genetic transformation of skin stem cells in the scalp into productive new hair follicles, (2) genetic modification of existing follicles to produce hair strands of different color or curl, (3) using the hair mill to generate full-length synthetic hair that's a phenotypic match to the user's original natural hair and then bonding these new hair strands to permanent biocompatible hairstalk anchors securely embedded in the scalp, or (4) installing minimills in the scalp that can fabricate and extrude new hair in the manner of nanorobotic artificial follicles; alternatively, programmable dermal display nanorobots embedded in a bald scalp would allow images and videos to be projected onto the bare skin of the

head (Section 6.5). The presence of hairbots in the hairbody can also produce a variety of **special effects** including (1) any coloration pattern or image imaginable, (2) sparkling glitteration throughout the hair, (3) shifting displays that reflect or reveal the user's emotional state, (4) the emission of fragrances and scents manufactured *in situ* by the nanorobots that can be detected and enjoyed by people close at hand, (5) audible sounds that can be heard by nearby human ears and spoken commands that can be heard and followed by the hairbots, and (6) purposeful tactile effects such as scalp massages (Section 6.6).

Microscale nanorobots capable of controlled flight (i.e., "flybots") can be attached to every strand of hair on a human head and then tow these strands along arbitrary circumcranial paths through the air, enabling **hairflight** (Section 7). Directly controlling the 3D physical movement of every single hair in real time allows the hairbody to (1) form active kinematic or reactive patterns reflecting the user's emotional state, surrounding the user's face or enhancing facial expressions, (2) create emotionally expressive shapes such as hearts or haloes, or (3) perform a "hair dance" in the air at speeds up to 10 cm/sec. Onboard energy storage should provide up to 3 hours of continuous hover power for ~3 million flybots positioned at 1 cm intervals along each hairstalk, drawing ~20 W for the entire hairbody. Users desiring nanorobot flight times beyond 3 hours can wear a necklace or hairstyle accessory that wirelessly broadcasts continuous radiofrequency power to the flybots.

Bionic hair provides the most complete solution to the challenge of coiffure flexibility, maintenance, and control (Section 8). Bionic hair comprises artificial nanomechanical hairstalks (i.e., "strandbots") each of which is an independently controlled single robotic tentacle manipulator entirely composed of strong diamondoid nanomachinery. After depilating natural hair to the base and placing its follicles in a reversible resting phase, a similar number of strands of bionic hair (manufactured in a specialized nanofactory having similar productivity and power requirements as the hair mill) are attached to a strong scalp- or skull-embedded biocompatible nanomechanical anchor that provides dislodgement resistance to leverage forces transmitted through the artificial hairstalk. Bionic hair provides arbitrary hairbody configurations with color variations and special effects, reactivity to external conditions or events, variable hair length control, and real time coiffure reconfiguration including up to an hour of stored or recorded choreographed programmed hair movements. Individual nanorobotic strandbots incorporate ~2 gigabits of onboard data storage and ~38 gigabits/sec of onboard data processing capacity (Section 8.1), and may be strong enough to lift a ~3 gm mass and throw it at ~45 cm/sec (Section 8.2). Bionic hair might also be able to provide some measure of physical protection for the user's head (Section 8.3), with ~2000 high-power defensive strandbots performing a cushioning maneuver to protect the human head during a simple fall or car crash, or even stopping bullets.

Today's practitioners of the cosmetic arts should be reassured that in the nanotech future described in this paper, some people, perhaps even most, may continue to prefer the human touch and the social interactions that take place during a visit to the hairstylist. The knowledge, experience, judgment, and creativity of such practitioners will remain valuable in this future era because the devices and techniques described in this paper will become available to them to use for the betterment of their clients.